Technical Report Documentation Page

1. Report No. ABC-UTC-2016-C2-FIU01-Final	2. Government Accession No.	3. Recipient's Catalog No.	
4. Title and Subtitle **Development of "ABC-UTC Non-Proprietary UHPC" Mix**		5. Report Date May 2021	
		6. Performing Organization Code	
7. Author(s) Esmail Shahrokhinasab (https://orcid.org/0000-0002-1927-1367) and David Garber (https://orcid.org/0000-0001-9561-0538)		8. Performing Organization Report No.	
9. Performing Organization Name and Address Department of Civil and Environmental Engineering Florida International University 10555 West Flagler Street, EC 3680 Miami, FL 33174		10. Work Unit No. (TRAIS)	
		11. Contract or Grant No. 69A3551747121	
12. Sponsoring Organization Name and Address Accelerated Bridge Construction University Transportation Center Florida International University 10555 W. Flagler Street, EC 3680 Miami, FL 33174	US Department of Transportation Office of the Assistant Secretary for Research and Technology And Federal Highway Administration 1200 New Jersey Avenue, SE Washington, DC 201590	13. Type of Report and Period Covered Final (May 2019 – May 2021)	
		14. Sponsoring Agency Code	
15. Supplementary Notes Visit www.abc-utc.fiu.edu for other ABC reports.			
16. Abstract Ultra-high performance concrete (UHPC) is generally known as a cementitious composite material with compressive strength (greater than 18 ksi) and high tensile strength (greater than 1 ksi). Commercially available UHPC products offer consistent quality and material properties, but their use has been limited due to their high cost, which around 25 to 30 times more expensive than conventional concrete. Non-proprietary UHPC is the non-commercial version of this material and can be produced at a more reasonable price. Non-proprietary UHPC mixes have been previously developed in different regions of the U.S., but still, more research is needed to verify previous efforts made with other types and quality of the material. The main objective of this study was to develop a non-proprietary UHPC mix design made with local materials that could achieve the necessary mechanical properties and durability for use in bridge components, repair, and connections.			
17. Key Words Non-proprietary UHPC; fibers; mix design and mechanical properties		18. Distribution Statement No restrictions.	
19. Security Classification (of this report) Unclassified.	20. Security Classification (of this page) Unclassified.	21. No. of Pages 130	22. Price

Form DOT F 1700.7 (8-72) Reproduction of completed page authorized

(this page is intentionally left blank)

Development of ABC-UTC Non-Proprietary UHPC Mix

Final Report

May 2021

Principal Investigator: David Garber

Department of Civil and Environmental Engineering
Florida International University

Authors
Esmail Shahrokhinasab and David Garber

Sponsored by
Accelerated Bridge Construction University Transportation Center

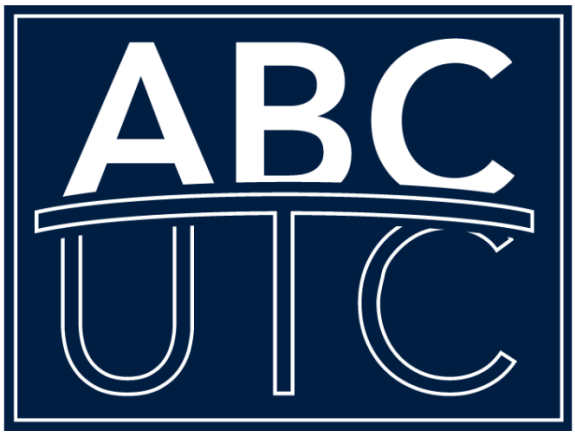

ACCELERATED BRIDGE CONSTRUCTION
UNIVERSITY TRANSPORTATION CENTER

A report from
Department of Civil and Environmental Engineering
Florida International University
10555 West Flagler Street, EC 3680
Miami, FL 33174
Phone: 305-348-2824 / Fax: 305-348-2802
https://cee.fiu.edu/

DISCLAIMER

The contents of this report reflect the views of the authors, who are responsible for the facts and the accuracy of the information presented herein. This document is disseminated in the interest of information exchange. The report is funded, partially or entirely, by a grant from the U.S. Department of Transportation's University Transportation Program. However, the U.S. Government assumes no liability for the contents or use thereof.

CONTENTS

LIST OF FIGURES

LIST OF TABLES

ACKNOWLEDGMENTS

This project was supported by the Accelerated Bridge Construction University Transportation Center (ABC-UTC at www.abc-utc.fiu.edu) at Florida International University (FIU), as lead institution, and Iowa State University (ISU), the University of Nevada-Reno (UNR), the University of Oklahoma (OU), and the University of Washington (UW) as partner institutions. The authors would like to acknowledge the ABC-UTC support.

The author would like to extend special appreciation to the ABC-UTC and the U.S. Department of Transportation Office of the Assistant Secretary for Research and Technology for funding this project.

This research project was a joint project between all the partner universities with OU as the lead university. The authors would like to thank Royce Floyd (OU) and his team for their guidance and leadership in the overall project.

CHAPTER 1: INTRODUCTION

1.1. Project Motivation

Ultra-high performance concrete (UHPC) is generally known as a cementitious composite material with compressive strength (greater than 18 ksi) and high tensile strength (greater than one ksi). Fibers are typically included in the mixture to achieve the required post-cracking behavior. Commercially available UHPC products offer consistent quality and material properties, but their use has been limited due to their high cost, which can be 25 to 30 times more expensive than conventional concrete.

This issue has motivated many scholars to develop less costly UHPC mix designs with at least the same or even improved mechanical properties compared to commercial products.

Non-proprietary UHPC mixes have been previously developed in different regions of the U.S., but more research was needed to verify previous efforts made with different types and quality of the material.

1.2. Research, Objectives, and Tasks

This research project was part of a more comprehensive research effort conducted at the five ABC-UTC partner universities. University of Oklahoma (lead), University of Washington, Iowa State University, University of Nevada Reno, and Florida International University were the five ABC-UTC partner universities that studied the different aspects of this research. OU, FIU, and ISU were responsible for material testing, and UNR and UW were responsible for structural application testing.

The main objective of this research was to develop a non-proprietary UHPC mix design, labeled "ABC-UTC Non-Proprietary UHPC Mix," made with local materials achieving the necessary mechanical properties and durability for use in bridge components, repair, and connections.

The main objective of this research project was accomplished through the following research tasks:

- *Task 1 – Review of Non-Proprietary UHPC Mix Designs:* A comprehensive literature review was conducted to gather available information related to the development of a non-proprietary UHPC mix. FHWA requirements and suggested ASTM tests were determined for evaluation of trial mixes.
- *Task 2 – Mechanical Testing and Customization of Non-Proprietary Mix:* The main goal of this task was to develop a qualified non-proprietary UHPC mix design based on locally available material and determine the effect of different constituents materials and fiber content on the final properties of "ABC-UTC Non-Proprietary UHPC Mix." Different variables include fiber type and content, cement type and content, high range water reducer (HRWR) dosage, and water to binder ratio, were studied through both small-scale trial batches (0.15 ft^3) and large batches (2.2 ft^3). The evaluation process was done based on tests recommended by FHWA for qualifying UHPC mix designs.
- *Task 3 – UHPC Durability Property Testing:* In addition to the mechanical testing conducted in Task 2, bulk resistivity tests were used to evaluate the permeability of the

developed mixtures. The bulk resistivity test was selected based on what has been recommended by other researchers and the availability of equipment for the tests.

- *Task 4 – Technology Transfer Workshop:* A technology transfer workshop was held as part of the 2019 International ABC Conference in Miami to share the performance, observations, and recommendations for the "ABC-UTC Non-Proprietary UHPC Mix."
- *Task 5 – Final Report*: A final report was developed to summarize all results from the experiments done at FIU.
- *Task 6 – Guide for ABC-UTC Non-Proprietary UHPC:* A "Guide for ABC-UTC Non-Proprietary UHPC" will be developed incorporating the research results from all partner universities. OU will coordinate the development of this guide, and all partner universities will contribute relevant sections.

1.3. Report Overview

This report is intended to summarize the results of an extensive literature review related to UHPC mixtures, mix optimization using particle size distribution analysis, development of a non-proprietary UHPC mix with locally available material in Florida, and the effect of different variables on final properties of UHPC mixture. Design recommendations for non-proprietary UHPC mix design are summarized.

CHAPTER 2. BACKGROUND ON UHPC

2.1. Introduction

Ultra-high performance concrete (UHPC) has recently become more popular between academia, engineers, and owners due to its unique properties. UHPC is generally known for its high compressive and tensile strength, self-consolidation, exceptional durability, and significant post-cracking ductility. Maximum water-to-binder ratios (w/b) of 0.24 in UHPC lead to compressive strengths of 22 ksi or more at 28-day age [1]. Low matrix porosity and high particle packing density result in higher durability for UHPC compared to conventional concrete [2]. UHPC has been shown to have a tenfold lower chloride diffusion rate and almost zero deterioration rate under freeze and thawing cycles[3], [4]. The use of steel fibers give UHPC the ability to resist direct tensile stresses of over 0.72 ksi, have a strain hardening response after initial cracking, and have limited crack width [5]. Large superplasticizer dosages allow for hydration of the cementitious materials in the mixture and give UHPC its self-consolidating properties.

These exceptional performance characteristics have made UHPC an ideal option for different sectors of the construction industry including precast concrete fields. UHPC can be used to ease the design and improve the performance of joints between precast elements. UHPC also allows designers to utilize smaller cross-sections, reduce the conventional reinforcement, increase the prestressing force, and consequently produce longer-span elements. UHPC has made a significant improvement in accelerating the construction process, through the use of UHPC in joints between conventional concrete precast elements and as the primary material for UHPC precast elements [6].

Despite all these advantages, the use of UHPC in the United States remains limited. Proprietary UHPC mixtures can cost up to 20 to 30 times more than conventional concrete. Non-propritary mixtures can decrease costs but often require much stricter quality control measures than conventional concrete. These enhanced quality control measures plus the high material cost for the material has limited the widespread use of UHPC in the U.S. infrastructure [5], [7].

For this reason, many research efforts have focused on the non-proprietary UHPC to make UHPC more accessible from locally available materials and give guidance on how to mix and use the material. This study investigates the development of non-proprietary UHPC using locally available material in Florida and gives details on how to mix and test the material.

2.2. Definition of UHPC and Typical Material Properties

Some of the typical material properties for UHPC are summarized in Table 2.1.

Table 2.1: Typical range of mechanical properties for UHPC [8], [9]

Property	Typical Range
7-day Compressive Strength	14.5 to 19.5 ksi
14-day Compressive Strength	18 to 22 ksi
Direct Tensile Cracking Strength	0.8 to 1.2 ksi
Direct Tension Bond Test	0.35 to 0.6 ksi

Property	Typical Range
Modulus of Elasticity	4,250 to 8,000 ksi
Long-term Drying Shrinkage	300 to 1,200 με
Long-term Autogenous Shrinkage	200 to 900 με
Initial setting time	4 to 10 hours
Final setting time	7 to 24 hours
Static flow	7.5 to 10 inches

UHPC typically is defined by some combination of its mechanical properties, however, the actual material properties that are typically included in the definition vary based on the researchers or organization that is providing the definition and the application for the UHPC. A summary of some of the typical minimum definitions of UHPC are summarized in Table 2.2.

Table 2.2: Minimum definitions of UHPC (modified from [3])

Document	Ref.	Country	Min. f'_c (ksi)	Min. Tensile Strength (ksi)	Other Criteria
ACI 239R-18	[10]	USA	22.0	--	--
AFNOR NF P 18-470	[11]	France	18.8	0.87 (first crack, f_t)	Durability, ductility, and fire resistance
ASTM C1856-17	[12]	USA	17.0	--	--
CSA A23.1	[13]	Canada	17.4	0.58 (first crack, f_t)	Durability and ductility
FHWA	[14]	USA	21.7	0.72 (post crack, f_t)	w/b ≤ 0.25
PCI	[3]	USA	18.0	1.50 (first crack, f_r), 2.00 (peak, f_r)	Durability and ductility
SIA 2052	[15]	Switz.	17.4	1.00 (first crack, f_t)	Ductility

The compressive strength is typically specified to be greater than or equal to 18 ksi [3] or 21.7 ksi [14]. Lower strengths are sometimes allowed or specified for specific applications, e.g., 14 ksi for the development length equations for the design of field-cast connections from FHWA [8] and 10 ksi for release strength for precast, prestressed UHPC [3].

UHPC definitions also typically include some requirement for tensile strength and sustained tensile or post-cracking strength. The definition is typically either measured using direct tension tests or modulus of rupture tests. The tensile strength at first cracking, the peak tensile strength, and some related deflections. Typical tensile strength curves are shown in Figure 2.1 for the tensile strength based on flexural stress modulus of rupture tests and direct tension.

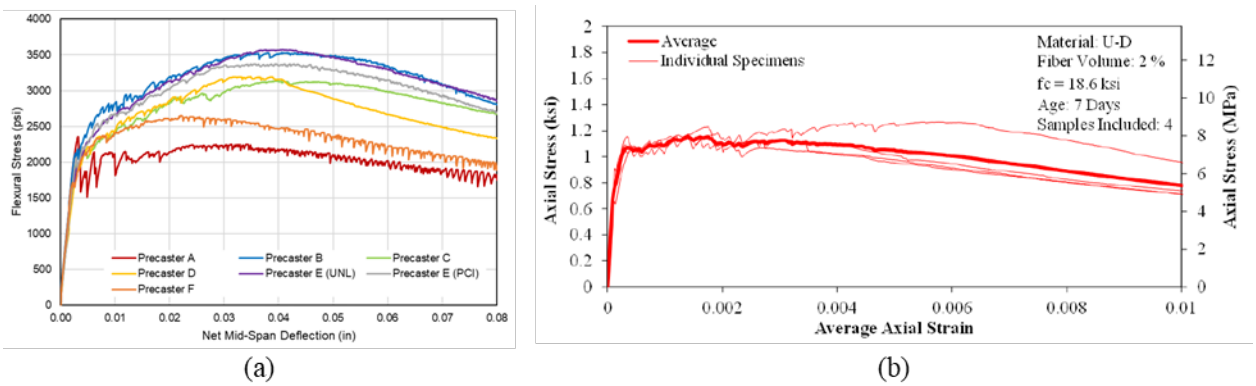

Figure 2.1: Tensile strength curves based on (a) flexural strength from modulus of rupture [3] and (b) direct tensile strength using prismatic samples [16]

The idealized stress-strain response of UHPC loaded under direct tension has a similar shape to conventional steel reinforcement, as shown in Figure 2.2. This idealized response illustrates four of the primary phases in the UHPC tensile response [7]:

1. *Elastic*: linear-elastic response, no crack formation
2. *First cracking*: beginning of the plastic response phase, multiple tightly spaced cracks form in the UHPC matrix
3. *Crack saturation*: start of the strain hardening response, larger cracks begin to develop in the UHPC matrix
4. *Localization*: sample reaches its ultimate tensile strength and begins to drop in strength, a single crack begins to open larger, fibers start to pull out of the UHPC matrix

The actual behavior of the UHPC in tension depends on many different factors, including fiber type, content, and distribution.

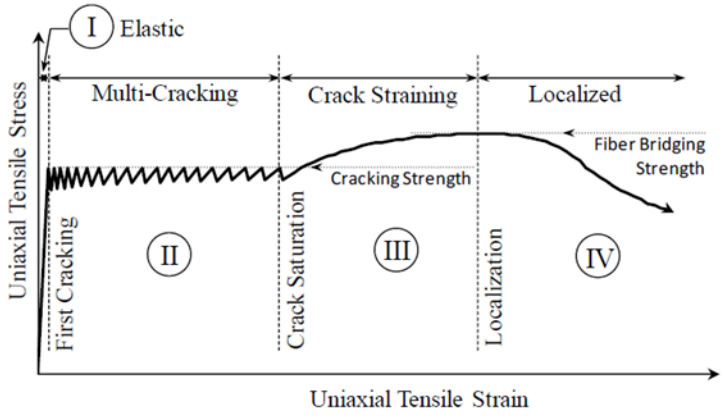

Figure 2.2: Idealized uniaxial tensile mechanical response of a UHPC [7]

2.3. UHPC Application

UHPC has been used in a wide variety of infrastructure applications including repair and retrofit of existing structures and the construction of new structures. UHPC's high compressive and tensile strength, self-consolidating nature, low permeability, long-term durability, and high bonding properties have helped UHPC perform well in different repair applications, such as thin-bonded overlay on deteriorated bridge decks, shown in Figure 2.3 (a), or as a shell around a damaged region of a component [7], [17]. In a recent study, the use of UHPC encasements was shown to increase the load-carrying capacity of timber piles more than 100 percent based on the initial timber pile diameter and UHPC shell thickness [18]. UHPC has also been used as formwork for cap beams and other elements to eliminate the need for assembling or stripping formwork [19].

UHPC also has been used in new construction in several different ways: (1) in the joints between precast elements, (2) as the material for full precast elements, and (3) as material for parts of a precast or prefabricated element. The primary application of UHPC to date has been for the field-cast connection between prefabricated bridge components [7]. The properties of UHPC lead to much shorter required development and splice lengths for reinforcement extending from the precast elements, and the presence of the steel fibers allow for connections to be designed without any field-placed reinforcement. The UHPC has enhanced bonding properties between the UHPC joint and precast element. UHPC joints can be designed to minimize the amount of material required, which helps to mitigate the higher cost of the material. The use of UHPC in the joint between precast elements has been considered recently by many owners, designers, and contractors, especially for joints between precast deck panels [7], [14]. An example of a UHPC joint between precast deck panels is shown in Figure 2.3 (b). UHPC has also been used to connect other prefabricated elements, such as precast barriers to decks or deck panels [20].

UHPC is also being used to produce full precast bridge elements, such as waffle deck panels, pile elements, and girders. The use of UHPC allows for optimized shapes for precast elements with decreased weights, less conventional reinforcement, increased span lengths, and decreased section profiles. An example of a UHPC precast waffle deck panel is shown in Figure 2.3 (c).

UHPC has also been used in application other than bridges. Many precast tunnel segments are made of UHPC or using UHPC as a thin fire resistance overlay due to its fire resistance property [21]. The high compressive strength and tensile resistance of UHPC have broadened its use even in military and critical infrastructures for security and blast mitigation purposes [22]. UHPC has also been used in the energy industry to construct taller and more efficient wind turbine towers [23], as shown in Figure 2.3 (d).

(a) (b) (c) (d)

Figure 2.3: Structural applications of UHPC; (a) overlay (UT) [9], (b) UHPC joints (OR) [9], (c) waffle deck panels (NE) [24], [25] and (d) wind turbine towers(IA) [23], [26]

UHPC has also been used for architectural elements like stairways, facades, street furniture, bus shelters, sun shades, and stuff like that for its high durability and resistance [27], [28]. Some architectural applications are shown in Figure 2.4.

(a) (b) (c) (d)

Figure 2.4: Architectural applications of UHPC; (a) Staircases (DK), (b) Sunshade (CA), (c) Gateway Pavilion (US) and (d) Facade Cladding Panels (Fr) [29]

UHPC is applicable to any applications where conventional concrete cannot address the minimum required mechanical properties [14]. For example, several researchers reported poor performance of normal concrete in the joint between bridge deck panels [9], [30]. UHPC has been used in these applications to improve the behavior of the joint and system.

2.4. UHPC Constituent Materials

The performance of UHPC is based on the properties and proportions of the different material components making up the UHPC mixture. The primary components of UHPC include cement, silica fume, an additional supplementary cementitious material of intermediate sizes (e.g., fly ash, slag), and fine sand (usually finer than conventional concrete sand). The proportions of these components are chosen based on their particle size distributions and reactive properties. A high-range water-reducing admixture (HRWR) or superplasticizer is responsible for providing the desirable flowability while the water-to-binder ratio (w/b) is around 0.2. Steel fibers are usually added at a dosage of 1 to 6 percent by volume to the mixture and provide post-cracking ductility and tensile strength for the UHPC.

One of the most popular proprietary UHPC product in the US is Ductal®, produced by Lafarge-Holcim [29]. This product meets the typical requirements for UHPC materials [31], also described above. The typical composition of Ductal® is shown in Table 2.3.

Table 2.3: Typical Composition of Ductal® [7]

Material	***lb/yd³***	***kg/m³***	***Percentage by Weight***
Portland Cement	1200	712	28.5
Fine Sand	1720	1020	40.8
Silica Fume	390	231	9.3
Ground Quartz	355	211	8.4
HRWR	51.8	30.7	1.2
Accelerator	50.5	30	1.2
Steel Fibers	263	156	6.2
Water	184	109	4.4

Most proprietary and non-proprietary UHPC mixtures have a similar composition to what is shown in Table 2.3. A further explanation of each constituent material is provided in the following sections.

2.4.1. Aggregate

UHPC materials typically only include fine aggregates, although coarser aggregates can be used in lower strength mixtures. Aggregate sizes up to 0.25 inches have been used successfully in UHPC mixture designs [8]. For high strength concrete, the failure cracking in the concrete matrix will often go through the weaker coarse aggregate, which will limit the achievable compressive strength. There have been a few studies that went beyond a maximum aggregate size of 0.25 inches and reported a decrease in the mechanical properties of UHPC. One study used coarse basalt aggregates with a maximum size of 0.63 inches in the UHPC mixture; using the larger aggregate size decreased splitting tensile strength and compressive strength by approximately 8 and 19%, respectively [32].

Using only fine aggregates allows for mixtures where the compressive strength is controlled by the strength of the hydrated cementitious materials and not the aggregate. The use of fine aggregates also provides a gradation of dry materials that facilitates the flowability of UHPC and a denser concrete matrix. Decreasing the maximum aggregate size to 0.23 inches (6 mm) and combining it with finer aggregate categories with a maximum grain size of 0.19, 0.09, and 0.008 inches resulted in a minimum 18 ksi compressive strength at 28 days [33]. Using two different aggregate sizes (0.003 to 0.008 inches and 0.016 to 0.031 inches) and combining them could result in a denser matrix and increased particle packing, which consequently leads to higher mechanical properties (compressive strength of 28 ksi in 28 days) [34]. Using multiple aggregate sizes and combining them based on optimized packing models is a verified solution to get the highest possible density out of available dry constituents and has been used successfully in several studies [32], [33], [35]–[37]. Different aggregate sizes and types used in previous studies are shown in Figure 2.5.

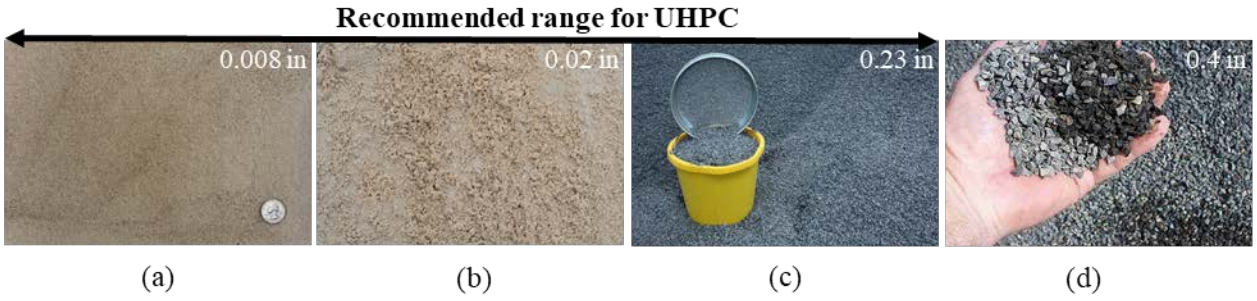

Figure 2.5:Range of the aggregate size used in UHPC; (a) Ultra fines recovery (UFR), (b) Fine sand-limestone, (c) limestone aggregates, (d) basalt aggregates

Different fine aggregate types, including limestone, basalt, and quartz, have also be used successfully in a UHPC mixtures [8], [38], [39]. Different types of aggregates have different properties. Quartz particles offer a higher strength than limestone particles. Previous studies reported using fine quartz particles in the UHPC matrix [38] and getting higher compressive strengths [40].

Other aggregate types have been explored for additional benefits, e.g., internal curing. Previous researchers used an aluminosilicate material (ECat) for this reason [41]. ECat has a chemical composition that encourages pozzolanic activity and a high specific surface area with water affinity, which leads to significant water absorption. This aggregate type was used initially to provide internal curing action on UHPC mixture and improve the mechanical properties of the UHPC.

Quartz particles were not available locally for this study, so ultra-fine recovery (UFR) or limestone powder was used as intermediate aggregates to enhance the density of the final mixture. UFR solid parts are recoverable fine materials coming from wastewater streams of aggregate plant system. The fine size of UFR (less than 150µm) has made it a conveyable and stackable material ideal for several industries.

A maximum grain size of 0.02 inches was used for the fine aggregate in this research to be consistent with the materials used by the University of Oklahoma (OU), who was the lead university for this research project. Limestone aggregate was used as it was the most widely available in South Florida.

2.4.2. Cement

A wide variety of portland cements are used in the construction industry, each one designed for a specific purpose and required performance. Although several studies have reported UHPC mix designs made by different cement types, few have been done to investigate the effect of various cement types on the final properties of UHPC. The most commonly used cement type in UHPC has been Type I/II cement which is a good candidate for UHPC mixtures due to its low cost and widespread availability [7], [5], [33], [34], [36], [42]–[45], [3]. There have been some studies that used Type I White, Type III and Type V cement successfully, but the final mixtures were produced at a higher cost than similar mixtures with Type I/II cement [34], [36], [43], [45].

Additionally, to minimize the workability challenges, it is recommended to use cement with a maximum C_3A content of 8 percent and a blain fineness of less than 281228 in^2/lb [46].

Five different cement types were investigated in this research to see their effect on the rheology and mechanical properties of the UHPC mixtures. Details on the five cement types investigated in this research are summarized in Table 2.4. The 28-day strength was reported by the manufacturer and found using ASTM C109 with a water-to-cement ratio of 0.485 [47].

Table 2.4: Manufacturer supplied properties of cements evaluated

Cement Type	***Producer***	***28-day strength, ksi (MPa)***	***C_3S***	***C_2S***	***C_3A***	***C_4AF***	***Blaine Fineness in^2/lb (m^2/kg)***	***Air Content %***	***Setting Time (min)***	
									Initial	***Final***
Masonry	Titan America	2.9 (20.2)	-	-	-	-	-	15	145	-
Type I-II	Titan America	6.8 (47.0)	63	9	6	11	279822 (398)	7	109	228
Type I-II	Ash Grove	4.7 (32.3)	59	19	6	10	-	6	115	115
Type III	Titan America	7.9 (54.7)	69	6	6	11	355050 (505)	6	75	155
Type I (white)	Lehigh	7.1 (49.1)	73	7	13	1	339583 (483)	6.7	100	200

2.4.3. Silica Fume

Silica fume plays an important role in UHPC mixtures due to its fine particle size and pozzolanic properties. These fine particles fill the gaps between coarser grains in the matrix and promote higher density. Besides its physical role, its pozzolanic activity provides additional strength and improved durability for the UHPC mixture. Typical UHPC mixtures have silica fume contents between 10 to 20 percent of cement weight [8].

A silica fume provided by BASF was used in this research at contents between 16 and 21 percent of the cement weight.

2.4.4. Supplemental Cementitious Materials (SCM)

Other supplemental cementitious materials are also used in UHPC mixtures. These materials typically are added to concrete to improve particle packing and make concrete mixtures more economical, sustainable, impermeable or improve mechanical properties [3], [8]. Fly ash, slag, and metakaolin are the most popular SCMs that have been used to date [48], [40].

Slag cement or blends of portland cement with ground-granulated blast-furnace slag (GGBS) has been used in several studies [34], [36], [43], [45]. Using GGBS typically helps to reduce the cost of the mixture and helps create a more sustainable cementitious material by using less ordinary portland cement. Using a 50:50 mix of Type I portland cement and GGBS as a binder not only offered a more reasonable cost but also satisfied typical requirements for UHPC mixtures in several studies [34], [36], [43], [45].

Fly ash has also been used in several studies but has generally shown less improvement in mechanical properties compared to UHPC mixtures made with GGBS [33], [36], [49]. Comparing the hydration process of mixes containing fly ash and slag revealed that fly ash

requires more water to be actively involved in the hydration process compared to slag. Therefore, in UHPC and other special concretes with low w/b, the pozzolanic reaction of fly ash is significantly retarded [49]. Fly ash can still be used in the UHPC mixture based on its availability and price. Although fly ash can be obtained at a more reasonable price than other SCM's like silica powder, it may not be as effective as other SCMs due to its higher water demand [5].

Several additional SCMs have been investigated for use in UHPC. These include nano-silica, silica powder, metakaolin, and nano-metakaolin.

Several studies used nano-silica particles with an average diameter between 1 and 100 nanometers to improve the durability of different types of cementitious material. Most of these studies reported significant improvement in strength development, modulus of elasticity and durability [50], [51], [51], [52]. Also, few studies used nano silica fume to investigate the final mechanical properties of UHPC mixtures. Using nano silica fume (5 percent of the cement weight) with silica fume (30 percent of the cement weight) resulted in a 21 ksi compressive strength at 28 days [53]. Nano-silica can be used in UHPC mixtures based on the availability and price. In this study nano-silica particles were not used to be consistent with other university partners.

One study investigated the use of silica powder in UHPC. They suggested to remove the silica powder from the mixture due to its relatively high cost and delayed reaction compared to silica fume [36].

Metakaolin is another SCM that has been used to improve the mechanical properties and durability of UHPC mixtures in a similar way as silica fume. Metakaolin can be more accessible than silica fume and has a white color, which makes it more appropriate for architectural purposes [40]. Kaolinite, the source of metakaolin is available in most countries and locations with more reasonable price compared to nano silica and silica fume. Metakaolin has also been used in the nano scale in some past studies to improve the particle packing of the UHPC. While replacing up to 10 percent of cement weight with nano-metakaolin improved the compressive strength at older ages, it also significantly decreased the flowability, so more HRWR was required to get the necessary flowability [54], [55]. Metakaolin was not used in this study to be consistent with other partner universities.

In general, most SCMs can be used in UHPC mix design based on availability but should be tested in small trial batches to ensure adequate performance before being used in field applications.

2.4.5. Fibers

Fibers have been used in cementitious composites since 1980 [56], [57] and play an important role in UHPC. Fibers are added to the UHPC matrix to provide post-cracking ductility and increase the tensile strength [21]. A fiber content of 2 percent of total mixture volume is typically used in UHPC, but contents as high as 6 percent have been used to attempt to increase the tensile strength [8]. Although higher fiber contents generally result in higher tensile strength, a higher dosage of fibers may cause negative results due to improper fiber distribution and decreased

workability. This issue can be even worse when fibers are relatively heavy, lengthy, and hooked. Dispersion of heavier fibers in the concrete matrix is more challenging and requires special mixing consideration. Deformed fibers like hooked end fibers perform better in terms of pullout resistance but need special attention as they are more susceptible to clumping during batching.

Fibers used for UHPC are classified based on the material type: metallic fibers (commonly made of steel) and non-metallic fibers (made of organic polymers; synthetic fibers). Steel fibers have higher yield strength (up to 400 ksi) compared to synthetic fibers (less than 100 ksi), which leads to UHPC with steel fibers having a much higher post-cracking tensile strength. Although steel fibers provide superior after-cracking behavior for UHPC, synthetic fibers can lead to improved fire resistance and also a softer UHPC response.

The effect of fibers on the mechanical performance of UHPC will depend on geometry, anchorage type, material, coating, chemical composition, weight, yield strength, volume fraction, dispersion, and orientation of the fibers [3].

The most commonly used steel fiber in UHPC is a brass-coated, straight, steel fiber with 0.008-inch (0.2-mm) diameter and 0.5-inch (13-mm) length and a specified minimum tensile strength of 290 ksi (2,000 MPa) [8]. The tensile strength of these fibers is typically around 400 ksi (2,758 MPa).

Four different steel fibers from various manufacturers and one synthetic fiber were used in this research at several different fiber contents. The properties of the fibers used in this research are summarized in Table 2.5 and a photograph of the different fibers is shown in Figure 2.6. The Bekaert OL 13/.20 and Hiper Fiber Type A fibers had the same physical properties and both were brass coated. Although the exact chemical composition of fibers was not obtained, the researchers were informed by the manufacturer that the Helix 5-13 fibers contained a higher zinc content. The manufacturer informed the researchers that the zinc content was decreased in the fibers, but new fibers were not obtained after this change had occurred.

The fiber types are given a short name in Table 2.5 for use in the mixture design tables.

Table 2.5: Fiber Properties

Name	***Fiber***	***Length,*** *in (mm)*	***Diameter,*** *in (mm)*	***Aspect Ratio (l/d)***	***Tensile strength,*** *ksi (MPa)*
A	Dramix 4D 65/35BG	1.4 (35.6)	0.020 (0.51)	70	268.0 (1,850)
H	Helix 5-13 (uncoated)	0.5 (12.7)	0.020 (0.51)	25	246.5 (1,700)
OL	Dramix OL 13/.20	0.5 (12.7)	0.008 (0.20)	63	400.0 (2,758)
HF	Hiper Fiber Type A	0.5 (12.7)	0.008 (0.20)	63	400.0 (2,758)
Sy	STRUX® 90/40	1.55 (40)	0.017 (0.43)	92	90.0 (620)

Figure 2.6: Different steel fibers (a) Bekaert 4D 65/35BG, (b) Helix 5-13, (c) BEKAERT OL 13/0.2 & Hiper Fiber and (d) STRUX® 90/40

2.4.6. Water

Like other cementitious composites, UHPC needs water to complete the hydration process. All water quality and control requirements relevant to conventional concrete are also applicable for UHPC mixtures [8]. Besides the role of water in the chemical reaction, its temperature during addition to the mixture plays a very important role in the final properties of fresh concrete. A lower temperature reduces the heat of hydration and results in higher flowability [8]. For this reason, cold water or ice cubes were used in many studies and are recommenced for casting in high-temperature climates [3]. Using ice particles not only improves the flowability by controlling the heat of hydration but also improves the mixing efficiency by gradually releasing water in the mixture and improving the mixing action [8].

2.4.7. Chemical Admixtures

The most common chemical admixtures in UHPC are high-range water reducers (HRWR) or superplasticizers. Both polycarboxylate-based superplasticizers and phosphonate-based superplasticizers have been used in UHPC mixtures to provide the required flowability for this concrete with low w/b. Other chemical admixtures like viscosity modifying admixtures (VMA) and corrosion inhibiter admixtures are also used in UHPC mixtures for specific actions [3].

VMA are water-soluble polymers that have been used in concrete technology to modify the viscosity of mixing water and increase the ability of cementitious paste to retain its constituents in suspension [58]. VMA have been widely used for self-compacting concrete (SCC) with slump flows ranging from 26 to 31 inches [58].

In this study, BASF Master Glenium 7920 was used as HRWR to provide required flowability. The BASF VMA 358 was also used for specific mix designs for uniform dispersion of heavier fibers and preventing fiber segregation.

2.5. Water-to-Binder Ratio

The water-to-binder ratio (w/b) is an important factor that affects the final mechanical properties of the cementitious composite. Lower w/b typically results in higher strength, but there are thresholds for high and low w/b defined based on the properties of the constituents in a mixture. In other words, decreasing the w/b will only increase strength to a certain point. After this point, further decreasing w/b will decrease the strength because there is not enough water to hydrate all

the cementitious materials and be available for later pozzolanic reactions. Additionally, low w/b will decrease the workability of a mixture and require more HRWR.

There are several different ways to measure the proportion of water in a concrete mixture. The water-to-cement ratio (w/c) is the weight of the total water in the mixture divided by the weight of cement, as shown in Equation 2-1. The w/c was initially used for conventional concrete with one single cementitious material as the binder.

Since the water in a mixture is also used to hydrate some SCMs or in the pozzolanic reaction for others (depending on SCM composition), the w/b became became more representative of the proportion of water in a concrete mixture. The w/b may also be written the water-to-cementitious material ratio (w/cm). The w/b is defined as the weight of the free water (including the natural moisture in aggregates) divided by the weight of all cementitious material [46], as shown in Equation 2-2.

For concrete mixtures with low w/b like UHPC, the water contained in the added chemical admixtures will influence the hydration and mechanical properties of the mixture [3]. The most accurate way to calculate the total water in a mixture includes all water components, including free water, moisture from aggregates, and the water content of chemical admixtures. This modified water-to-binder ratio (w^*/b) can be found as shown in Equation 2-3. Most past researchers have not considered the water content from the chemical admixtures when finding w/b.

Water-to-cement: $$w/c = (W_1 + W_2)/C_1 \quad \text{Equation 2-1}$$

Water-to-binder: $$w/b = (W_1 + W_2)/(C_1 + C_2) \quad \text{Equation 2-2}$$

Modified water-to-binder: $$w^*/b = (W_1 + W_2 + W_3)/(C_1 + C_2) \quad \text{Equation 2-3}$$

where:

W_1 = weight of free water

W_2 = weight of water available as moisture content in aggregates

W_3 = weight of liquid portion of chemical admixtures (defined by manufacturer)

C_1 = weight of cement

C_2 = weight of SCMs

All three equations were used to report results in this research to make them more comparable with previous studies.

2.6. Previous Efforts on Developing Non-Proprietary UHPC Mixture.

There have been several previous research efforts for developing non-proprietary UHPC mixture made with locally available materials in different regions of the U.S. Most of the studies satisfied the typical minimum requirements for UHPC mixtures and in some cases ended up with much

higher mechanical properties [2], [5], [34], [38], [41]–[44], [59]. A summary of previous studies on non-proprietary UHPC mixtures is shown in Table 2.6.

Table 2.6: Previous research projects for developing non-proprietary UHPC mixes.

Researcher	Year	Location	Selected-UHPC Mix Parameters						Performance	
			C: SF: SCM	*Other SCMs Used*	*w/c*	*w/b*	*Agg.:b*	*Fiber vol. fraction (%)*	*Flow (in.)*	f'_c *(ksi)*
Tadros et al.[1]	2020	A	1.0: 0.25: 0.00	-	0.25	0.200	0.88	0 and 2	8-11	25.0
		B	1.0: 0.25: 0.11	LP	0.25	0.184	1.10	0 and 2	8.9, 9.2	23.4
		C	1.0: 0.25: 0.00	-	0.24	0.195	0.77	0 and 2	9.1	23.1
		D	1.0: 0.20: 0.18	LP	0.29	0.202	0.77	0 and 2	9.1	21.4
		E	1.0: 0.25: 0.00	-	0.23	0.188	1.10	0 and 2	8.9	23.6
Lawler et al.	2019	FL	1.0: 0.15: 0.15	FA (Class F)	0.23	0.170	1:0 to 2:0	1.5 and 2	8-10	18-19
Karim et al.[2]	2019	Iowa	1.0: 0.07: 0.00	-	0.20, 0.25	0.18, 0.2, 0.23	1.12, 1.3	2	8-9	10-17
Matos et al.	2019	Portugal	1.0: 0.54: 0.27	-	0.40	-	1.0	3	11.2-12.2	21-22
Looney et al.	2019	OK	1.0: 0.17: 0.50	S	0.18 to 0.22	0.18 to 0.23	0.75, 1.0	1 and 2	9-11	16-18.2
Berry et al.	2017	Montana	SF/FA = 0.75	FA	0.24	-	1.4 [3]	0 and 2	8-11	20-21
El-Tawil et al.	2016	Michigan	1.0: 0.25: 1.0	S	0.22	0.18	1.0	1.5	-	20.9-28.3
Graybeal	2013	WA, OR, ND, SD, NY, PA	1.0: 0.25: 0.25	FA	0.22 to 0.24	0.15 to 0.16	1.0	1 and 2	10.4-12.4	22.5-29
Tafraoui et al.	2009	France	1.0: 0.25: 0.25	Metakaolin	0.27	0.22	0.9, 1.18	0 and 2	-	15-27.5

c = cement; b = all cementitious materials; FA=fly ash; LP=limestone powder; S=slag or GGBS

[1]liquid portion of chemical admixtures was included in w:c and w:b calculations

[2]compressive strength was measured at 7 days

[3] this is sand to cement ratio

2.7. Available Constituent Materials

The materials selected for this research were chosen based on their local availability in South Florida. Five different types of cement and five different types of fibers were studied in this research. The amounts of the other SCMs, fine aggregate, and chemical admixtures were varied but the type was the same in all mixtures in this research. The material details, supplier information, and abbreviations used throughout this report are summarized in Table 2.7.

Table 2.7: Material detail, suppliers, and abbreviations

Material	***Details***	***Sign***	***Supplier***
Fibers	Dramix 4D 65/35BG	A	Bekaert
	Helix 5-13	H	HELIX
	Dramix OL 13/.20	OL	Bekaert
	Hiper Fiber	HF	Hiper Fiber
	STRUX® 90/40	Sy	GCP Applied Technology
Cement	Type M- Masonry Cement	C-M	Titan America
	Type I-II	C-T-I/II	
	Type III	C-T-III	
	Type I-II	C-A-I/II	Ash Grove
	Type I	C-W-I	Lehigh White Cement
Ground-Granulated Blast-Furnace Slag (GGBFS)	-	S	ARGOS USA Cement
Silica Fume	Master Life® SF 10	SF	BASF
Sand	Fine Masonry	FA	Titan America
UFR	-	UFR	Titan America
HRWR	Glenium 7920	HRWR	BASF
VMA	VMA 358	VMA	BASF

2.8. Base Mixture

The base mixture for this research was given by the lead university for the overall project, the University of Oklahoma (OU), and based on work done by Looney et al. [45]. The mixture design is shown in Table 2.8.

Table 2.8: Non-proprietary UHPC mix design initially proposed by OU

Type	**Quantity**
Type I Cement, lb/yd^3	1179.6
Slag, lb/yd^3	589.8

Type	Quantity
Silica Fume, lb/yd^3	196.6
w/*b*	0.20
Fine Masonry Sand, lb/yd^3	1966
Steel Fibers, lb/yd^3	255.2
Steel Fibers, %	2.0
Glenium 7920, oz./cwt	15.77

This mixture design was used as a starting point in this research and was modified to determine the effects of different materials and quantities on the mechanical properties.

2.9. UHPC Standard Tests

Most tests for conventional concrete can be used as is or with slight modifications for evaluating the performance of UHPC material. There are some additional tests that should be used to properly test the enhanced properties of UHPC. A summary of some of the most important tests used previously by other researchers that will be used in this study is shown in Table 2.9.

Table 2.9: Conducted tests for qualified UHPC mixtures [12], [60]–[67]

Property	Test Method	Specimen Geometry	Age for Testing (# specimens to test)
Flowability	ASTM C1437 ASTM C230	n/a	tested during casting
Compressive Strength	ASTM C39 ASTM C1856	3”x6” cylinders	3 days (3), 28 days (3)
Modulus of Elasticity	ASTM C469 ASTM C1856	3”x6” cylinders	28 days (3)
Splitting Tensile Strength	ASTM C496	3”x6” cylinders	28 days (3)
Flexural Strength	ASTM C78	3”x3”x11” prisms	28 days (3)
Total and Drying Shrinkage	Embedded VWGs ASTM C157	6”x12” cylinders	Begin measuring after casting (3)
Set Time	ASTM C403	6”x6” cylinder	at time of casting (3)
Bulk Resistivity Test	ASTM C1760	4”x8” cylinders	3,7,14,28,56 and 90 days (4)

More details on these tests will be provided in the following chapters when discussing experimental procedures.

CHAPTER 3. MIXTURE OPTIMIZATION

3.1. Particle Packing Theory

There are two dependent approaches for optimizing cementitious materials. The first approach, known as particle packing theory, is related to the physical characteristics of constituents and their proportions in the final mix. The second approach relates to the chemical composition of the constituents and the reaction between components; this approach focuses on choosing appropriate SCMs to expedite and improve cement hydration. This chapter will focus on particle packing theory and its application to this research.

Different models can be used for the particle packing of UHPC. The most-used particle packing model was originally developed by Andreasen and Andreasen [68]. The model provides an equation that represents the optimal partical size distribution based on the physical characteristics of the constituents; the density and strength of a mixture will theoretically be higher the closer the actual particle size distribution curve is the the optimal curve. Andreasen and Andreasen's model was modified by Funk and Dinger [69] to account for the smallest particle size; this model is shown in Equation 3-1.

$$D(P) = \frac{D^q - D_{min}^q}{D_{max}^q - D_{min}^q} \qquad \text{Equation 3-1}$$

where:

- $D(P)$ = percent passing for each diameter evaluated
- D = particle diameter being evaluated
- D_{min} = smallest particle diameter used in the mix design
- D_{max} = largest particle size used in the mix design
- q = distribution modulus

The distribution modulus (q) defines the coarseness of the final mixture: q closer to 1.0 produces a more coarsely graded mixture, while q closer to 0 produces a more finely graded mixture. Typical q values used for UHPC mixtures are in the range of 0.19 to 0.37 [3], [34], [36], [70].

Many previous studies have used the particle packing theory and tried to best match actual particle size distributions to the optimal curves from Andreasen and Andreasen [68] and Funk and Dinger [69]. A recent study by Tadros et al. [3] used particle packing optimization in five different locations across the U.S. to develop five different UHPC mixtures with 28-day compressive strengths greater than 22 ksi. Particle packing optimization has also been used to create sustainable concrete mixtures with reduced portland cement contents (50 percent reduction) while keeping similar mechanical properties [71]. It has also been used for developing special concretes like self-compacting concrete (SCC), high-performance concrete (HPC), recycled aggregate concrete, and 3D printable concretes [72]–[74].

3.2. Particle Packing Analysis

The first step in the particle packing optimization process is to determine the particle size distribution curves for each of the possible constituent materials. Samples of the different constituent materials were obtained from each of the producers for characterization and review.

Dry constituents in UHPC are very fine, so their full particle size distributions cannot typically be determined using a physical sieving process. Commercial laser diffraction devices can be used to determine the particle size distributions for very fine particles (4.0×10^{-6} in. to 4.0×10^{-2} in. [0.1 µm to 1000 µm]). The particle size distributions of the powder materials were determined by laser particle size analysis using a Malvern Mastersizer 2000 by Titan America in Miami.

The particle size distributions for the primary dry materials used in this study are shown in Figure 3.1 (a). The size of the smallest and largest particles is also determined using the laser particle size analysis. The largest particle size in this study was 2.0×10^{-5} in. (500 µm), measured in the fine sand aggregates. The smallest particle diameter was around 3.9×10^{-8} in. (1 µm), measured from the silica fume. The silica fume used in the testing was coarser than expected, so the particle size analysis was performed on different samples to verify the results. The silica fume contained some larger particles (by observation) than would typically be expected from silica fume. The ideal curves found using Equation 3-1 with the measured minimum and maximum particle size is shown in Figure 3.1 (b) for different values for the distribution modulus (q). A distribution modulus q of 0.25 was considered for the particle packing analysis in this study, based on previous researchers [3], [36], [45].

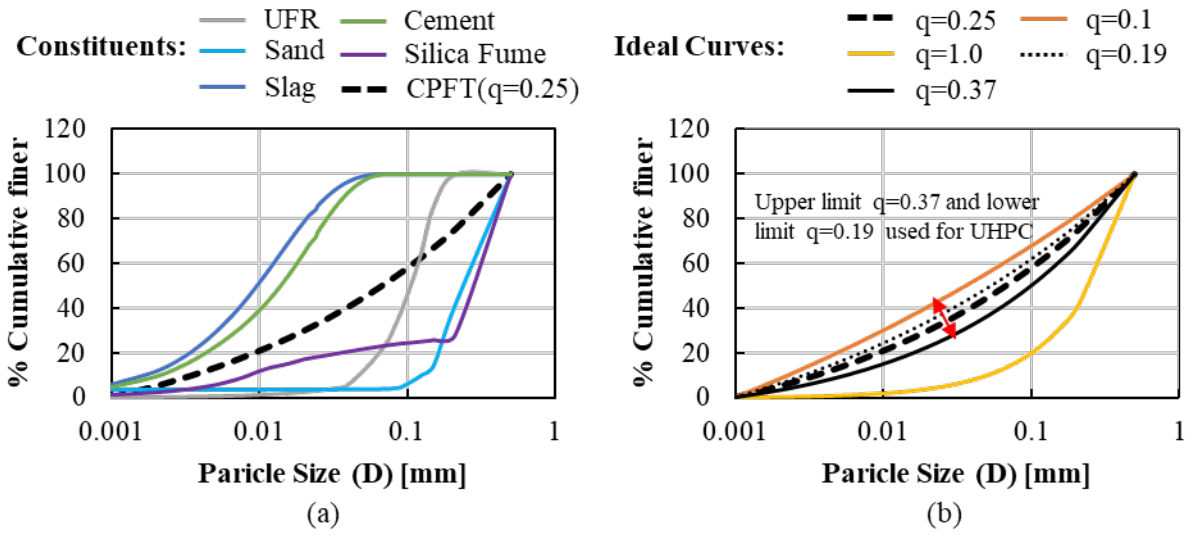

Figure 3.1: Particle packing analysis: (a) distribution curves of different constituents and (b) effect of varying "q" parameter in Modified Andreasen and Andersen model with D_{max} = 0.5 mm and D_{min} = 0.001 mm.

3.3. Qualified UHPC Mixtures

A spreadsheet tool was developed to evaluate different proportions of the constituent materials and the resulting particle size distribution curves. The proportions of the constituent materials

was generally kept within the ranges typically used for UHPC mixtures. Several different aggregate-to-cementitious material ratios (agg/cm) were investigated, including 0.8, 0.9, 1.0, 1.1, and 1.2. The trial-and-error process revealed an optimum agg/cm of 1.0. Several different proportions of cementitious materials were investigated to reveal the optimal cement to slag to silica fume ratio of 0.6 to 0.3 to 0.1.

Using agg/cm equal to 1.0 and the proportions of cementitious materials kept at 0.6:0.3:0.1, several mixture designs were evaluated with different proportions of aggregates. Five of these iterations with different proportions of sand and UFR are shown next to the optimal particle size distribution curve (with q = 0.25) in Figure 3.2. The closer the particle size distribution curve is to the optimal curve, the better the particle packing density for the mixture.

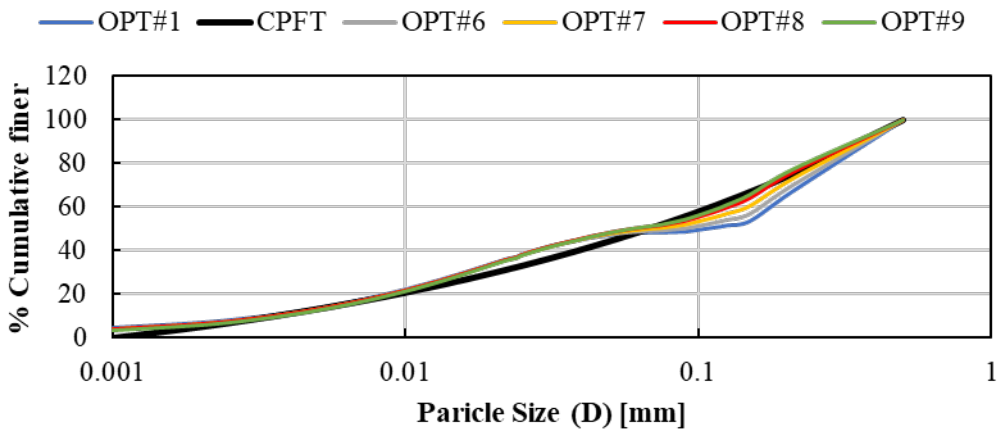

Figure 3.2: Particle size distributions for five mix design and the optimal particle size distribution curve with q = 0.25

A summary of the proportions of the constituent materials in these five mixtures developed based on the particle packing analysis is provided in Table 3.1. An ideal cement to the slag to silica fume ratio (0.6:0.3:0.1) was determined based on this analysis, OPT#1. Modifying the sand to UFR ratio was found to improve the particle packing in the range where there was the largest difference between the mixture curves and idealized curves; four mixtures with UFR were designed as comparisons OPT#6 through OPT#9.

Table 3.1: Proportions of the initially qualified mixes

Mixes	***Agg./C***	***Cement %***	***Slag %***	***Silica Fume %***	***Sand %***	***UFR %***
		Cementitious Materials			Aggregate	
OPT#1	1.0	0.6	0.3	0.1	1.00	0.00
OPT#6	1.0	0.6	0.3	0.1	0.90	0.10
OPT#7	1.0	0.6	0.3	0.1	0.80	0.20
OPT#8	1.0	0.6	0.3	0.1	0.70	0.30
OPT#9	1.0	0.6	0.3	0.1	0.65	0.35

These proportions were used as the starting point for the experimental work.

CHAPTER 4. SMALL-SCALE BATCHES

4.1. Introduction

For more efficient use of material, two different experimental steps were defined for developing the UHPC mixtures. The first series of experimental testing was conducted as a trial-and-error process using 0.15 ft^3 mixtures (small-scale batches) using only compressive strength and flow table testing. A total of 115 0.15-ft^3 batches and 690 3-in. by 6-in. cylinders were cast during this portion of the experimental program. Several of these mixtures were then selected for casting of larger volume mixtures (2.2 ft^3) for conducting a larger range of experimental tests.

Variables investigated in the small-scale batches included water-to-binder ratio (w/b), cement type, proportions of cementitious materials, aggregate type and proportions, aggregate preparation (wet versus dry), fiber type and fiber content, HRWR dosage, VMA dosage, and mixing time and procedure. Mixtures were developed in the small-scale batches with compressive strengths greater than 18 ksi and flowability between 8 and 10 inches.

4.2. Determining Amount of Material for Mixtures

The base proportions of the constituent materials was determined based on the particle packing analysis described in Chapter 3. The actual amount of material to include in each 0.15 ft^3 mixture was determined by first determining the amount of material per cubic foot and then multiplying these amounts by 0.15 ft^3, which was the desired volume.

An example for determining the amount for a specific mix is provided below. Some of the information that is needed for the base mixture is shown in Table 4.1 for the proportions. The proportions of cement, slag, and silica fume are based on only the cementitious materials. The proportion of fine sand and UFR are based on only the fine aggregate. The aggregate to cementitious materials ratio was 1.0 for most of the mixtures that were investigated. The total units equals 2.0 based on 1.0 unit for cementitious materials and 1.0 unit for aggregates.

Table 4.1: Example information needed to determine materials for small-scale batch mixture

Constituent	Proportion	Variable
agg/cm	1.0	
Cement	0.6	P_c
Slag	0.3	P_s
Silica Fume	0.1	P_{sf}
Fine Sand	0.9	P_{sand}
UFR	0.1	P_{UFR}
Total Units	*2.0*	P_{tot}

Additional information is needed on the desired fiber content, fiber density, desired water-to-binder ratio (w/b), HRWR content, VMA content, and the estimated density of the UHPC mixture without fibers. Values for this example are shown in Table 4.2. These HRWR content is typical for some of the mixtures. The density is the measured density from one of the base mixtures.

Table 4.2: Additional information needed for example to determine materials for small-scale batch mixture

Property	Value	Variable
Fiber Content [%]	2.0	FC
Fiber Density [lb/ft^3]	490	ρ_f
Water-to-binder ratio	0.2	w/b
HRWR [oz./cwt]	27.5	v_{HRWR}
VMA [oz./cwt]	0.0	V_{VMA}
Estimated Density [lb/ft^3]	148.6	ρ_c

The information from Table 4.1 and Table 4.2 can be used to determine the amount of material required per cubic foot of material. The amount of cement, slag, and silica fume can be found using Equation 4-1, Equation 4-2, and Equation 4-3, respectively. An example is provided for determining the amount of cement, slag, and silica fume in the example mixture.

Cement (lb/ft^3):

$$W_c = \frac{\rho_c P_c (1 - FC)}{P_{tot}} \quad \text{Equation 4-1}$$

$$W_c = \frac{\left(148.6\ {}^{lb}/_{ft^3}\right)(0.6)(1 - 0.02)}{2.0} = 43.7\ {}^{lb}/_{ft^3}$$

Slag (lb/ft^3):

$$W_s = \frac{\rho_c P_s (1 - FC)}{P_{tot}} \quad \text{Equation 4-2}$$

$$W_s = \frac{\left(148.6\ {}^{lb}/_{ft^3}\right)(0.3)(1 - 0.02)}{2.0} = 21.8\ {}^{lb}/_{ft^3}$$

Silica Fume (lb/ft^3):

$$W_{sf} = \frac{\rho_c P_{sf} (1 - FC)}{P_{tot}} \quad \text{Equation 4-3}$$

$$W_{sf} = \frac{\left(148.6\ {}^{lb}/_{ft^3}\right)(0.1)(1 - 0.02)}{2.0} = 7.3\ {}^{lb}/_{ft^3}$$

The amount of water can be found by summing the weight of the cementitious materials and multiplying by w/b, as shown in Equation 4-4. The weight of water per cubic foot for the example is also shown.

Water (lb/ft^3):

$$W_w = \left(W_c + W_s + W_{sf}\right)\left({}^{w}/_{b}\right) \quad \text{Equation 4-4}$$

$$W_w = \left(43.7\ {}^{lb}/_{ft^3} + 21.8\ {}^{lb}/_{ft^3} + 7.3\ {}^{lb}/_{ft^3}\right)(0.2) = 14.6\ {}^{lb}/_{ft^3}$$

The amount of fine sand and UFR can be found using a similar procedure as the cementitious materials, as shown in Equation 4-5 and Equation 4-6.

Fine Sand (lb/ft^3): $$W_{sand} = \frac{\rho_c P_{sand}(1 - FC)}{P_{tot}}$$ Equation 4-5

UFR (lb/ft^3): $$W_{UFR} = \frac{\rho_c P_{UFR}(1 - FC)}{P_{tot}}$$ Equation 4-6

The weight of fibers to include can be found just by taking the fiber density (ρ_f) times the fiber content (*FC*) as shown in Equation 4-7. The weight of the steel fibers for the example mixture are also shown below.

Steel Fibers (lb/ft^3): $$W_{fibers} = \rho_f(FC)$$ Equation 4-7

$$W_{fibers} = \left(490\ {}^{lb}/_{ft^3}\right)(0.02) = 9.8\ {}^{lb}/_{ft^3}$$

The amount of HRWR and VMA can be determined using Equation 4-8 and Equation 4-9. The amount of HRWR per cubic foot for the example is also shown.

HRWR (oz/ft^3): $$V_{HRWR} = v_{HRWR}\frac{\left(W_c + W_s + W_{sf}\right)}{100}$$ Equation 4-8

$$W_w = \left(27.5\ {}^{oz}/_{cwt}\right)\left(43.7\ {}^{lb}/_{ft^3} + 21.8\ {}^{lb}/_{ft^3} + 7.3\ {}^{lb}/_{ft^3}\right)/100 = 20.0\ {}^{oz}/_{ft^3}$$

VMA (oz/ft^3): $$V_{VMA} = v_{VMA}\frac{\left(W_c + W_s + W_{sf}\right)}{100}$$ Equation 4-9

The amount of all the different constituents in the example mixture is shown in Table 4.3. Amounts are shown per cubic foot and per 0.15 cubic foot, which was the size of the small-scale batch mixtures.

Table 4.3: Amount of materials per 1 ft^3 and 0.15 ft^3 for example mixture

Constituent	**Amount per ft^3**	**Amount per 0.15ft^3**
Cement [lb]	43.7	6.6
Slag [lb]	21.8	3.3
Silica Fume [lb]	7.3	1.1
Water [lb]	14.6	2.2
Fine Sand [lb]	65.5	9.8
UFR [lb]	7.3	1.1
Steel Fibers [lb]	9.8	1.5
HRWR [oz]	20.0	3.0

Constituent	Amount per ft^3	Amount per $0.15ft^3$
VMA [oz]	0.0	0.0

This procedure was performed to find the amount of material to use for each of the mixtures. A similar procedure was also used for the large-scale batches (2.2 ft^3).

4.3. Mixing Procedure

Due to the low w/b and the small particle size of UHPC, relatively higher mixing energy is required to complete the wetting process compared to conventional concrete. A 1.5-HP planetary mixer with 0.2 ft^3 capacity was used to make 0.15 ft^3 trial mixtures; the mixer was found to exert a sufficient amount of mixing energy.

The mixing process included two 10-minutes phases. The first 10-minute mixing phase involved mixing all the dry components (other than the fibers), and the second 10-minute mixing phase involved the addition of the liquid components (water and chemical admixtures) and the steel fibers.

The mixing procedure for the small-scale batches is shown in Figure 4.1. All constituents were premeasured in cylinder molds and graduated cylinders before the beginning of the mixing procedure, shown in Figure 4.1 (a) and (c). The sand, cement, slag, silica fume, and UFR were all added to the mixer and mixed on low speed for 10 minutes, as shown in Figure 4.1 (b). A plastic sheet was wrapped around the mixer at this time to try and keep all the dry materials and dust in the mixer during this phase.

For the second 10-minute mixing phase, half of the HRWR was added to the required water, as shown in Figure 4.1 (d), and poured into the mixer over 2 minutes, as shown in Figure 4.1 (e). The remainder of the HRWR was then added to the mixture and left to mix until the powder material became a flowable paste, which typically took 6 to 11 minutes of additional mixing time. Once the UHPC paste was produced, the fibers were added to the mixture and allowed to mix for an additional 2 minutes, as shown in Figure 4.1 (f). The transition from a powder to a fluid takes additional time depending on the water-to-cementitious ratio and the HRWR dosage. The average total mixing time varied between 20 to 25 minutes.

Due to the very low water to binder ratio and very fine particles, UHPC is very sensitive to moisture. To avoid any variability in results, the required aggregates (fine sand and UFR) for most of the mixtures were oven-dried and stored in sealed containers to reach room temperature 24 hours before mixing. There were a few mixtures where the aggregates were not oven-dried before mixing. Not oven drying the materials led to increased variability in test results. For field cast applications, it is probably not practical to use oven-dried material. The moisture content of aggregates should be measured and monitored continuously before the mixing process.

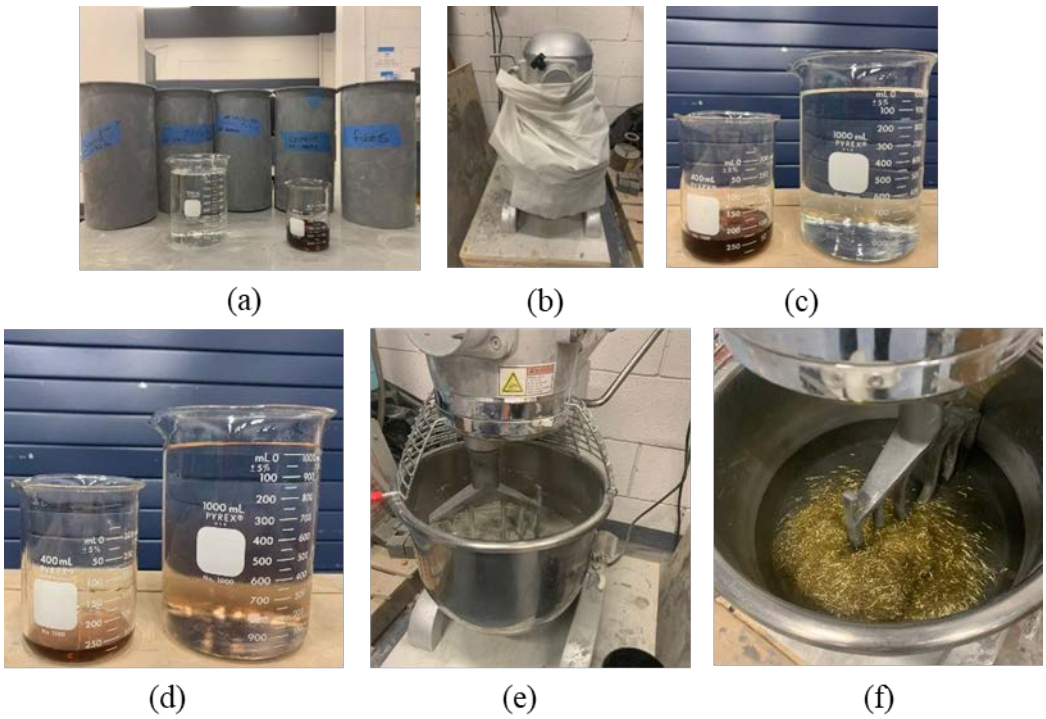

Figure 4.1: General Mixing procedure (a) weighted material, (b) dry mixing, (c) weighted water and HRWR, (d) blending half of HRWR with required water, (e) second 10 minutes of mixing with water and HRWR, and (f) adding fibers.

4.4. Initial Evaluation of Small-Scale Batches

The small-scale batches were evaluated based on their rheology, flowability, and compressive strength. The target compressive strength was 18 ksi at 28 days and target flowability of the fresh UHPC between 9 and 11 inches. The general working time and fiber segregation were also observed duing the mixing and placing process. Each 0.15 ft^3 batch of UHPC was enough to conduct the flow table test and fill six 3 by 6-inch cylinder samples. Two cylinder samples were tested to measure the compressive strength at 3, 7, and 28 days. The general procedure for mixture optimization is shown in Figure 4.3.

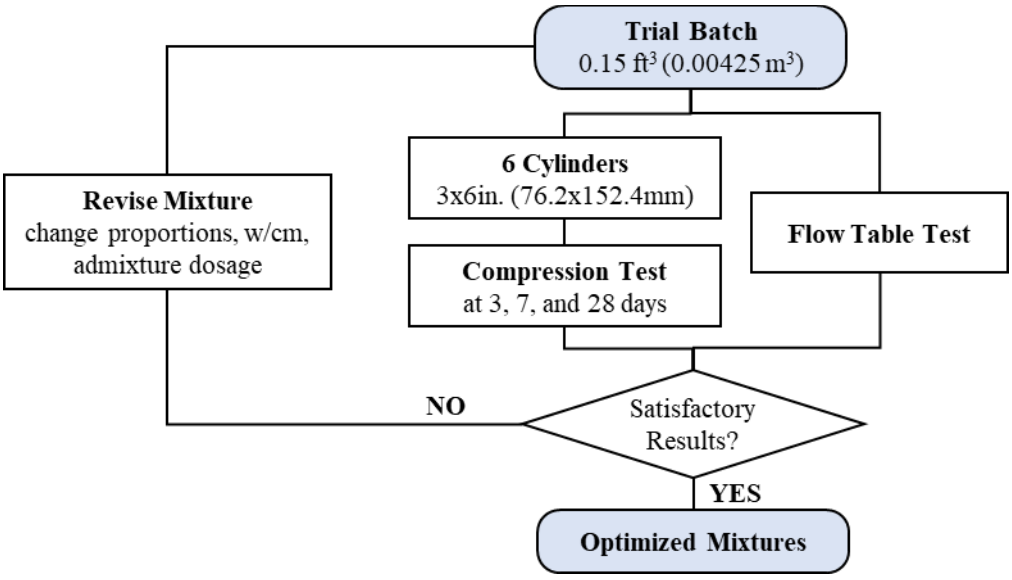

Figure 4.2: Mixture optimization process

4.5. Preparation and Initial Tests

Flow table tests were used to measure the flowability of the mixture and highlight any fiber segregation issues in the mixture. The UHPC was then placed into six 3 by 6-inch plastic single-use cylinder molds. After labeling and cleaning the concrete leftovers from external parts of mold, they were capped and stored in a temperature-controlled room until the test dates.

4.5.1. Flow Table Test Procedure

The flowability of UHPC mixtures was determined using flow table test for cement mortar in the static mode according to ASTM C230/C230M (Standard Specification for Flow Table for Use in Tests of Hydraulic Cement) [12], [67]. The spread cone, shown in Figure 4.3 (a), was filled immediately after the mixing process was finished and then slowly lifted for measuring the spreading flow. The material on the base plate was allowed to spread for 60 seconds, and then the diameter of the spread was measured in two directions. The minimum and maximum diameters were measured, as shown in Figure 4.3 (b) and (c), and the flow for a mix was taken as the average of the two readings.

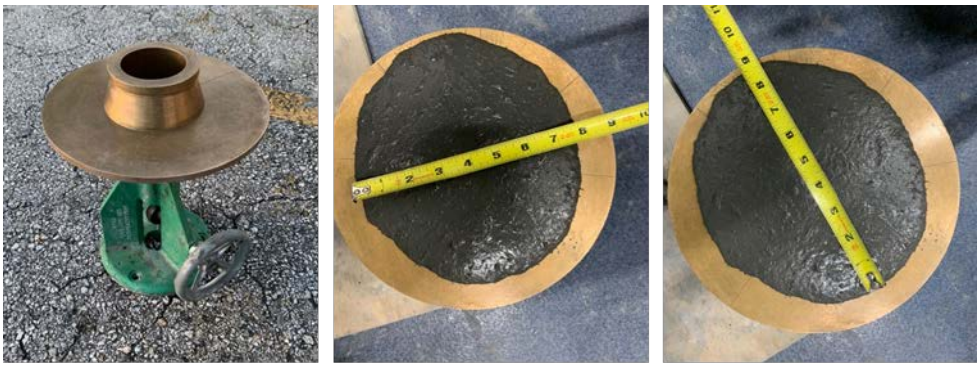

(a) (b) (c)

Figure 4.3: Flowability Test; (a) Flow table apparatus (b) minimum spread measurement and (c) maximum spread measurement

The flow table test was also used to determine if there were any issues with fiber distribution and fiber segregation in a mixture. Poor fiber distribution was observed in two different ways: (1) if there were not many fibers in the UHPC taken from the mixer for the flow table test, as shown in Figure 4.4 (a), and (2) if all the fibers clumped together in the middle of the spread, as shown in Figure 4.4 (b). Poor fiber distribution in the flow table test correlated well with poor fiber distribution in the overall mixture.

(a) (b)

Figure 4.4: Photographs of two flow table tests performed on C6 with poor fiber distribution, (a) without many fibers and (b) with all fibers clumped in middle of test

4.5.2. Compressive Test Procedure

The compressive test was conducted in accordance with ASTM C39 (Compressive Strength of Cylindrical Concrete Specimens) and ASTM C1856 (Standard Practice for Fabricating and Testing Specimens of Ultra-High Performance Concrete) [12], [61]. All cylinder samples were capped, stored in a temperature-controlled room, and demolded 24 hours before the test. No special curing methods were used in the small-scale batch study. The surface of the cylinders after demolding is shown in Figure 4.5 (a). After demolding and before compressive tests, all samples were ground on both ends using an automatic cylinder end grinder machine, shown in Figure 4.5 (b), to satisfy the planeness required by ASTM C39 and ASTM C1856. A sample cylinder after the grinding process was completed is shown in Figure 4.5 (c). The volume and

mass measurements were then taken, and all information was recorded (hand-written) in developed testing sheets. The cylinders were then placed in the compressive test machine, Figure 4.5 (d) and tested to failure using the appropriate loading rate from ASTM C39 and ASTM C1856. A cylinder after failure is shown in Figure 4.5 (e). Photographs were taken of all cylinders before and after failure. The failure load and failure mode were documented on the testing sheets. After testing, the data for all cylinders was input into spreadsheets developed to collect the test data. The compressive strength for each cylinder was calculated in these spreadsheets using all the input data.

Figure 4.5: Compression testing procedure, (a) demolded sample, (b) grinding machine used to smooth each end of the cylinders, (c) sample after cylinder grinding, (d) compressive test machine with cylinder installed, and (d) diagonal break pattern of cylinder

4.6. Experimental Results for Small-Scale Batches

Four different series of small-scale tests were cast to study the effect of the different variables discussed above. An overview of the four different series of small-scale batches is shown in Table 4.4.

Table 4.4: Series OU, A, and B with aggregates in natural moisture

Series	n_{mixes}	Cement type	Initial goal	Moisture Condition
OU	7	C-M	Effect of C-M	N
A	10	C-T-I/II	Finding proper amount of water and HRWR dosage	N
B	20	C-T-I/II	Optimum SCM proportions	N
C	53	All cement types	Find the qualified mixtures	D

For Moisture Condition: D = oven-dried; N = natural moisture

Only the results from some of the mixtures are presented in this section. The results are organized by the influence of different variables:

- Sand moisture and water content
- Cement type
- Water-to-binder ratio (w/b)
- HRWR content
- VMA content
- Effect of fiber type and content

- Effect of fine aggregate type and content

All results related to small-scale trial batches are provided in Appendix A.

4.6.1. Fine Aggregate Moisture

Three different series of small-scale mixtures were cast using aggregate that was not oven dried. The aggregate for these mixtures was stored outside and moved inside 2 days before casting. There was a large variation in the results when the aggregate was not oven dried. A sample of some of similar mixtures with w/b of 0.18 and 0.20 with aggregate that was not oven dried is shown in Table 4.5. The three mixtures with similar w/b ratios had the same mixture proportions, same mixing procedures, and similar HRWR contents.

Table 4.5: Mixture proportions and characteristics for investigation of variation in results due to moist fine aggregate

Mix.	Cement Type	w/b	Mix Proportions						Fiber		Admixtures		Density (lb/ft^3)	Sand Moisture
			agg/cm	*C*	*S*	*SF*	*FA*	*UFR*	*Type*	*Content (%)*	*HRWR (oz./cwt)*	*VMA (oz./cwt)*		
B11	Titan Type I/II	0.18	1.0	0.6	0.3	0.1	1.0	0.0	-	0.0	23.81	0.00	146.10	N
B17	Titan Type I/II	0.18	1.0	0.6	0.3	0.1	1.0	0.0	-	0.0	23.81	0.00	146.40	N
B31	Titan Type I/II	0.18	1.0	0.6	0.3	0.1	1.0	0.0	-	0.0	23.81	0.00	144.90	N
B1	Titan Type I/II	0.20	1.0	0.6	0.3	0.1	1.0	0.0	-	0.0	15.75	0.00	138.60	N
B23	Titan Type I/II	0.20	1.0	0.6	0.3	0.1	1.0	0.0	-	0.0	23.81	0.00	146.00	N
B24	Titan Type I/II	0.20	1.0	0.6	0.3	0.1	1.0	0.0	-	0.0	21.97	0.00	145.80	N

The compressive strength for these mixtures are shown in Figure 4.6. There is a large variation in the compressive strengths at different ages between the three mixtures in each w/b group. As an example, the coefficient of variation of the 28-day compressive strength between the three mixtures was 0.13 and 0.12 for w/b of 0.18 and 0.20, respectively. This is a larger coefficient of variation than was measured for similar mixtures with oven-dried aggregate.

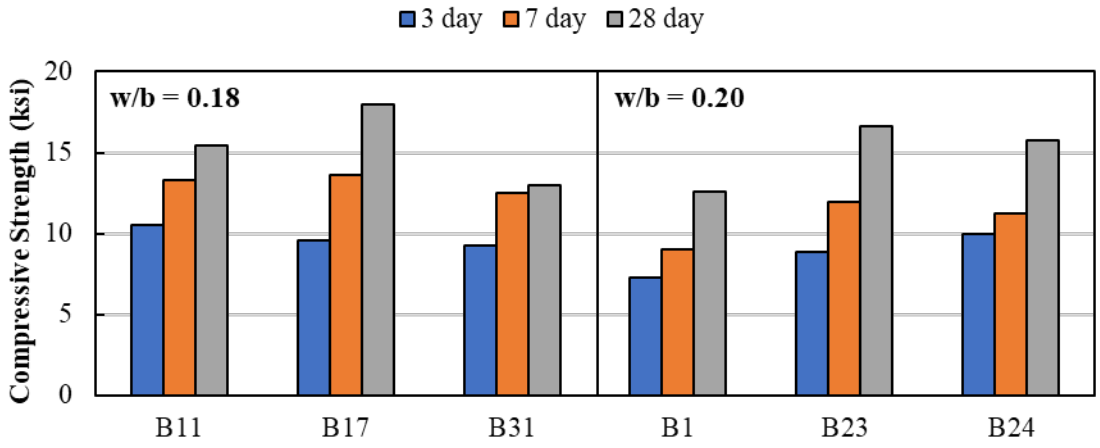

Figure 4.6: Effect of moisture content in aggregate on compressive strength

A summary of results related to these three series is available in Appendix A.

4.6.2. Cement Type

Five different cement types were used in this project to estimate their effect on the final properties of the UHPC. Five different mixes with the same mix proportions (OPT#1) were cast to determine the effect of cement on mixture properties. Details of each mix design are summarized in Table 4.6.

Table 4.6: Mixture proportions and characteristics for investigation of cement type

Mix.	Cement Type	w/b	Mix Proportions						Fiber		Admixtures		Density (lb/ft^3)	Sand Moisture
			agg/cm	*C*	*S*	*SF*	*FA*	*UFR*	*Type*	*Content (%)*	*HRWR (oz./cwt)*	*VMA (oz./cwt)*		
OU2	Masonry Cement	0.20	1.0	0.6	0.3	0.1	1.0	0	A	2.0	15.77	0	135.7	N
C3	Ash Grove Type I-II	0.20	1.0	0.6	0.3	0.1	1.0	0	OL	2.0	22.25	0	149.0	D
C32	Titan Type I/II	0.20	1.0	0.6	0.3	0.1	1.0	0	OL	2.0	27.47	6.5	146.9	D
C37	Titan Type III	0.20	1.0	0.6	0.3	0.1	1.0	0	OL	2.0	27.47	0	149.0	D
C4	Lehigh White Cement	0.20	1.0	0.6	0.3	0.1	1.0	0	OL	2.0	23.35	0	146.5	D

One of the mixtures (OU2) did not use oven-dried sand and used Dramix 4D 65/35BG fibers; the other four mixtures used oven-dried sand and Dramix OL 13/.20 fibers. Flowability and compressive strengths are shown in Figure 4.7.

Specimens with masonry cement had the lowest compressive strengths of the five different types of cement. The masonry cement led to an average 28-day compressive strength of 10.2 ksi and a density less than 140 lb/ft^3; this was likely due to the masonry cement's high air content. Samples made by masonry cement all had higher porosity and lower density than other samples made by other cement. Masonry cement is not recommended for UHPC mixtures.

The Type I/II cement and Lehigh White cement had similar performance with compressive strength around 14.5 ksi at 28 days. Lehigh White cement is usually available with premium cost compared to Type I/II cement.

Specimens with Type III cement had the highest compressive strengths of the group reaching an average compressive strength of 17.9 ksi at 28 days. Type III cement had good initial flowability, but had a noticeably shorter working time than UHPC made with the other types of cement. Considering the decreased working time for Type III cement, it was not used for the large-scale batches. The working time issue would need to be addressed before Type III cement is used in UHPC.

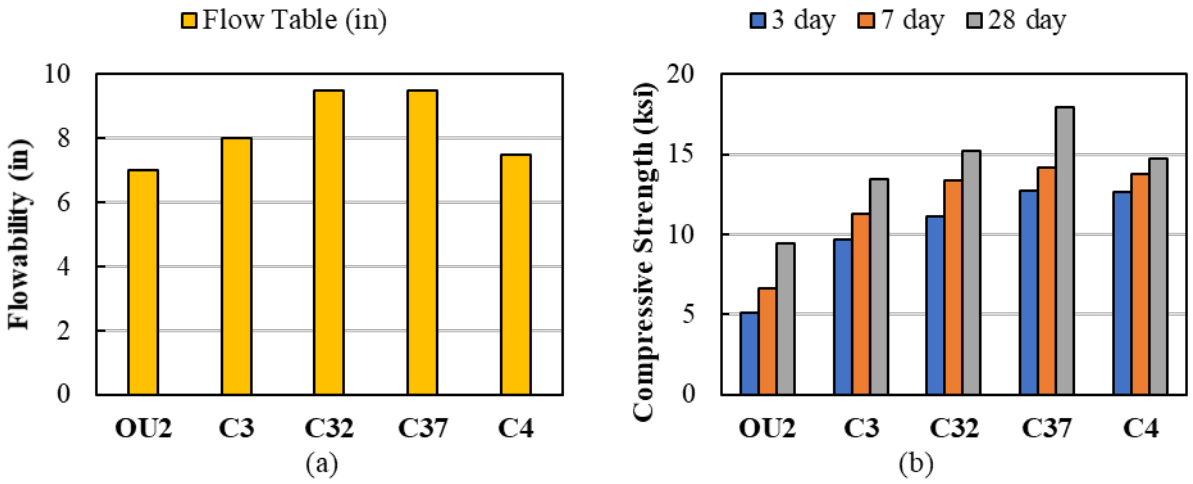

Figure 4.7: Effect of cement type on (a) flowability and (b) compressive strength

Type I/II cement was used for the majority of small-scale batches and all the large-scale batches due to its good performance, working time, and low cost.

4.6.3. Water-to-Binder Ratio

Water to binder ratio (w/b), discussed in §2.5, is one of the most important criteria determining the final mechanical properties of any cementitious material. Any cementitious mix needs enough water to hydrate the cementitious materials and be available for pozzolanic reactions, but excess water will lead to more pores and decreased strength. There is no exact w/b to guarantee the full hydration process, as it depends on cement fineness, the chemical composition of the clinker used, and grain size. Previous studies [75]–[77] reported numbers between 0.35 to 0.45 for full cement hydration for conventional concrete, but it differs for each mixture design and depends on the constituents used in the concrete matrix. To find the optimum w/b of the UHPC for this research, mixtures with w/b between 0.17 to 0.24 were tested, which coincides with typical w/b ratios for UHPC mixtures [5], [7], [78], [79].

Five mixtures used to compare the effect of the w/b are shown in Table 4.7. The HRWR content was increased for smaller w/b to keep a relatively consistent workability between the mixtures, although the flow still decreased with the w/b ratio even with the increased HRWR content, as shown in Figure 4.8 (a).

Table 4.7: Mixture proportions and characteristics for investigation of water to cement ratio (dried sand used in all mixtures)

Mix.	Cement Type	w/b	Mix Proportions						Fiber		Admixtures		Density (lb/ft^3)
			agg/cm	*C*	*S*	*SF*	*FA*	*UFR*	*Type*	*Content (%)*	*HRWR (oz./cwt)*	*VMA (oz./cwt)*	
C17	Titan Type I/II	0.24	1.0	0.6	0.3	0.1	1.0	0	OL	2.0	16.39	2.47	142.8
C11	Titan Type I/II	0.22	1.0	0.6	0.3	0.1	1.0	0	OL	2.0	19.87	6.5	144.6
C32	Titan Type I/II	0.20	1.0	0.6	0.3	0.1	1.0	0	OL	2.0	27.47	6.5	146.9
C34	Titan Type I/II	0.18	1.0	0.6	0.3	0.1	1.0	0	OL	2.0	27.47	6.5	149.8
C26	Titan Type I/II	0.17	1.0	0.6	0.3	0.1	1.0	0	OL	2.0	35.52	0	150.0

The optimum w/b was found to be around 0.18 to 0.20, as shown in Figure 4.8. The compressive strength increased as the w/b decreased from 0.24 to 0.18. The compressive strength then decreased when the w/b was further reduced from 0.18 to 0.17. The w/b shown here do not include the water from the admixtures.

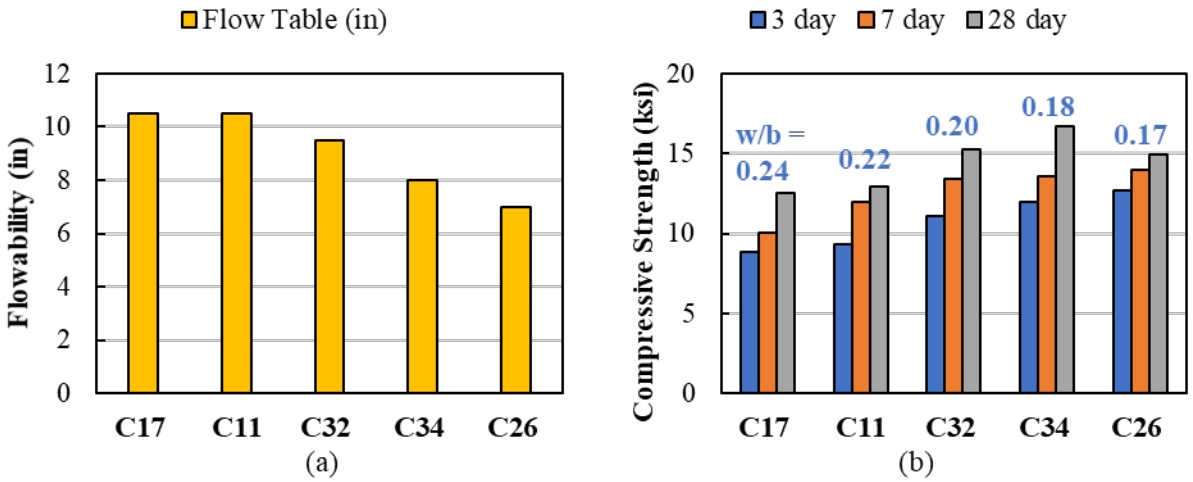

Figure 4.8: Effect of water-to-binder ratio on (a) flowability and (b) compressive strength

A w/b of 0.20 was used as the base value for the large-scale batches. One large-scale batch was cast with a w/b of 0.18.

4.6.4. HRWR Content

HRWR was used to provide workability and flowability of mixtures with low w/b. The base HRWR content was recommended by the University of Oklahoma (OU) as 18 oz/cwt. This was used as the starting point and modified throughout the testing program to maintain a flow between 8 and 10 inches. Three mixtures that had similar mixture proportions with different HRWR contents are summarized in Table 4.8.

Table 4.8: Mixture proportions and characteristics for investigation of HRWR effect (dried sand used in all mixtures)

Mix.	Cement Type	w/b	Mix Proportions						Fiber		Admixtures		Density (lb/ft^3)
			ag/cm	*C*	*S*	*SF*	*FA*	*UFR*	*Type*	*Content (%)*	*HRWR (oz./cwt)*	*VMA (oz./cwt)*	
C28	Titan Type I/II	0.20	1.0	0.6	0.3	0.1	1	0	OL	2.0	21.70	0	147.1
C2	Titan Type I/II	0.20	1.0	0.6	0.3	0.1	1	0	OL	2.0	22.25	0	144.5
C31	Titan Type I/II	0.20	1.0	0.6	0.3	0.1	1	0	OL	2.0	27.47	0	147.4

As expected, increasing the HRWR content increased the flow of the mixture, shown in Figure 4.9 (a). Increasing the HRWR content decreased the 28-day compressive strength for these three mixtures, as shown in Figure 4.9 (b). This was possibly due to the water content in the HRWR adding additional water to the mixture and thus increasing the w*/b, as described in §2.5. The water content of the chemical admixtures was not included in the w/b shown in Table 4.8. The water content of the chemical admixtures is typically neglected when determining the mixing

water and w/b. The results from Figure 4.9 (b), showing increased HRWR decreasing the strength of the mixture, would support that the liquid part of chemical admixtures should be considered for calculation of w/b and the amount of mixing water to add to a mixture.

Due to its small flowability, the concrete for C28 needed to be actively compacted into the mold to ensure that no voids were present in the cylinder molds. In general, flowabilty below 8 inches required this active compaction, which is not practical for field applications.

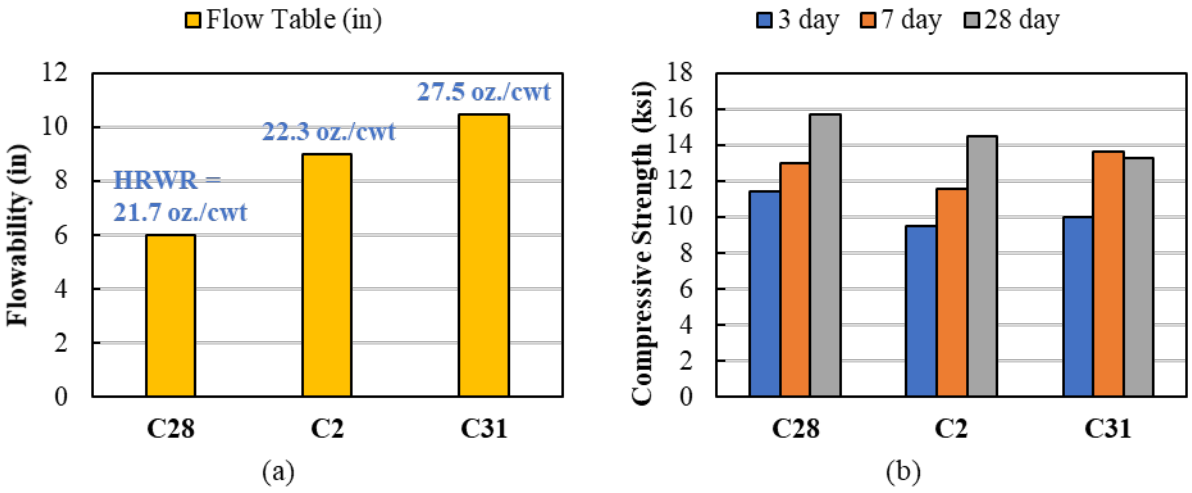

Figure 4.9: Effect of HRWR content on (a) flowability and (b) compressive strength

A HRWR content of 27.5 oz/cwt was used as the base amount for the large-scale batches to ensure sufficient workability to cast all the specimens.

4.6.5. VMA Content

Viscosity modifying admixture (VMA) is a water-soluble polymer that is used in concrete technology to modify the viscosity of mixing water and increase the ability of the cementitious paste to retain its constituents in suspension [58]. VMA is widely used for self-consolidating concrete (SCC) where the flowability exceeds 26 inches [58]. Its usage is not limited to SCC; VMA is also used for pumped concrete, under water concrete, lightweight concrete, sprayed concrete or shotcretes, and even for porous concrete [80].

VMA was used in this research to help prevent steel fiber segregation in the UHPC mixes, especially when heavier fibers or longer fibers were used. The effect of VMA was investigated on a fiber type that did not require VMA to stabilize the fiber in the mixture (Dramix OL 13/0.2); this allowed for a 0 oz/cwt to be compared to mixtures with VMA. The three mixture designs used to compare the effects of VMA are shown in Table 4.9. The water content of the VMA was not considered in the w/b calculation due to its small proportion compared to the total water.

Table 4.9: Mixture proportions and characteristics for investigation of VMA effect (dried sand used in all mixtures)

Mix.	Cement Type	w/b	Mix Proportions						Fiber		Admixtures		Density (lb/ft^3)
			ag/cm	*C*	*S*	*SF*	*FA*	*UFR*	*Type*	*Content (%)*	*HRWR (oz./cwt)*	*VMA (oz./cwt)*	
C28	Titan Type I/II	0.20	1.0	0.6	0.3	0.1	1.0	0	B	2.0	21.70	0	147.1
C16	Titan Type I/II	0.20	1.0	0.6	0.3	0.1	1.0	0	B	2.0	26.55	3.02	148.7
C29	Titan Type I/II	0.20	1.0	0.6	0.3	0.1	1.0	0	B	2.0	21.70	6.50	146.5

The flow and compressive strength for similar mixtures with different amounts of VMA are shown in Figure 4.10. VMA increased the flow (comparing C28 and C29 with similar HRWR contents); see Figure 4.10 (a). The VMA content did not change the compressive strength of mixtures, as shown in Figure 4.10 (b).

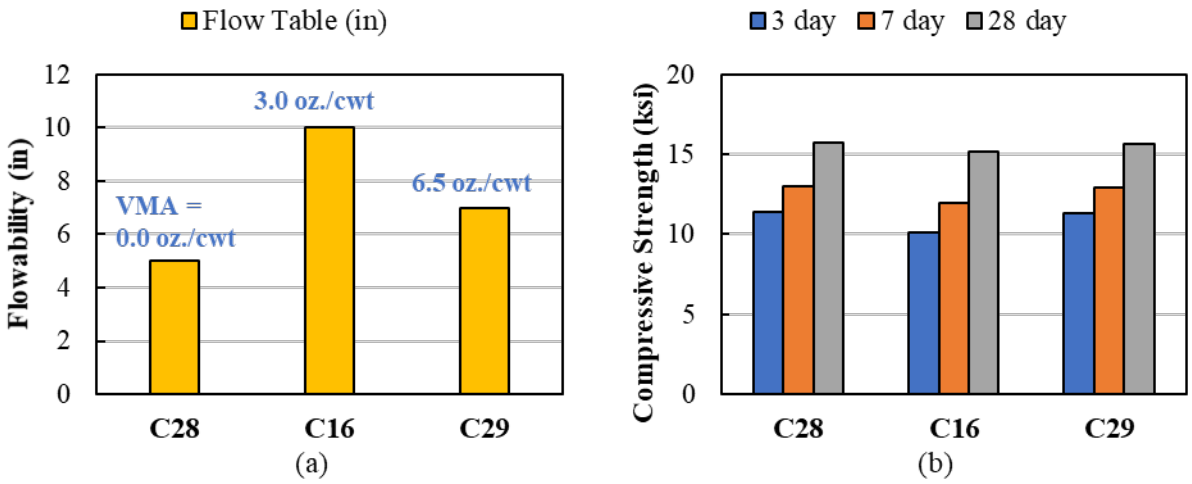

Figure 4.10:Effect of VMA content on (a) flowability and (b) compressive strength

VMA is not suggested to be used with the standard fiber types used for UHPC (i.e., 0.5-in. length and 0.008-in. diameter), but it can be used to stabilize other kinds of fibers that may tend to settle or clump together during the mixing procedure without affecting the strength of the mixture. VMA was only used for the large-scale batch with Dramix 4D 65/35BG, since these fibers are longer and heavier. Other large-scale batches did not include any VMA.

Four additional mixtures also were developed to determine the VMA influence on rheological properties and working time of the fresh UHPC. Details on these four mixtures are provided in Table 4.10.

Table 4.10: Mixture proportions and characteristics for investigation of working time (dried sand used in all mixtures)

Mix.	Cement Type	w/b	Mix Proportions						Fiber		Admixtures		Density (lb/ft^3)
			ag/cm	*C*	*S*	*SF*	*FA*	*UFR*	*Type*	*Content (%)*	*HRWR (oz./cwt)*	*VMA (oz./cwt)*	
C35	Titan Type I/II	0.20	1	0.60	0.3	0.1	1	0	B	2	27.47	0.00	150.5
C36	Titan Type I/II	0.20	1	0.60	0.3	0.1	1	0	B	2	27.47	6.50	150.2

Mix.	Cement Type	w/b	Mix Proportions						Fiber		Admixtures		Density (lb/ft^3)
			ag/cm	*C*	*S*	*SF*	*FA*	*UFR*	*Type*	*Content (%)*	*HRWR (oz./cwt)*	*VMA (oz./cwt)*	
C40	Titan Type I/II	0.17	1	0.6	0.3	0.1	1	0	B	2	29.39	0.00	156.5
C41	Titan Type I/II	0.17	1	0.60	0.3	0.1	1	0	B	2	29.39	9.16	151.6

The mixing procedure for these four mixtures was the same as the other mixtures. But plastic cylinders were cast in different time intervals after completing the mixing process. Two cylinders were cast at three different times after casting (6 cylinder samples for each mixture).

The flow was measured every 10 minutes for 30 to 70 minutes until the flow of the mixture dropped below 6 inches. The flow versus time for these four mixtures is shown in Figure 4.11. The mixture with a w/b of 0.20 had a higher flow over time with VMA than the same mixture without VMA, shown in Figure 4.11 (a). The VMA content did not affect the flow for the mixtures with a w/b of 0.17 and smaller initial flow, shown in Figure 4.11 (b).

All mixtures were slightly agitated by hand mixing at the end of the testing; in all cases, the hand mixing process increased the flow. This shows that UHPC can be agitated (by hand or in a separate mixer) to increase the working time, which would be useful for field applications.

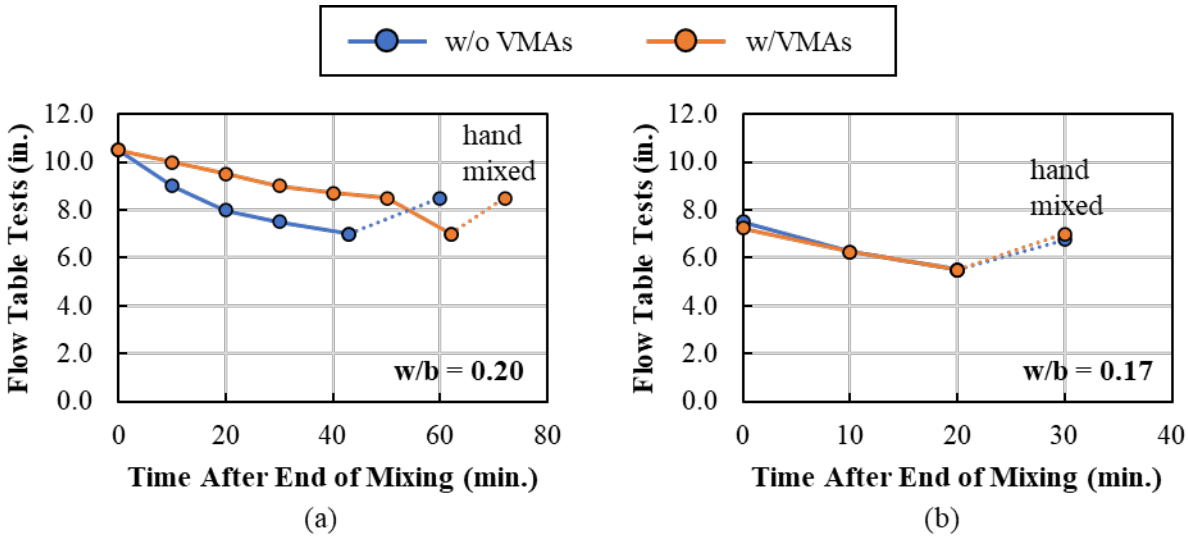

Figure 4.11: Flow versus time for mixtures with and without VMA and (a) w/b of 0.2 and (b) w/b of 0.17

There were only two samples cast for each time after mixing was complete for each w/b, so all the samples for each w/b were tested at the same age: 7 days for w/b of 0.20 and 28 days for w/b of 0.17. The compressive strength of the cylinders plotted versus the time they were cast after the end of the mixing is shown in Figure 4.12. There was a slight increase in compressive strength with time after casting for w/b of 0.20, see Figure 4.12 (a). There was no significant change in compressive strength with time after casting for w/b of 0.17. Similar compressive strengths were observed for specimens with and without VMA for both w/b ratios.

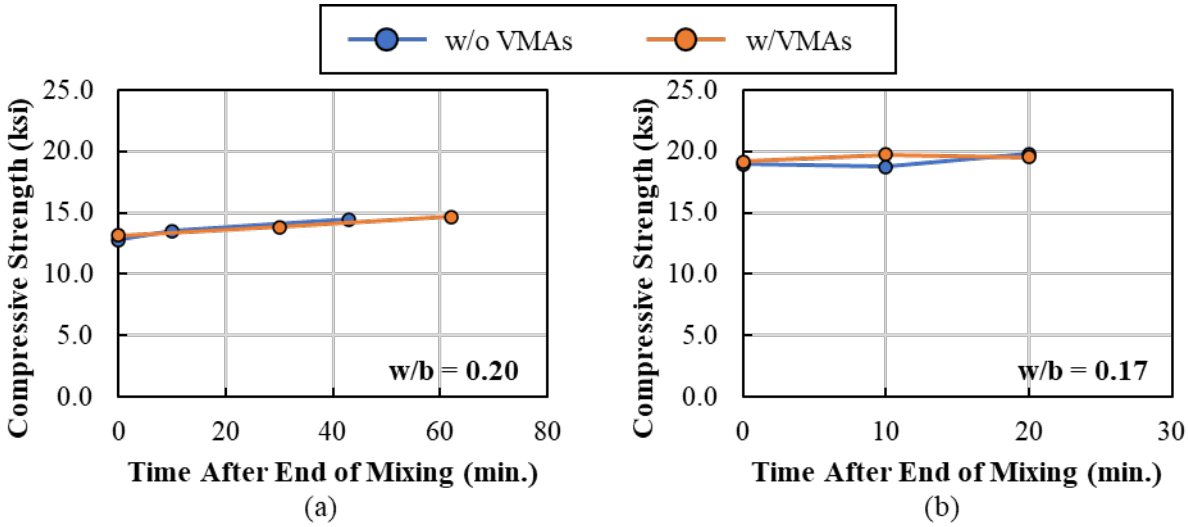

Figure 4.12: Compressive strength versus time after mixing for mixtures with and without VMA and (a) w/b of 0.2 (measured at 7 days) and (b) w/b of 0.17 (measured at 28 days)

4.6.6. Effect of Fiber Type

There are several studies that focused on the effect of different fiber contents ranging from 1 to 5 percent by volume [5], [34], [38], [42], [45]. The most common fiber content used by previous researchers and in field applications is 2 percent by volume. Mixtures with 0 percent fiber content and 2 percent fiber content were investigated in the small-scale batches. The results for 2 percent fibers by volume with different types of fibers are presented in this section.

Four different fiber types were investigated in the small-scale batch mixtures:

- Dramix 4D 65/35BG (A)
- Helix 5-13 Uncoated (H)
- Dramix OL 13/.20 (OL)
- Hiper Fiber Type A (HF)

See Table 2.5 for details on the fiber properties.

Details on the four mixtures used for this comparison are shown in Table 4.11. The base mix design (OPT#1) was used for the comparison. VMA was used in two mixtures containing Helix (H) fibers and Bekaert 4D 65/35BG (A) fibers to stabilize fibers. The recommended dosage by the manufacturer was 10 oz/cwt, but a smaller dosage was found to effectively prevent segregation. Bekaert 4D 65/35BG fibers were the heaviest and most challenging fiber to keep in suspension in the concrete mixture; their anchorage end shape and longer length led to them clumping together in several of the mixtures. The results provided in this section are for mixtures with good fiber distribution.

Table 4.11: Mixture proportions and characteristics for investigation of fiber type (dried sand used in all mixtures)

Mix.	Cement Type	w/b	Mix Proportions						Fiber		Admixtures		Density (lb/ft^3)
			ag/cm	*C*	*S*	*SF*	*FA*	*UFR*	*Type*	*Content (%)*	*HRWR (oz./cwt)*	*VMA (oz./cwt)*	
C5	Titan Type I/II	0.20	1.0	0.60	0.3	0.1	1.0	0	H	2.0	24.72	6.41	146.2
C6	Titan Type I/II	0.20	1.0	0.60	0.3	0.1	1.0	0	A	2.0	24.72	8.24	146.4
C2	Titan Type I/II	0.20	1.0	0.60	0.3	0.1	1.0	0	OL	2.0	22.25	0	144.5
C42	Titan Type I/II	0.20	1.0	0.60	0.3	0.1	1.0	0	HF	2.0	27.47	0	148.6

The flowability and compressive strength for the four mixtures with different fiber types are shown in Figure 4.13. The fiber type did not have a significant effect on the flowability of the mixtures; flowability was kept between around 8 and 10 inches, shown in Figure 4.13 (a). The mixtures contained Hiper Fiber (HF in C42) and Dramix OL 13/.20 (B in C2) showed higher compressive strengths than the other types of fibers, shown in Figure 4.13 (b).

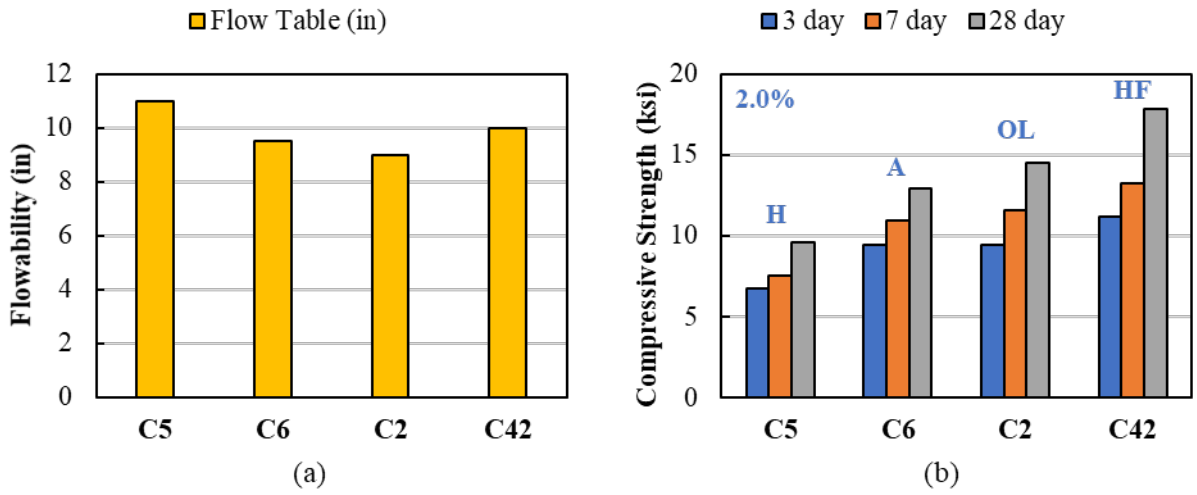

Figure 4.13: Effect of Fiber type on (a) flowability and (b) compressive strength

All mixtures in this group had a reasonable distribution of fibers, with the help of VMA for some of the mixtures. Photographs of a representative cylinder for each mixture after compression failure are shown in Figure 4.14.

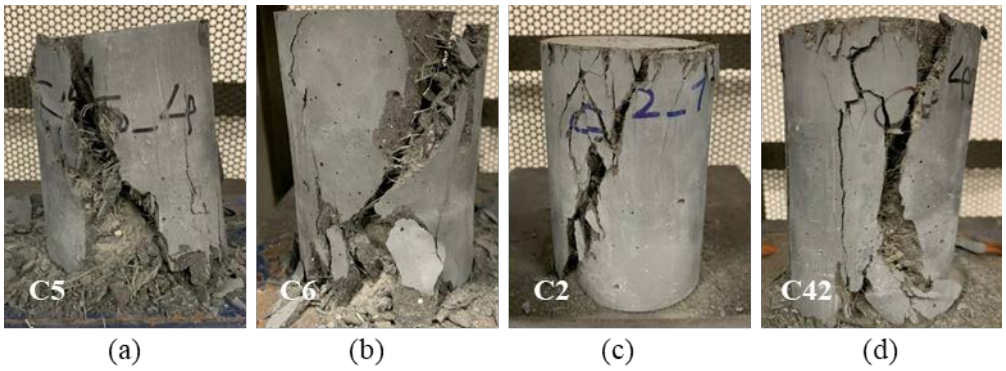

Figure 4.14: Sample cylinders after compressive failure for different fiber types: (a) Helix 5-13, (b) Dramix 4D 65/35BG, (c) OL 13/.20, and (d) Hiper Fiber Type A

The Helix 5-13 Uncoated (H) fibers had a higher zinc content and no brass coating, which led to an expansive reaction between the fibers and UHPC paste for some of the samples, as shown in Figure 4.15. The concrete expanded about 0.5 in. outside the top of the cylinder before demolding, see Figure 4.15 (a). When the cylinder was removed, part of the cylinder broke off the top, see Figure 4.15 (b). The resulting compressive strength was low (5.9 ksi) relative to the samples with other fiber types. A photograph of the cylinder after failure is shown in Figure 4.15 (c). These results suggest that higher zinc content in fibers can negatively affect the mechanical properties of the UHPC mixture. This observation highlights the importance of creating trial mixes before using any new constituents in the mix design.

The manufacturer of the fiber communicated to the research team that the issue has been fixed, but the testing schedule did not allow for new samples to be cast and tested with the improved fibers.

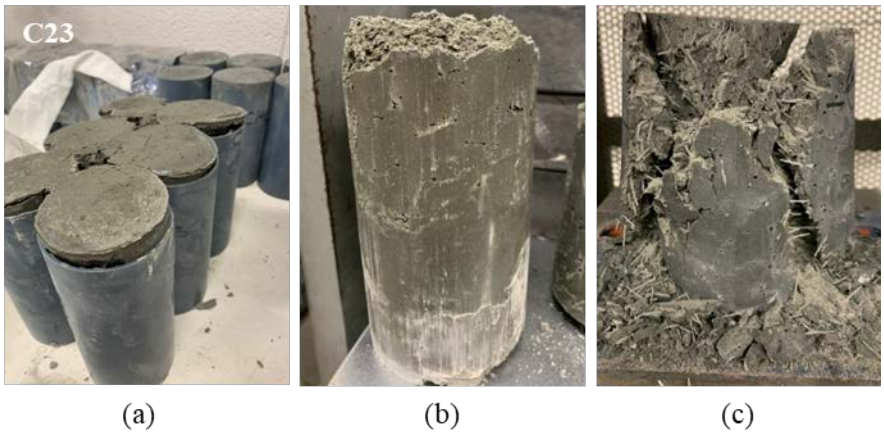

Figure 4.15: Example of expansion caused by concrete mixture reacting with zinc in fibers for C23 (a) before demolding, (b) after demolding before testing, and (c) after testing

Three of the four steel fibers (all but the Helix 5-13 Uncoated) were used in the large-scale batches. A synthetic fiber was also tested in the large-scale batches. This synthetic fiber was obtained later in the research project, so it was only tested in the large-scale batches.

4.6.7. Effect of Fine Aggregate Type and Content

Ultra-fines recovery (UFR) was used in some mixtures to improve the particle packing of the mixture. Its very small size allows it to fill the gap between other coarser particles in the mixture minimizing the porosity and increasing the density. UFR is made of limestone with lower stiffness and strength than quartz particles made of rock crystal quartz. The particle packing analysis showed that replacing 10 to 35 percent of regular sand with UFR brought the base mix distribution curve (OPT#1) closer to the ideal curve (shown in Figure 3.1 and Figure 3.2).

Five mix designs with UFR replacement between 0 and 35 percent were used to determine the effect of UFR on the flowability and compressive strength. A summary of the mix designs is shown in Table 4.12. Adding UFR to the concrete mix increased the total special surface area, which required more HRWR to result in the same flowability.

Table 4.12: Mixture proportions and characteristics for investigation of using ultra-fine recovery (UFR) (dried sand used in all mixtures)

Mix.	Cement Type	w/b	Mix Proportions						Fiber		Admixtures		Density (lb/ft^3)
			ag/cm	*C*	*S*	*SF*	*FA*	*UFR*	*Type*	*Content (%)*	*HRWR (oz./cwt)*	*VMA (oz./cwt)*	
C28	Titan Type I/II	0.20	1.0	0.6	0.3	0.1	1.00	0.00	OL	2.0	21.70	0	147.1
C45	Titan Type I/II	0.20	1.0	0.6	0.3	0.1	0.90	0.10	OL	2.0	27.47	0	146.5
C46	Titan Type I/II	0.20	1.0	0.6	0.3	0.1	0.80	0.20	OL	2.0	27.47	0	148.4
C47	Titan Type I/II	0.20	1.0	0.6	0.3	0.1	0.70	0.30	OL	2.0	29.39	0	147.6
C48	Titan Type I/II	0.20	1.0	0.6	0.3	0.1	0.65	0.35	OL	2.0	29.39	0	147.3

The measured flow and compressive strength for these mixtures with varying UFR amounts and w/b of 0.20 are shown in Figure 4.16. Compressive strength results showed that replacing 10, 20, 30, and 35 percent of sand with UFR increased the 28-strength 7.0, 9.3, 8.9, and 13.6 percent, respectively, compared to the mixtures without any UFR. Although the flow was 8 inches, it was harder to work with the UHPC with a 35-percent UFR replacement.

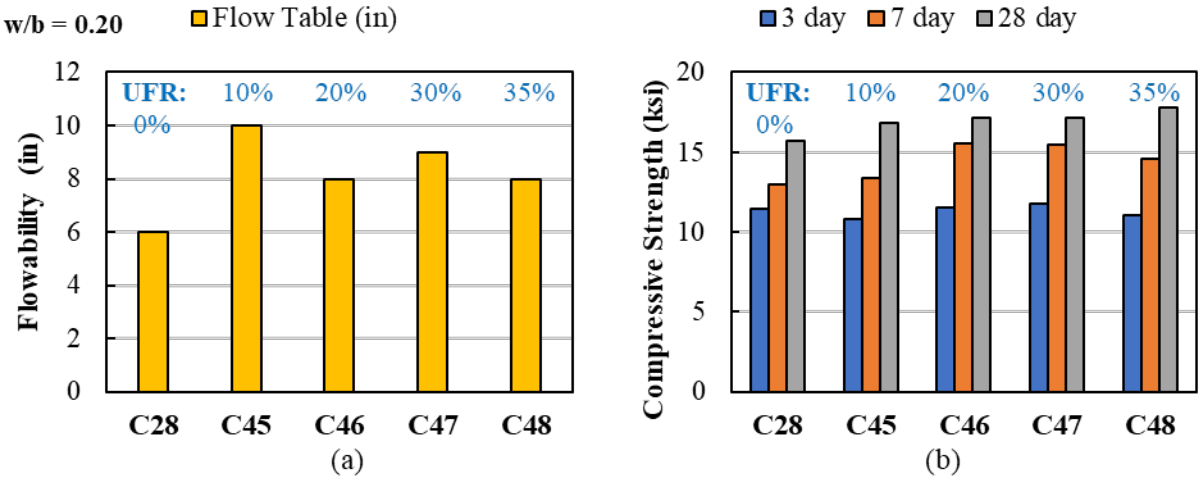

Figure 4.16: Effect of fine aggregate content on (a) flowability and (b) compressive strength (with w/b = 0.20)

Two additional mixtures were cast with a lower w/b and and UFR contents of 20 and 30 percent. Details for these mixtures are provided in Table 4.13.

Table 4.13: Mixture proportions and characteristics for investigation of using ultra-fine recovery (UFR) with w/b of 0.18 (dried sand used in all mixtures)

Mix.	Cement Type	w/b	Mix Proportions						Fiber		Admixtures		Density (lb/ft^3)
			ag/cm	*C*	*S*	*SF*	*FA*	*UFR*	*Type*	*Content (%)*	*HRWR (oz./cwt)*	*VMA (oz./cwt)*	
C28	Titan Type I/II	0.18	1	0.6	0.3	0.1	1.00	0.00	OL	2.0	27.47	0	149.4
C45	Titan Type I/II	0.18	1	0.6	0.3	0.1	0.80	0.20	OL	2.0	38.08	0	150.7
C46	Titan Type I/II	0.18	1	0.6	0.3	0.1	0.70	0.30	OL	2.0	38.08	0	150.8

The measured flow and compressive strength for these mixtures with varying UFR amounts and w/b of 0.18 are shown in Figure 4.17. Compressive strength results showed that replacing 20 and 30 percent of sand with UFR increased the 28-strength 19.1 and 17.6 percent, respectively, compared to the mixtures without any UFR.

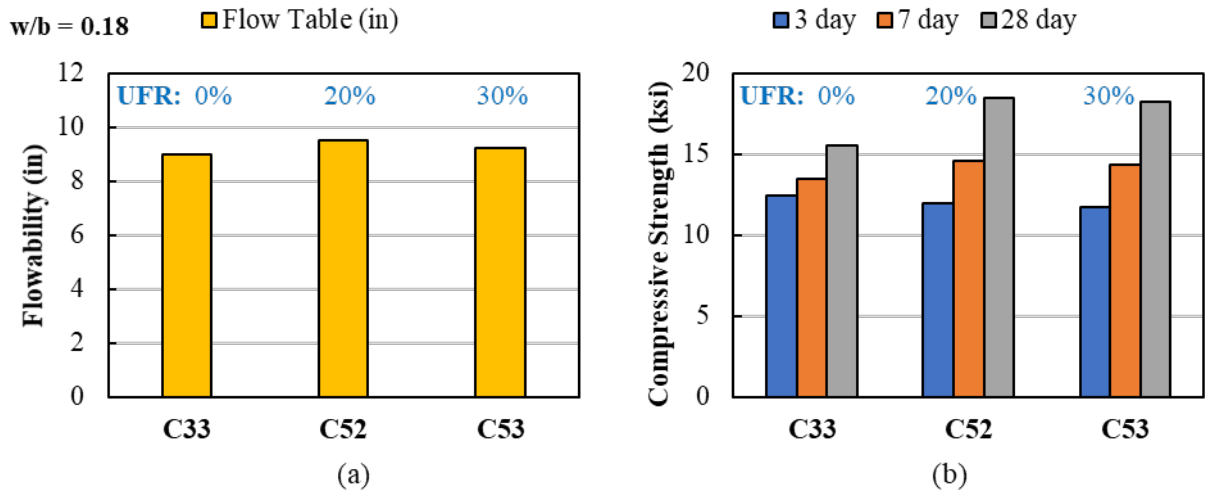

Figure 4.17: Effect of fine aggregate content on (a) flowability and (b) compressive strength (with w/b = 0.18)

A 20 and 30 percent replacement of the fine masonry sand with UFR was found to increase the compressive strength for w/b of 0.18 and 0.20. One large-scale batch with a 30-percent UFR replacement was cast. The other large-scale batches were cast without UFR to be consistent with the base mix design used by the other partner universities in this project.

4.7. Summary and Observations

A total of 690 3 by 6-inch cylinder from 115 0.15-ft^3 batches were cast with different mixture designs. The mixture designs were developed to investigate the effect of aggregate moisture, cement type, water-to-binder ratio, HRWR content, VMA content, fiber type, and fine aggregate type and content on the flow and compressive strength of the UHPC. The following observations were made based on these small-scale batches:

- The fine aggregate moisture content effected the repeatability of the UHPC mixtures. Fine aggregates should be oven dried to ensure consistent material properties can be achieved. This may be difficult for field applications. More research should be done to investigate mixtures with fine aggregates with natural moisture contents.
- Type I/II or Lehigh White cement resulted in similar compressive strengths and workability. Type III cement led to higher compressive strength but shortened the working time for the UHPC.
- A water-to-binder ratio between 0.18 and 0.20 produced the highest compressive strength while maintaining a good flow and working time. The water content in the chemical admixtures can affect the compressive strength and should be considered when determining how much water should be added to a mixture.
- VMA content did not influence the compressive strength. VMA can be used at dosages less than 10 oz./cwt to stabilize heavier steel fibers in the mixtures.
- The use of fibers with 0.5-inch length, 0.008-inch diameter, and tensile strength of 400 ksi led to the highest compressive strengths. This size fiber reasonably distributed in the mixture without the addition of any VMA.
- Uncoated fibers with high zinc contents can lead to an expansive reaction in the UHPC that greatly decreases its strength. This reaction can be observed in small-scale (0.15 ft^3) trial batches.
- Ultra-fines recovery (UFR) materials can replace the fine masonry sand at 20 to 30 percent replacement to increase strengths by 10 to 15 percent. More HRWR is needed for mixtures with UFR to achieve flows between 8 and 10 inches.

These observations were considered when developing the large-scale batches described in the next chapter.

CHAPTER 5. LARGE-SCALE BATCHES

5.1. Introduction

Ten large-scale batches (2.2-ft^3) were used to further evaluate the UHPC mixtures and the effect of fiber type and content on the mechanical properties. A total of 360 3-in. by 6-in. cylinders, 40 4-in. by 8-in. cylinders, 30 6-in. by 12-in. cylinders, and 50 3-in. by 3-in. by 11-in. prisms were cast in this phase to test the compressive strength, modulus of elasticity, splitting tensile strength, flexural strength, shrinkage, set time, and bulk resistivity.

5.2. Mixture Designs for Large-Scale Batches

The mixture design for the large-scale batches was based on the mix design from OU taking into consideration everything learned from the small-scale batches. The ten mixture designs used for the large-scale batches are summarized in Table 5.1. The water-to-binder ratio not considering the water content in the chemical admixtures (w/b) and considering the water content in the chemical admixtures (w*/b) are both shown; see §2.5 for more details on calculating w/b and w*/b. A w/b of 0.2 not considering the water content in the chemical admixtures was selected as the base value to be consistent with OU's mixture design.

Table 5.1: Mix proportions of large-scale batches

Mix.	Fiber Type	Vol. %	w*/b	w/b	Agg./b	C	Slag	SF	Sand	UFR	Cement Type	Glenium (oz/cwt)	VMA (oz/cwt)
L1	OL	2	0.21	0.20	1.00	0.60	0.30	0.10	0.7	0.3	C-T-I/II	29.4	0.00
L2	OL	2	0.21	0.20	1.00	0.60	0.30	0.10	1.0	0.0	C-A-I/II	22.0	0.00
L3	OL	2	0.21	0.20	1.00	0.60	0.30	0.10	1.0	0.0	C-T-I/II	27.5	0.00
L4	OL	2	0.19	0.18	1.00	0.60	0.30	0.10	1.0	0.0	C-T-I/II	27.5	0.00
L5	HF	2	0.21	0.20	1.00	0.60	0.30	0.10	1.0	0.0	C-T-I/II	27.5	0.00
L6	A	1.5	0.21	0.20	1.00	0.60	0.30	0.10	1.0	0.0	C-T-I/II	27.5	4.49
L7	OL	4	0.21	0.20	1.00	0.60	0.30	0.10	1.0	0.0	C-T-I/II	27.5	0.00
L8	HF	4	0.21	0.20	1.00	0.60	0.30	0.10	1.0	0.0	C-T-I/II	27.5	0.00
L9	Sy	2	0.20	0.20	1.00	0.60	0.30	0.10	1.0	0.0	C-T-I/II	27.5	0.00
L10	Sy	1	0.20	0.20	1.00	0.60	0.30	0.10	1.0	0.0	C-T-I/II	27.5	0.00

The mixtures were selected to investigate several different variables:

- L2 is the same material (shipped from Oklahoma) and same mixture design as that used by OU. The results from this mixture will be compared with results from OU in the ABC-UTC Guide document to show variability that may occur based on different people with different experience levels creating the mixture.
- L3 is the same mixture design as OU but using materials from South Florida. The results from this mixture can be compared to the mixture with Oklahoma materials to see the effect of material obtained from different parts of the country with the same mix design. Materials from South Florida were also shipped to OU for them to test at their lab.
- L1 and L4 have the same fiber type and fiber content as L3. L1 has all the same proportions as L3 except with 30 percent UFR replacement of the fine masonry sand. L4 has all the same proportions as L3 except with a w/b of 0.18. These mixtures will give

more insight to the effect of w/b and UFR replacement for mixture sizes that would be used in field applications.

- L3 and the other mixtures not mentioned so far (L5 to L10) were used to investigate the effect of three different steel fibers and one synthetic fiber at two different fiber contents on the mechanical properties of the mixtures. The OU mix design was used as the base mix design for all large-scale batches.

The actual quantity of materials for the 2.2 ft^3 mix was determined using the same procedure described in §4.2, but by taking the amounts per cubic foot times 2.2.

Comparisons are made in the following section based on the test.

5.3. Mixing Procedure

The mixing procedure and sequence of adding UHPC constituents was like the procedure followed for the small-scale batches with a slight variation in the mixing time after the water and chemical admixtures were added.

Before the mixing procedure began, the fine aggregates were all oven dried and stored in sealed containers. The proper amounts of all constituents were measured and stored in five-gallon buckets with lids prior to mixing.

Mixing of the UHPC was done using an Imer Mortarman vertical shaft paddle mixer (MIX 750 MBP). This mixer has a specified capacity of 27 ft^3 and specified batch output of 17 ft^3, but the actual amount of UHPC that can be mixed is less than the specified capacities due to the increased mix energy required by UHPC. The amount of UHPC mixed for this project was 2.2 ft^3; this mixer has been used in other projects to successfully mix up to 2.5 ft^3.

First, all the dry materials were added through the top of the paddle mixer and allowed to mix for 10 minutes, shown in Figure 5.1 (a). The water and chemical admixtures were then added slowly to the dry mixture, shown in Figure 5.1 (b), and allowed to mix until the powder material became a flowable paste. It typically took 10 to 20 minutes for the mixture to become a flowable paste. Like the small-scale batches, the fibers were added to the mixture once the concrete paste was produced and allowed to mix for an additional 2 minutes, shown in Figure 5.1 (c).

(a) (b) (c)

Figure 5.1: Sequence of adding material, (a) adding dry constituents and mix for 10 minutes, (b) adding water and chemical admixtures, and (c) adding fibers

The UHPC was then poured into five-gallon buckets and used for the flow table test and to create all the samples required for the testing program. Photographs from the sample fabrication and flow table tests are shown in Figure 5.2. A cart with all the samples from one of large-scale batches is shown in Figure 5.2 (e).

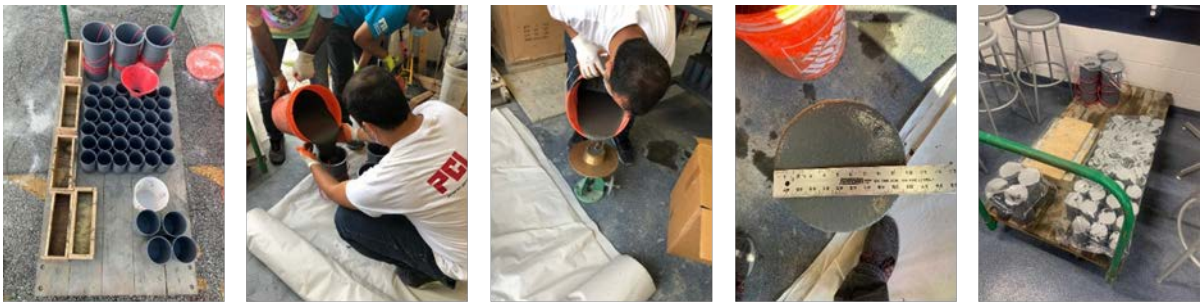

Figure 5.2: Sampling process: (a) preparing plastic and wooden molds, (b) casting samples, (c) fresh concrete flowability test, (d) spread flow, and (e) storing samples

5.4. Curing and Storage

The effect of curing conditions on the final compressive strength was investigated by storing half of the 3 by 6-inch cylinder samples in a lime water bath 24 hours after casting until test day. The rest of the samples were capped and kept in a temperature-controlled room until they were demolded 24 hours before testing.

5.5. Test Procedures

5.5.1. Flowability

The flowability tests for the large-scale batches were performed using the same procedure described in §4.5.1.

5.5.2. Setting Time

The setting time of UHPC mixtures was determined using mortar penetration tools according to ASTM C403/C2403M-16 (Time of Setting of Concrete Mixtures by Penetration Resistance) [66]. According to ASTM C403/C2403M-16, a cylinder container with a minimum 6-in. diameter and 6-in. height is required for the setting time test. For measuring the initial and final setting time of non-proprietary UHPC concrete, a 2-gallon bucket with 10-in. diameter and 10-in. height was used. The bucket was filled up to 80 percent height of bucket (around 8 in.) immediately after the mixing process was concluded and stored in a temperature-controlled room. Then, at specific intervals of 30 minutes or 60 minutes, the resistance of the UHPC mix to penetration was measured using standardized needles designed for the test, shown in Figure 5.3 (a). Two samples after the end of testing are shown in Figure 5.3 (b) and (c).

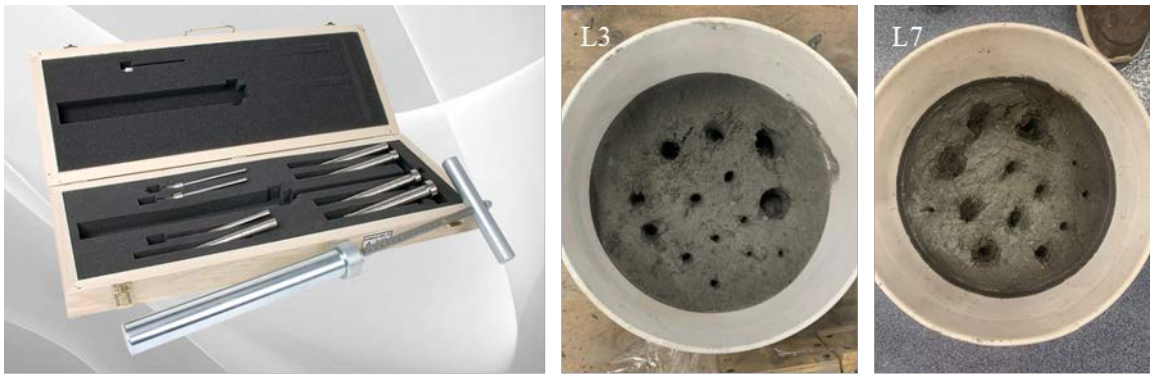

Figure 5.3: Setting time test; (a) testing apparatus [81], (b) sample left from L3, and (c) sample from L7

Sample data from the setting time test for L4 is shown in Table 5.2. The time of measurement, needle size, and resistance penetration load measured using the testing apparatus are needed to calculate the mortar resistance. The mortar resistance can be found simply by dividing the resistance penetration load by the cross-sectional area of the head of the needle.

Table 5.2: Sample data for setting time measurement (example: L4)

Time (min.)	Needle Diameter (#)	Needle Area (in^2)	Resistance Penetration Load (lbf)	Mortar Resistance (psi)
0	#1	1.0	0	0
60	#1	1.0	2	2
120	#1/2	0.5	10	20
180	#1/2	0.5	20	40
240	#1/4	0.25	110	440
300	#1/10	0.1	90	900
360	#1/20	0.05	100	2000
420	#1/40	0.025	80	3200
480	#1/40	0.025	100	4000

The mortar resistance plotted versus time for L4 is shown in Figure 5.4. The standard definition for initial and final setting time is the time required for the concrete to reach specified resistance values to penetration: 500 psi and 4000 psi for initial and final set, respectively. The initial and final setting time are highlighted as 250 minutes and 480 minutes, respectively, in Figure 5.4 for the example data provided for L4. A linear interpolation was used between measurements taken at 240 minutes and 300 minutes to determine the approximate time when the mortar resistance reached 500 psi.

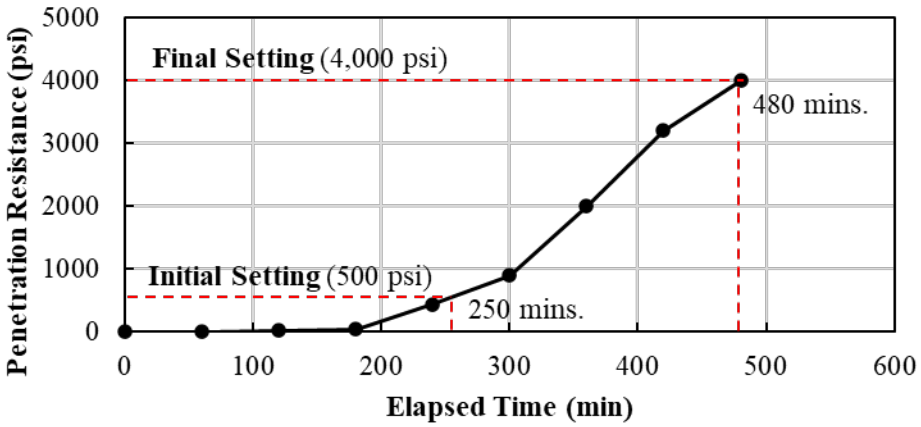

Figure 5.4: Example of initial and final setting time for L4

A similar procedure was used to determine the setting time for all large-scale batches.

5.5.3. Compressive Strength

The compressive strength tests for the large-scale batches were performed using the same procedure described in §4.5.2.

5.5.4. Modulus of Elasticity

The modulus of elasticity test was conducted in accordance with ASTM C469/C469M − 14 (Static Modulus of Elasticity and Poisson's Ratio of Concrete in Compressive) [63]. The modulus of elasticity of 3 in. by 6 in. cylinder samples was determined within the typical working stress range of 0 to 40 percent of the ultimate concrete strength. The compressive test machine was used to apply load at a constant rate (36.3±7 psi/s) until an applied load between 40 and 50 percent of the ultimate strength was reached. This test was done for concrete samples at 28 days for six samples (3 moist cured samples and 3 uncured samples) per batch.

All cylinders were prepared the same way as for the compressive strength cylinders, shown in Figure 4.5 and discussed in §4.5.2. Two samples were first tested in compression to determine the ultimate compressive strength of the mix. This tested strength was used to determine the 40-percent load for the modulus of elasticity testing.

The test setup for the modulus of elasticity testing is shown in Figure 5.5 (a) with a closer view of the instrumented specimen in Figure 5.5 (b). A compressometer/extensometer device with two linear strain conversion transducers (LSCT) was used to measure the longitudinal and diagonal deflections during the test, shown in Figure 5.5 (c). A basic data acquisition system, shown in Figure 5.5 (d), was used consisting of the LSCT sensors, a 250-kip capacity load cell, measurement hardware, a Campbell Scientific CR6 datalogger, and a computer with programmable software were used to collect data on load and deflection during the modulus of elasticity tests, shown in Figure 5.5 (e). Three load cycles were applied on each of the 3 in. by 6 in. cylinder samples to minimize the measurement errors during the acquisition of data.

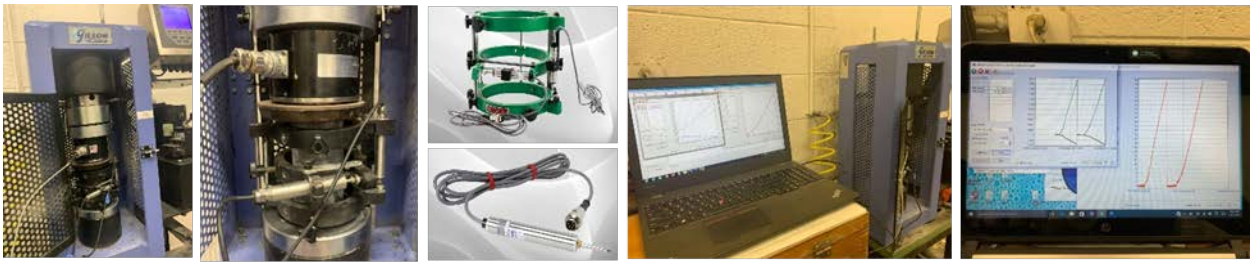

Figure 5.5: Modulus of elasticity test setup; (a) compression machine with instrumented sample, (b) closer view of instrumented sample, (c) compressometer/extensometer with LSCT [82], (d) data acquisition system, and (e) sample measured load and deflection

Data was collected at a frequency of 10 Hz, which led to large data files for each test. The data was analyzed and reduced by taking the average of specific increments of data; this helped to reduce file sizes and eliminate noise in the dataset. The reduced data was compared to the original data to ensure that the reduced data properly represented the original data set. A sample of original and reduced data is shown in Figure 5.6 for L1-21-2.

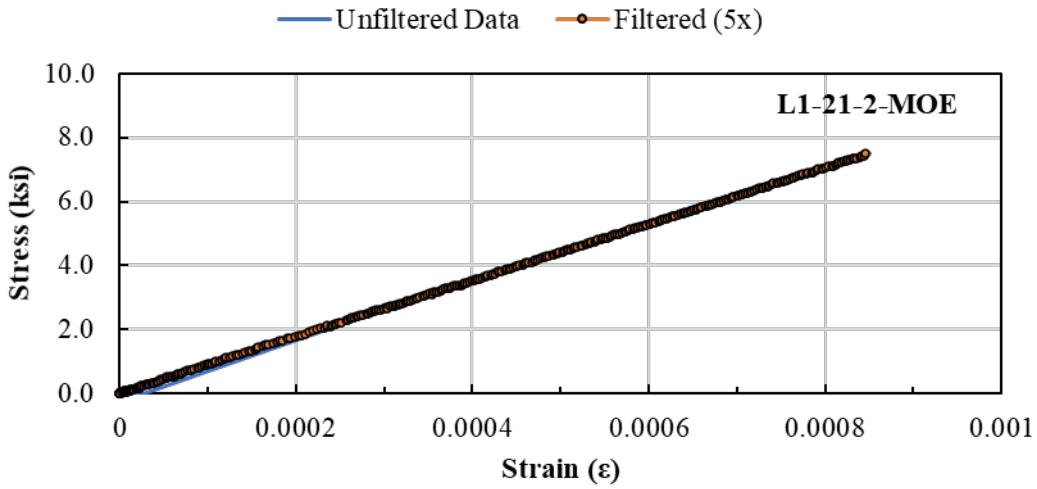

Figure 5.6: Example of noise and data reduction process for modulus of elasticity test

The data from the three tests was used to determine the modulus of elasticity using Equation 5-1 from ASTM C469/C469M [63]. The average of the three calculated modulus of elasticity values was recorded as the measured value for that sample.

$$E_c = \frac{S_2 - S_1}{\varepsilon_2 - 0.000050} \qquad \textit{Equation 5-1}$$

where:

E = chord modulus of elasticity, (ksi)

S_2 = stress corresponding to 40% of ultimate load, (ksi)

S_1 = stress corresponding to a longitudinal strain, ε_1, of 50 millionths, (ksi)

ε_2 = longitudinal strain produced by stress S_2

The values required for Equation 5-1 were determined based on the measured data for each test; an example is shown in Figure 5.7 (a) for sample L1-21-2. The calculation for the modulus of elasticity for this sample is provided below as an example.

Using Equation 5-1:
$$E_c = \frac{S_2 - S_1}{\varepsilon_2 - 0.00005} = \frac{7.55\ ksi - 0.48\ ksi}{0.000847 - 0.00005} = 8{,}865\ ksi$$

The modulus of elasticity was also determined based on the slope from a linear regression of the data within the range up to 40 percent of the ultimate compressive strength, as shown in Figure 5.7 (b). The stiffness for L1-21-2 was found to be 8,809 ksi using the slope of the linear regression.

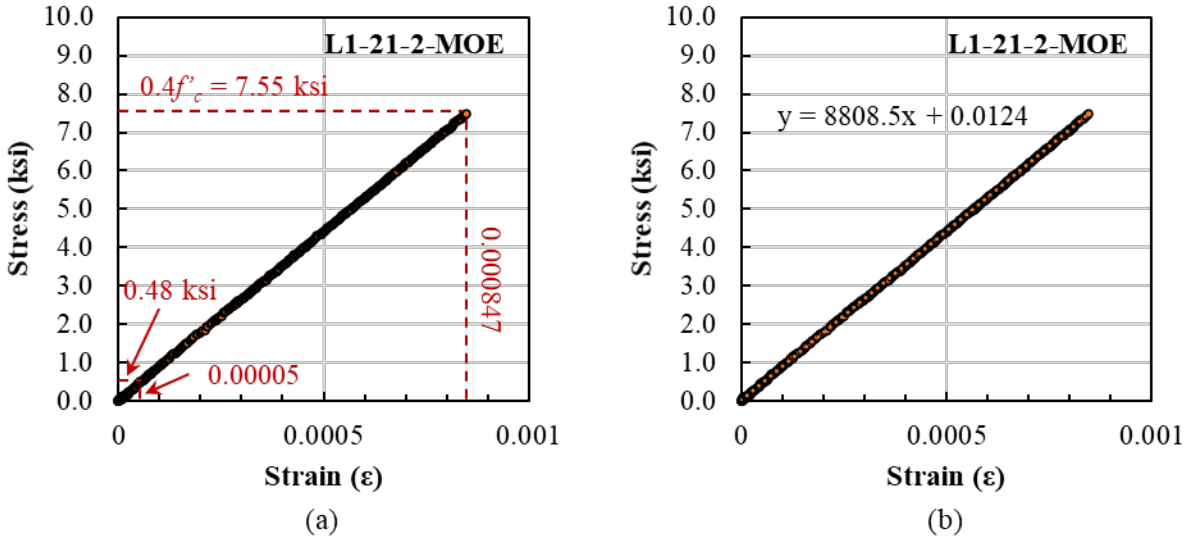

Figure 5.7: Procedures for determining modulus of elasticity with (a) ASTM C469 and (b) linear regression of measured data (L1-21-2)

The value from ASTM C469 was recorded as the modulus for the sample. The slope from the linear regression was used to verify the results from the ASTM C469 calculations.

5.5.5. Splitting Tensile Strength

The splitting tensile strength (f_{sp}) was determined using ASTM C496/C496M−17 (Splitting Tensile Strength of Cylindrical Concrete Specimens) [64]. The splitting tensile strength test is an indirect way to measure the tensile strength of concrete samples. The compression applied along the long side of a concrete cylinder causes transverse tension to develop along the length of the sample, as shown in Figure 5.8 (a). Splitting tensile strength is usually greater than direct tensile strength (f_t) and less than flexural strength (f_r).

All cylinders were prepared using the same end grinding procedure performed on the cylinders for compression tests, shown in Figure 4.5 and discussed in §4.5.2. The length of the cylinders

was measured in three locations and diameter measured in two directions using calipers. The weight of the cylinders was also measured prior to testing. These values were all hand recorded on a testing sheet.

The test setup used for the splitting tensile strength is shown in Figure 5.8 (b). Steel filler plates were used to decrease the space in the compression testing machine. Wood paint strips were placed on the top and bottom of a 3 by 6-inch cylinder laying on its side. The load was applied until the cylinder split in half, as shown in Figure 5.8 (c) through (e).

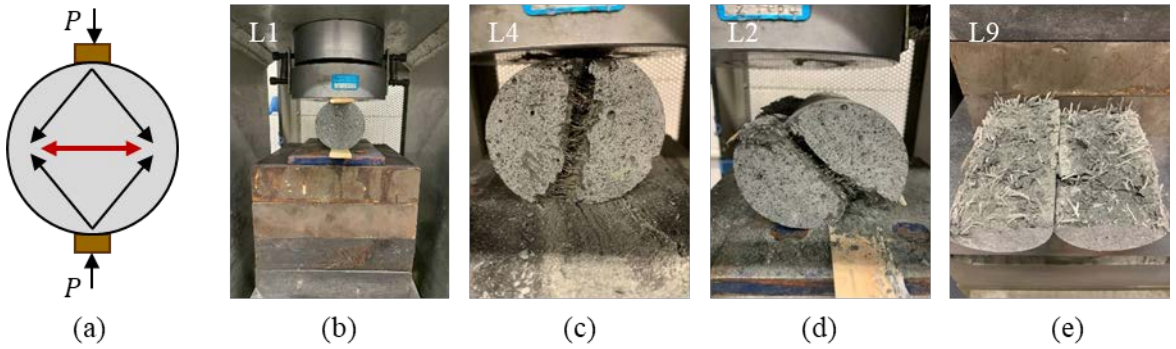

Figure 5.8: Split cylinder test, (a) stress flow in test, (b) test setup with wood bearing strips along length, (c) splitting failure from L4 with steel fibers, (d) splitting failure from L2 with steel fibers, and (e) splitting failure of L9 with synthetic fiber

The maximum applied load was recorded on the testing sheet for each of the samples. All specimen details and test results were collected in a test records spreadsheet, where the splitting tensile strength was calculated using Equation 5-2, from ASTM C496/C496M−17 [64].

$$f_{sp} = 2P/\pi ld \qquad \textit{Equation 5-2}$$

where:

f_{sp} = splitting tensile strength (ksi)

P = maximum applied load by the testing machine (kips)

l = length (in.)

d = diameter (in,)

Examples for some of the splitting tensile strength tests for L4 are shown in Table 5.3.

Table 5.3: Splitting cylinder test for L4

Mix/Cylinder ID:	**L4-SP1**	**L4-SP2**	**L4-SP3**	**L4-SP4**	**L4-SP5**	**L4-SP6**
Curing Condition	Not Cured			Moist Cured		
Weight [lb]:	3.091	3.481	3.4295	3.1645	3.204	3.185
Length of Cylinders [in]:	5.003	5.582	5.497	5.109	5.130	5.123

Mix/Cylinder ID:	L4-SP1	L4-SP2	L4-SP3	L4-SP4	L4-SP5	L4-SP6
	5.014	5.588	5.497	5.102	5.131	5.128
	5.008	5.583	5.501	5.107	5.132	5.126
Diameter of Cylinders [in]:	3.000	3.006	3.003	3.004	3.007	3.003
	3.003	3.009	3.006	3.007	3.006	3.005
Ultimate Load [kips]:	74.2	68.73	69.63	72.1	67.93	68.22
Splitting tensile strength [ksi]	3.14	2.60	2.68	2.99	2.80	2.82

An example of how the tensile splitting strength was calculated for L4-SP1 is shown below. The average length and average diameter are used in the calculation.

$$f_{sp} = \frac{2P}{\pi l d} = \frac{2(74.2\ kips)}{\pi\left(\frac{5.003" + 5.014" + 5.008"}{3}\right)\left(\frac{3.003" + 3.000"}{2}\right)} = 3.14\ ksi$$

This was done for all the tensile splitting strength specimens.

5.5.6. Modulus of Rupture

The modulus of rupture test was conducted in accordance with ASTM C78/C78M – 18, Flexural Strength of Concrete (Using Simple Beam with Third-Point Loading) [62].

Five 3 in. by 3 in. by 11 in. prism specimens were cast using wooden formworks for each large-scale batch, as shown in Figure 5.9 (a) and (b). Before filling the formwork with fresh concrete, all internal faces were coated with a thin layer of form oil to make the later demolding process easier. All samples were filled with fresh UHPC concrete immediately after the mixing process. The top open face of filled formworks was covered with a plastic sheet immediately after casting. All samples were stored in a temperature-controlled room until 24 hours before testing. A day before testing, they were demolded, measured, and weighted.

A four-point loading test setup according to ASTM C78 was used, as shown in Figure 5.9 (c) through (e). The loading blocks and support blocks were designed so that forces were applied to the beam perpendicularly to the side faces of the beam and applied without eccentricity. The compressive test machine was again used to apply load at a constant rate between 125 and 175 psi/min until it reached its ultimate flexural strength. Two LSCT sensors and a 250-kip loadcell were connected to the CR6 data acquisition system to measure load and displacement during the test. LSCT sensors were placed on both sides of the specimen at midspan to measure the average midspan deflection during testing.

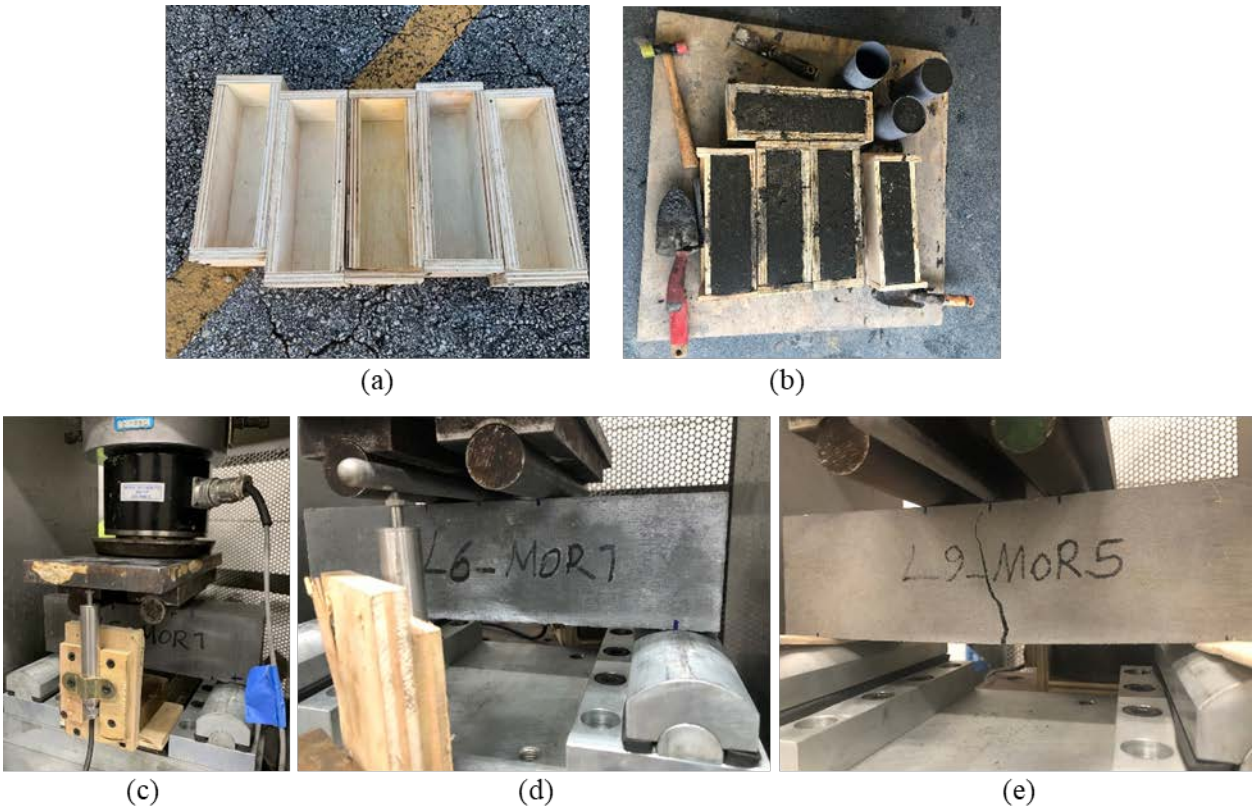

Figure 5.9: Modulus of rupture test; (a) wooden formworks, (b) filled specimens with fresh UHPC, (c) test setup, (d) LSCT sensor reads the mid-span deflection, and (e) typical flexural failure of beams

The width and depth of the specimens across one of the fractured faces were measured after conducting the test. Three measurements were taken at different locations to determine the average width and the average depth. The modulus of rupture was calculated for each sample using Equation 5-3 for failures in the middle third and Equation 5-4 for failures outside the middle third by not more than 5 percent of the span length.

Failure in middle third of span: $$R = \frac{PL}{bd^2}$$ *Equation 5-3*

Failure outside middle third of span (by not more than 0.05L): $$R = \frac{3Pa}{bd^2}$$ *Equation 5-4*

where:

R = modulus of rupture, (ksi),

P = maximum applied load indicated by the testing machine, (kips),

L = span length, (in.),

b = average width of the specimen, (in.), at the fracture.

d = average depth of the specimen, (in.), at the fracture.

a = average distance between the line of fracture and the nearest support measured on the tension surface of the beam, (in.).

Modulus of rupture test data was collected through the data acquisition system. All modulus of ruptures were calculated based on the unfiltered stored data. The filtered data was used for creating the comparison plots, to remove noise and decrease file sizes. Filtered data, unfiltered data, and strain after crack behavior of UHPC for L6-MOR3 are shown in Figure 5.10.

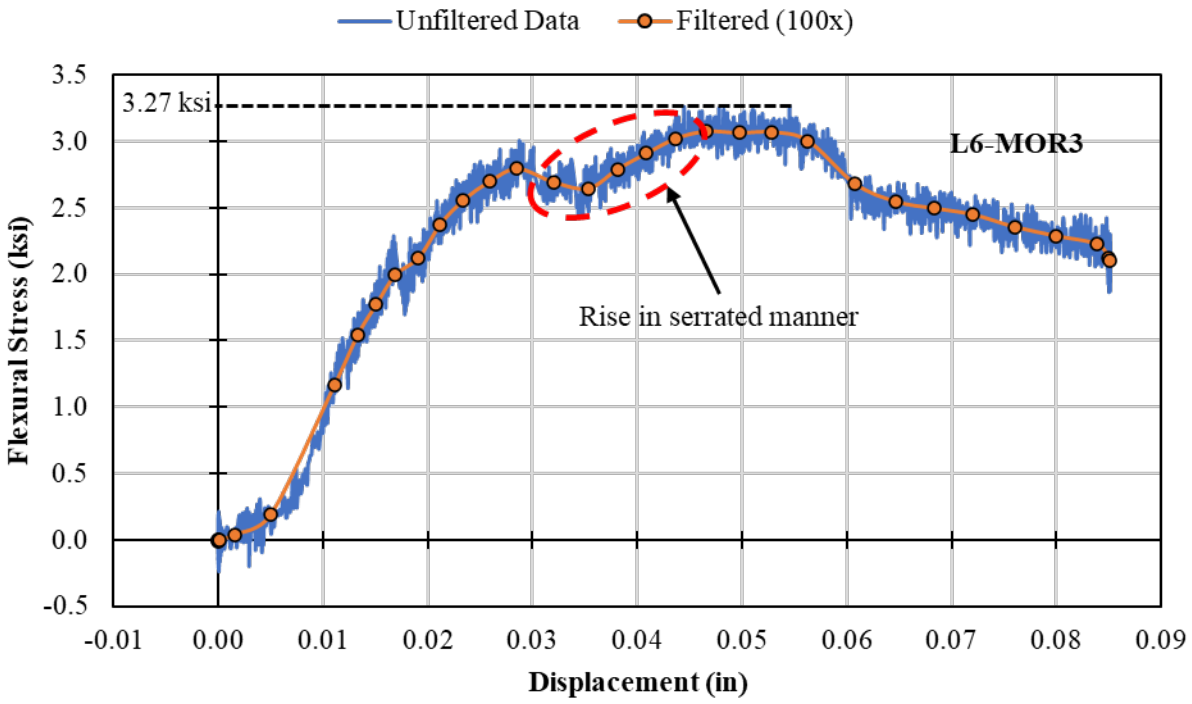

Figure 5.10: Example of modulus of rupture – L6-MOR3

The failures occurred in the middle third of the span length for all samples, so Equation 5-3 was used for calculating the modulus of rupture. An example of how the modulus of rupture was calculated for L6-MOR3 is shown below:

Using Equation 5-3: $$R = \frac{PL}{bd^2} = \frac{(8.22\ kips)(10.989")}{(3.0030")(3.0305")^2} = 3.27\ ksi$$

This procedure was done for all the modulus of rupture specimens for all large-scale batches.

5.5.7. Bulk Resistivity

The durability of UHPC has been investigated in several different studies. Alkali-silica reaction tests, freeze-thaw tests, chloride ion penetrability tests, and electrical and surface resistivity tests have all been used by previous researchers [8], [37], [83]. The electrical bulk resistivity test was used to determine the long-term durability of the UHPC in this study, based on available equipment.

ASTM C1760-12 [60] was used to determine the bulk electrical conductivity of the saturated specimens of hardened UHPC to provide a rapid indication of the resistance of the concrete to the penetration of chloride ions. Saturated cylinder samples (4 in. by 8 in.) were tested to measure the electrical current based on a constant potential difference of 60V across their ends. After 24 hours of casting, cylinder samples were demolded, ground at both ends, and measured (length and dimeter).

The resistivity of the samples was measured at different ages (3, 7, 14, 28, 56, and 90 days) using a Resipod Concrete Resistivity Meter, which has a wide range of resistance measurements (1 to 1,000 kΩ-cm), shown in Figure 5.11 (a). The maximum range of the device (1,000 kΩ-cm) controlled for several of the specimens. Electrical plates with conductive foam inserts were placed at each end of the 4 in. by 8 in. concrete cylinder samples and connected to the meter through cables, shown in Figure 5.11 (b).

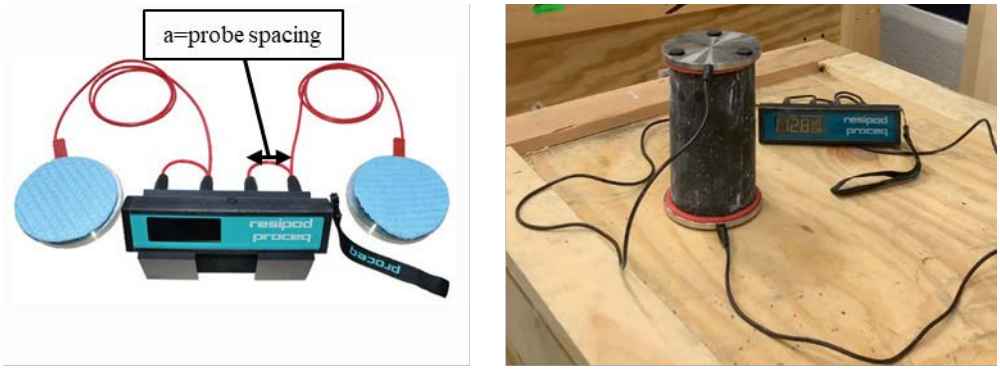

Figure 5.11: Bulk resistivity test; (a) resistivity meter device and attachments [84] and (b) test setup

The current was measured after 60 seconds of applying potential difference. The measured dimension was used to calculate the bulk resistivity using Equation 5-5 from Proceq Resipod User Manual [64], which simplifies to Equation 5-6.

$$\rho = \left(\frac{R_{Cylinder}}{2\pi a}\right)\left(\frac{A}{L}\right) \qquad \text{Equation 5-5}$$

Simplified to:

$$\rho = R_{Cylinder}\left(\frac{d^2}{8aL}\right) \qquad \text{Equation 5-6}$$

where:

$R_{cylinder}$ = measured value of resistivity by Resipod (kΩcm)

a = probe spacing (1.5 in. [3.8 cm], specified in the Resipod manual [85])

d = diameter of the sample (in.)

A = cross sectional area of tested cylinder (in.^{2})

L = length of the sample (in.)

A sample result for the bulk resistivity of cylinder samples is summarized in Table 5.4.

Table 5.4: Example of bulk resistivity test- L4

Test #:	**L4**					
Cylinder ID:	L4-4×8-1					
Mass of Cylinder before Capping [lb]:	7.95					
Length of Cylinders [in]:	7.2970					
	7.2900					
	7.2725					
Diameter of Cylinders [in]:	3.9890					
	3.9900					
Age [day]	3	7	14	28	56	90
K [A/L, in]:	1.72					
$R_{Cylinder}$ [kΩ-cm]:	15.5	30.1	43.1	71.2	141.8	248.9
Bulk Resistivity ρ [kΩ-cm]:	2.83	5.49	7.86	12.99	25.88	45.42

An example of how the bulk resistivity of cylinder samples of L1 at 3 days was calculated is shown below. The measurement is taken in kΩcm, using a in cm converts the data to kΩ-in.

$$\rho = R_{Cylinder}\left(\frac{d^2}{8aL}\right) = (15.5\ k\Omega.cm)\left[\left(\frac{\left(\frac{3.9890" + 3.9900"}{2}\right)^2}{8(1.5")\left(\frac{7.2970" + 7.2900" + 7.2725"}{3}\right)}\right)\right] = 2.83\ k\Omega.cm$$

This procedure was done for all the bulk resistivity samples for all large-scale batches.

5.5.8. Shrinkage

The shrinkage test was according to ASTM C157/C157M – 17 (Length Change of Hardened Hydraulic-Cement Mortar and Concrete). GEOKON vibrating wire embedment strain gauges (VWSG) designed for direct embedment in concrete were used to measure the strain variation of concrete due to total shrinkage. Three 6 in. by 12 in. cylinder samples with one vertically-oriented VWSG at the center of the sample were used for the shrinkage tests. A photograph of the VWSG, location of the VWSG in the cylinder, and photograph of the installed VWSG before cylinder casting are shown in Figure 5.12. Steel wire was used to hold the VWSG in the correct location during cylinder casting.

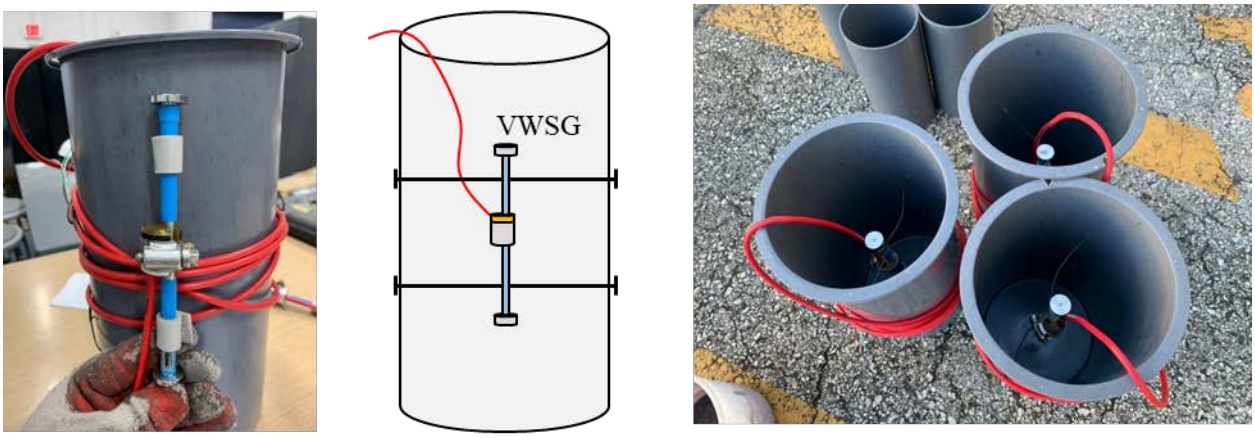

Figure 5.12: Shrinkage test; (a) Geokon Model 4200 VWGS, (b) schematic installation of the sensor, and (c) prepared samples

The UHPC samples were demolded 24 hours after casting and sensors were attached to a data acquisition system to continuously monitor the data after casting. These samples were stored in a climate-controlled room at temperatures between 71°F and 75°F. Photographs of the cylinders attached to the data acquisition system are shown in Figure 5.13.

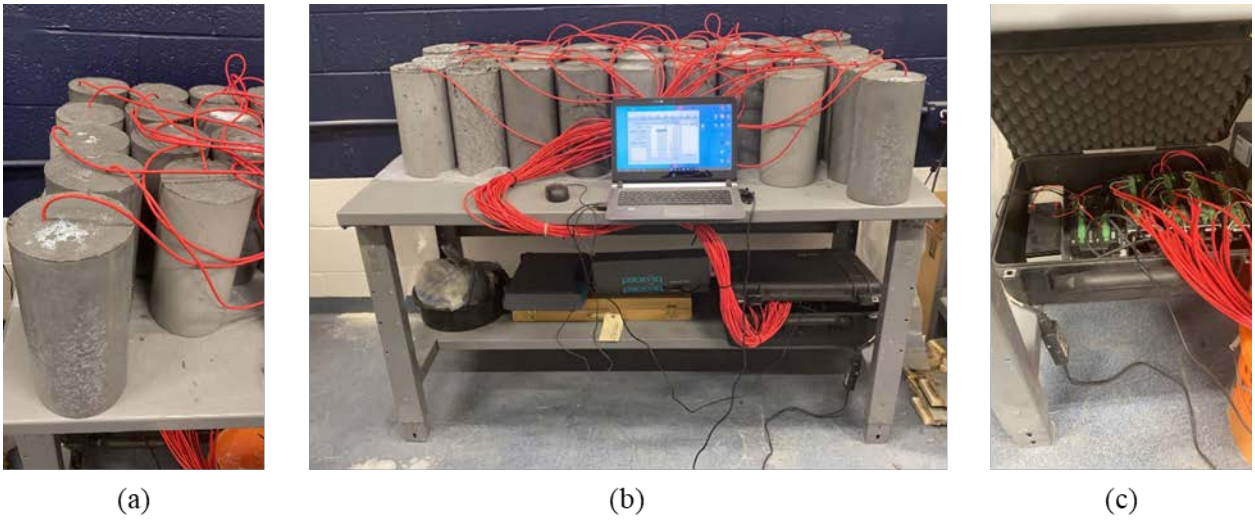

Figure 5.13: Shrinkage test; (a) shrinkage samples with embedded VWSG sensors, (b) test setup, and (c) data acquisition system

The beginning strain in the VWSG was set as zero strain; all subsequent strains are the total shrinkage that occurs in the sample. The data was reduced using the average of a specific interval of data points to reduce noise and file sizes. The reduced data was compared to the original dataset to ensure the reduced data represented the original data well. An example of data from a shrinkage test for L4 is shown in Figure 5.14.

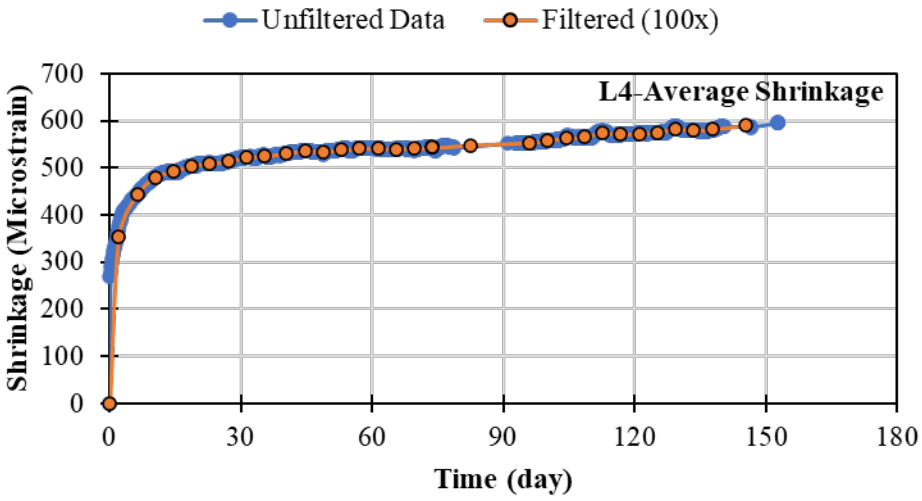

Figure 5.14: Shrinkage example (L4-2% OL fibers)

A similar procedure was followed for all large-scale batches.

5.6. Evaluation of Large Batches

The tests described in the previous section were performed on all ten of the large-scale batches shown in Table 5.1. Results are organized by test. Discussion of results is divided into two groups for most tests:

- *Group I – Effect of Fiber Content*: This group includes L3 and L5 to L10. All mixes in this group were made using the same mix proportions, HRWR dosage, and w/b, but with different fiber types and fiber contents.
- *Group II – Effect of w/b and UFR*: This group includes L1, L3, and L4 to study the effect of w/b and using UFR. The fiber type and fiber content were kept the same for all mixes in this group.
- *Group III – Effect of Material Source*: This group compares L2 and L3 to see the influence of the source of the material. L2 materials were shipped from Oklahoma. L3 materials were obtained from local suppliers in south Florida.

More details of all conducted tests are provided in §5.5.

5.6.1. Flowability Results

The base HRWR dosage (27.5 oz./cwt.) was modified for some of the mixtures to get between an 8- and 10-inch spread flow. The flowability for all of the mixtures is shown in Figure 5.15. L4 had less flowability than mixtures with similar HRWR contents due to its lower w/b ratio (0.18 compared to 0.2 for other mixtures). Additionally, higher fiber contents led to less flowability than other mixtures; seen by comparing the similar mixtures with 2 and 4 percent fibers.

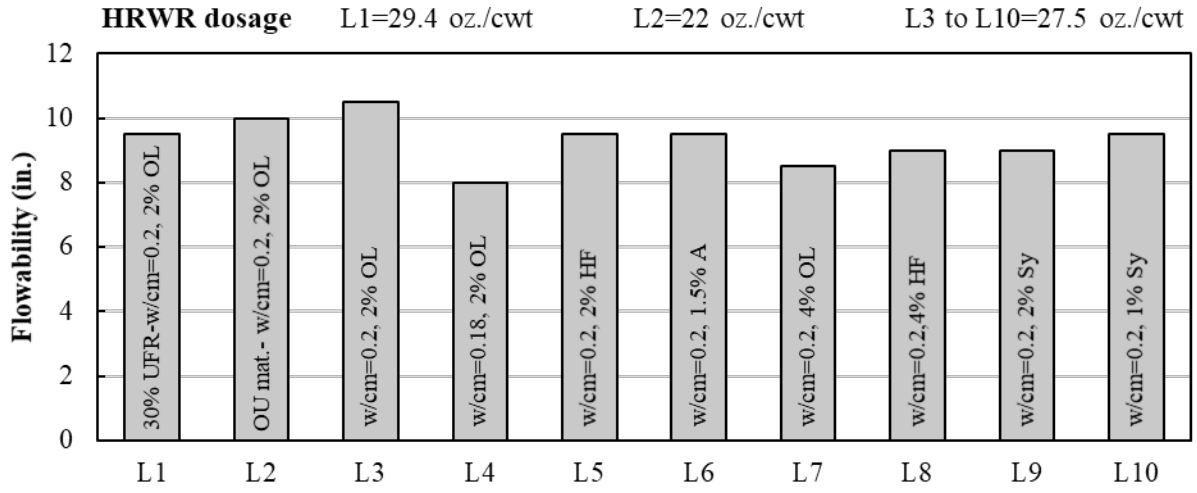

Figure 5.15: Measured flowability of large batches with HRWR dosage (oz./cwt)

5.6.2. Setting Time Results

The setting time of all ten large batches was measured by penetrating special needles and recording the penetration resistance, as described in §5.5.2. The calculated initial and final setting times for all large-scale batches are shown in Table 5.5.

Table 5.5: Initial and final set time for all large-scale batches

Mixture	*L1*	*L2*	*L3*	*L4*	*L5*	*L6*	*L7*	*L8*	*L9*	*L10*
w/b	0.20	0.20	0.20	0.18	0.20	0.20	0.20	0.20	0.20	0.20
Sand:UFR	0.7:0.3	1:0	1:0	1:0	1:0	1:0	1:0	1:0	1:0	1:0
Fiber Type	OL	OL	OL	OL	HF	A	OL	HF	Sy	Sy
Fiber Content	2.0	2.0	2.0	2.0	2.0	1.5	4.0	4.0	2.0	1.0
Initial Set (hr)	6.3	5.8	5.5	4.1	5.2	5.1	5.0	4.3	4.6	4.6
Final Set (hr)	11.0	9.0	10.0	8.0	11.0	10.0	9.0	9.5	10.5	11.5

The penetration stress versus time for the mixtures with different fiber type and fiber contents are shown in Figure 5.16. The mixtures with higher fiber contents had shorter final set times. As an example, mixtures with 4 percent OL fibers (L7) had final set time of 9.0 hrs. compared to 10.0 hrs. for 2 percent OL fibers (L3). A similar comparison can be made for mixtures with HF fibers (L5 for 2 percent and L8 for 4 percent) and with Sy fibers (L10 for 1 percent and L9 for 2 percent). There was no clear correlation between fiber content and initial set time.

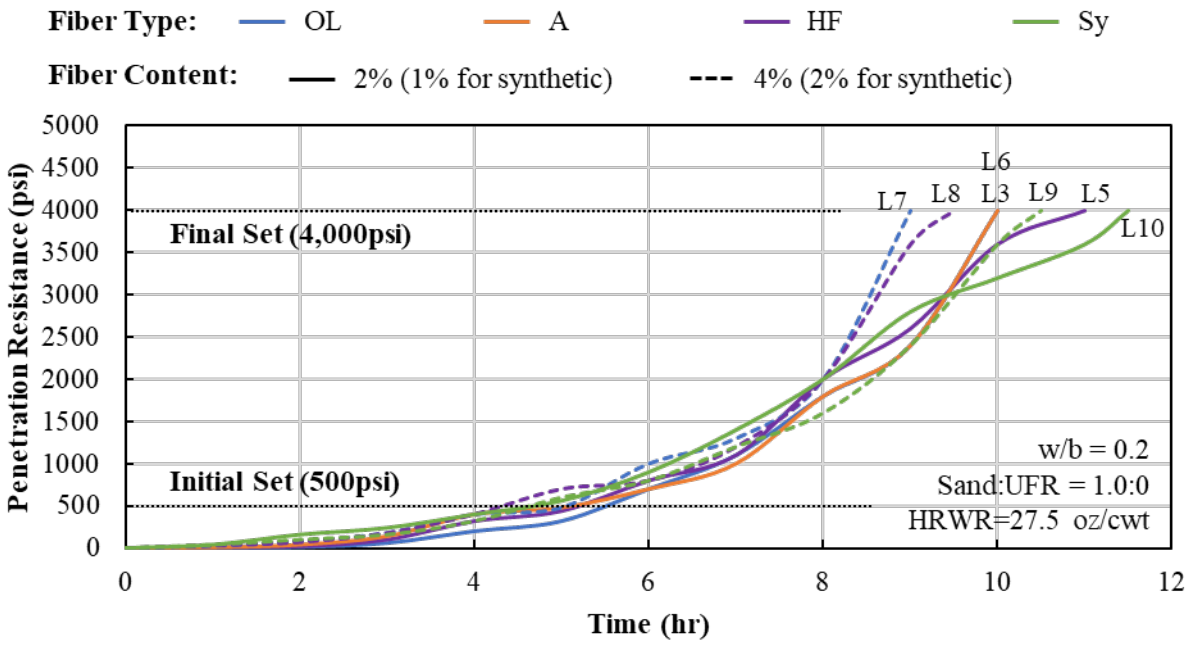

Figure 5.16: Effect of fiber type and content on setting time

The shorter final set time for mixtures with higher fiber contents may have occurred as a result of the fibers resisting the penetration needle, as shown in Figure 5.17.

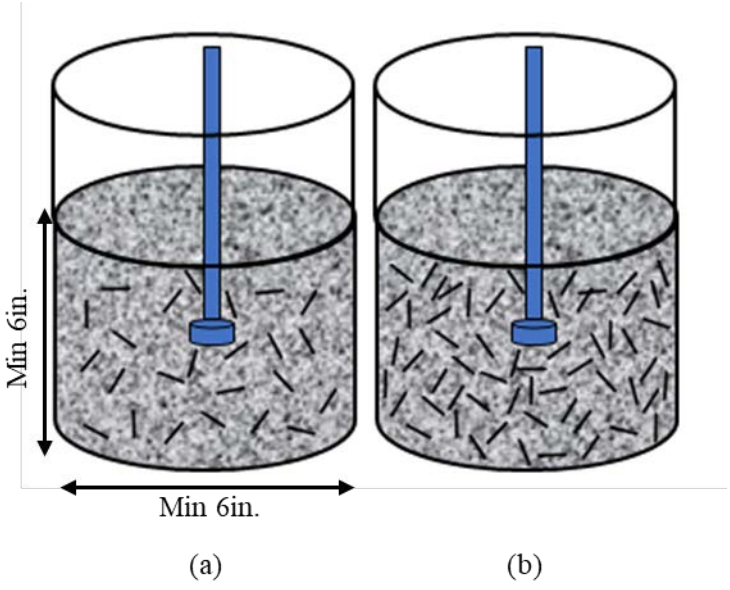

Figure 5.17: Schematic of setting time test; (a) low volume content fibers and (b) high volume content

The effect of different w/b and UFR on the penetration stress over time is shown in Figure 5.18. The smaller w/b resulted in an earlier initial set and final set time, comparing L4 with w/b of 0.18 and L3 with w/b of 0.20. The use of UFR at a 30 percent replacement of the fine masonry

sand led to slightly increased initial and final set times; this may be due to the larger HRWR content or that UFR leads to an improved particle packing.

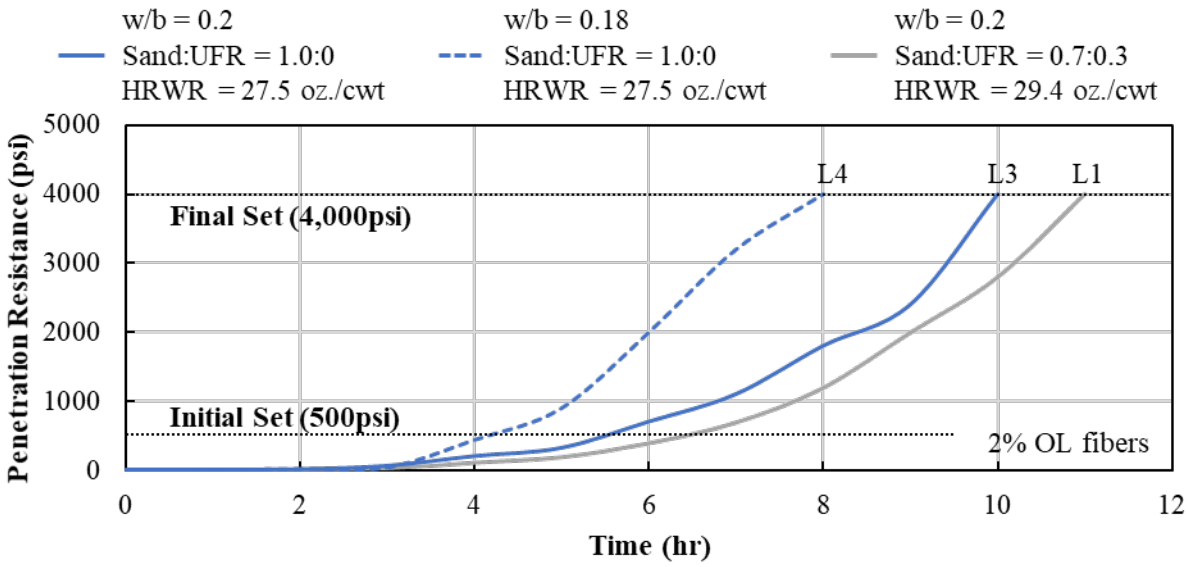

Figure 5.18: Effect of w/b and UFR on setting time

The penetration stress versus time curves for the two mixtures with similar proportions using materials from Oklahoma (OK) and south Florida (FL) are shown in Figure 5.19. The two sources of materials led to similar initial set time. The mixture with OK materials had a shorter final set time, but this may have been due to less HRWR being used.

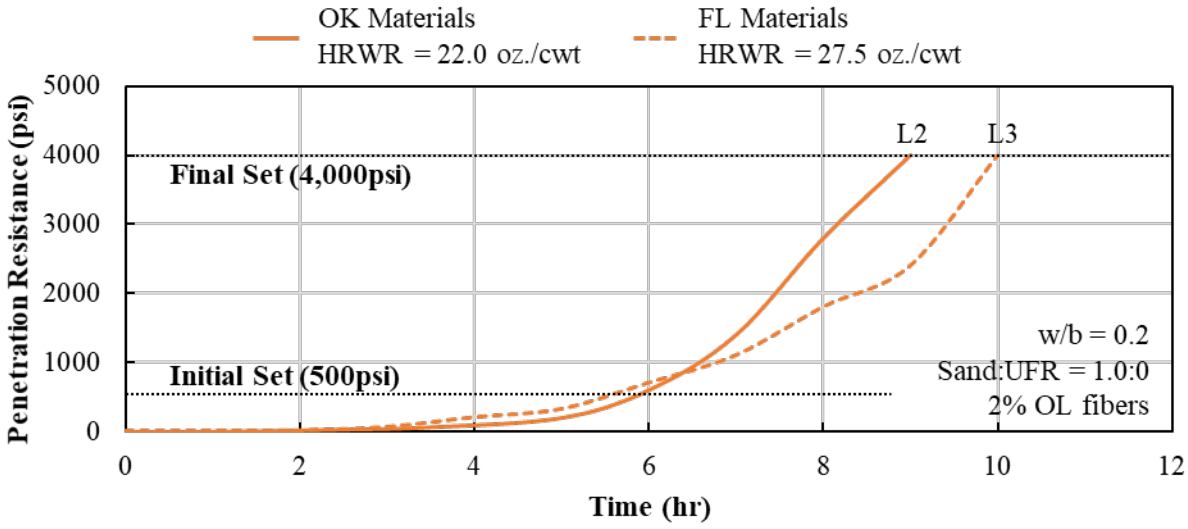

Figure 5.19: Effect of material source on setting time

5.6.3. Compressive Strength Results

Six 3 in. by 6 in. cylinders were tested at five different ages (3, 7, 14, 28, and 56 days). Three were moist cured and three left in the capped cylinder mold until testing at each age to determine the effectiveness of curing on compressive strength and density. The average compressive strength for all large-scale batches without moist curing are summarized in Table 5.6.

Table 5.6: Average measured compressive strength for large-scale batches

Mix.*	**w/b**	**Sand:UFR**	**Fiber**		**Compressive Strength (ksi)**				
			Type	*Content*	*3 day*	*7 day*	*14 day*	*28 day*	*56 day*
L1	0.20	0.7:0.3	OL	2.0%	11.8	14.6	15.5	16.7	18.1
L2	0.20	1:0	OL	2.0%	11.0	14.0	15.7	17.6	18.2
L3	0.20	1:0	OL	2.0%	12.2	14.4	15.5	17.1	17.6
L4	0.18	1:0	OL	2.0%	12.0	14.9	16.4	17.8	18.1
L5	0.20	1:0	HF	2.0%	12.1	14.3	15.4	17.5	18.0
L6	0.20	1:0	A	1.5%	11.7	14.9	16.2	17.3	17.6
L7	0.20	1:0	OL	4.0%	12.0	14.3	15.0	17.0	17.1
L8	0.20	1:0	HF	4.0%	12.8	14.3	15.6	17.3	17.4
L9	0.20	1:0	Sy	2.0%	9.7	10.8	11.2	11.1	13.4
L10	0.20	1:0	Sy	1.0%	10.9	12.4	13.4	15.4	16.0

*materials for L2 were shipped from Oklahoma; all other materials were obtained in South Florida

The measured compressive strength and density for the large-scale batches used to evaluate fiber type and fiber content are shown in Figure 5.20. The mixtures with steel fibers all had average 28-day compressive strengths between 17 and 18 ksi. There was no clear trend between fiber type and fiber content (for 2 and 4 percent fibers) and compressive strength for these large-scale batches. The fiber content did have a slight effect on the density of the concrete; the mixtures with 4 percent fibers had a slightly higher density than those with 2 percent fibers (3 to 4 percent increase in density).

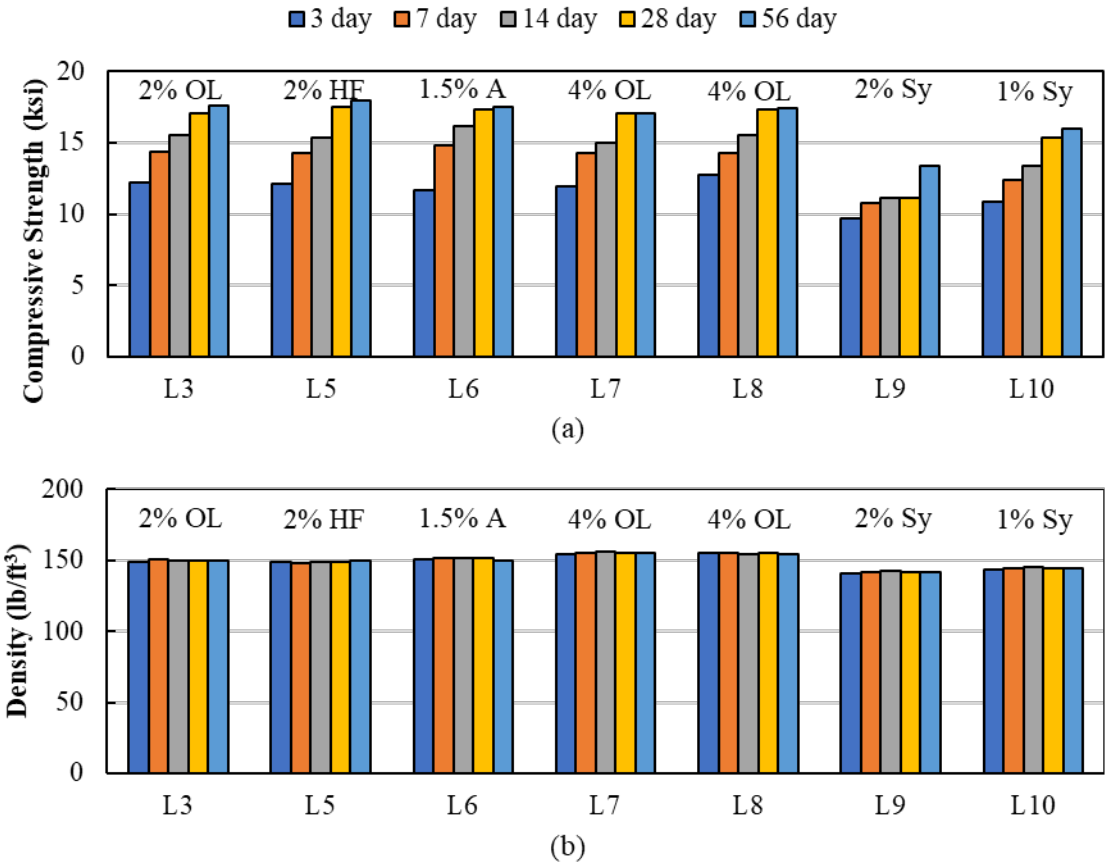

Figure 5.20: Effect fiber type and content on (a) compressive strength and (b) density

The mixtures with synthetic fibers (L9 and L10) had lower compressive strengths and densities than those with steel fibers. The mixture with 2 percent synthetic fibers had the smallest compressive strengths of all the different fiber types and contents tested (13.4 ksi at 56 days), compared to 16.0 ksi for 1 percent synthetic fibers and between 17 and 18 ksi for steel fibers.

The lower compressive strength of the mixtures made with synthetic fibers (L9 and L10) could be due to the lower strength of the synthetic fibers compared to steel fibers. Additionally, more fiber clumps were observed in mixtures containing synthetic fibers than mixtures with steel fibers. Clumping of the fibers occurred in some cases where the fibers were added rapidly to the mixer, when long or heavy fibers were used, or when synthetic fibers were used. A schematic of fiber clumping in cylinders is shown in Figure 5.21 (a). Photographs after compression failure for two cylinders from mixtures with 2 percent and 1 percent synthetic fibers are shown in Figure 5.21 (b) and (c), respectively. Clumping of the fiber led to weak local spots in the cylinders, which could lead to lower compressive strengths.

Figure 5.21: (a) Schematic of fiber clumping, (b) sample cylinder failure for L9 with 2% synthetic fibers (L9-20-28day), and (c) sample cylinder failure for L10 with 1% synthetic fibers (L10-27-56day)

The measured compressive strength and density for the large-scale batches used to evaluate the effect of w/b and UFR content are shown in Figure 5.22. Decreasing the w/b from 0.20 to 0.18 increased the compressive strength between 2 and 6 percent at different ages. The addition of UFR did not increase the strength for the large-scale batches, comparing L1 and L3 in Figure 5.22 (a). The addition of UFR was found to increase the compressive strength in the small-scale batches; it is unclear why it did not affect the strength in the large-scale batches. The w/b and UFR content had no effect on the density of the mixtures, shown in Figure 5.22 (b).

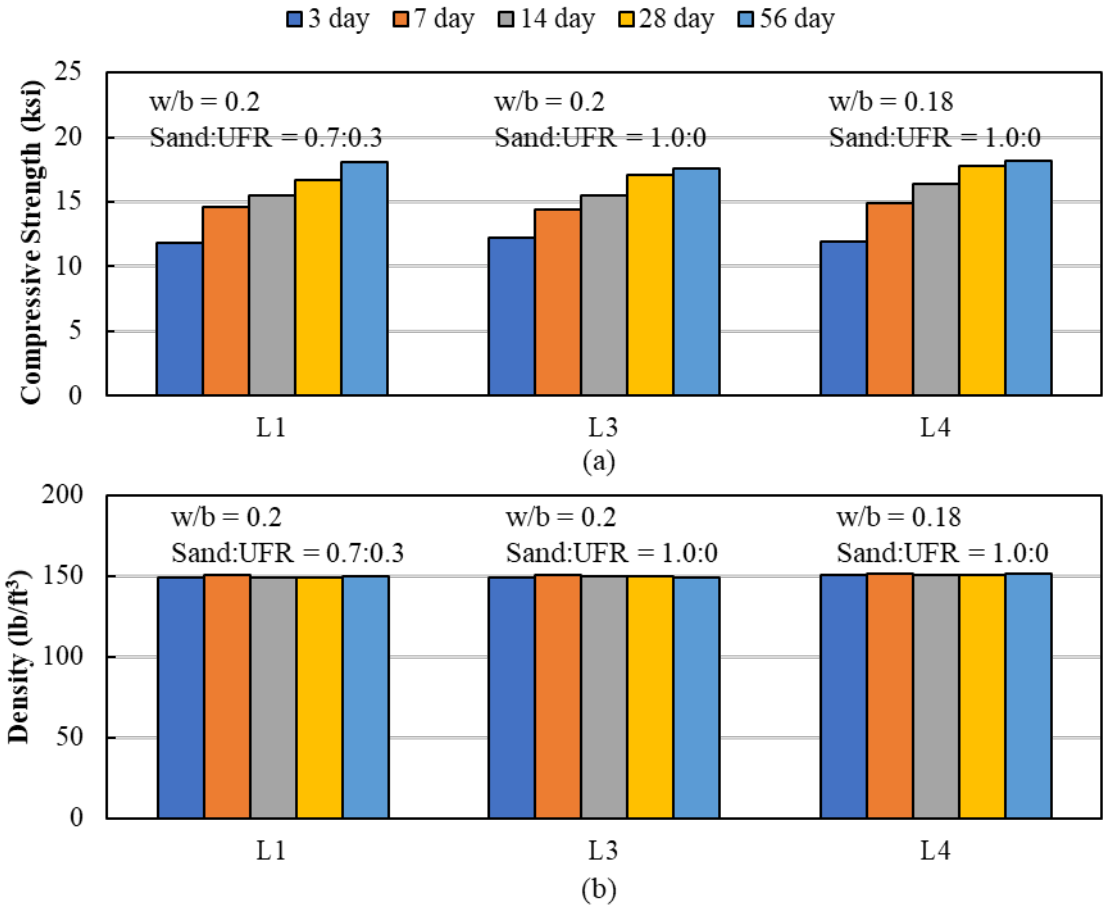

Figure 5.22: Effect w/b and UFR on (a) compressive strength and (b) density

The compressive strength and density for the two mix designs used to compare the behavior of materials from Oklahoma (OK) compared to those from south Florida (FL) are shown in Figure 5.23. The compressive strength for L2 (OK) was 2.9 and 3.4 percent higher than L3 (FL) at 28 and 56 days, respectively. The density for the mixtures with OK materials was on average 2.3 percent higher than that made with the FL materials.

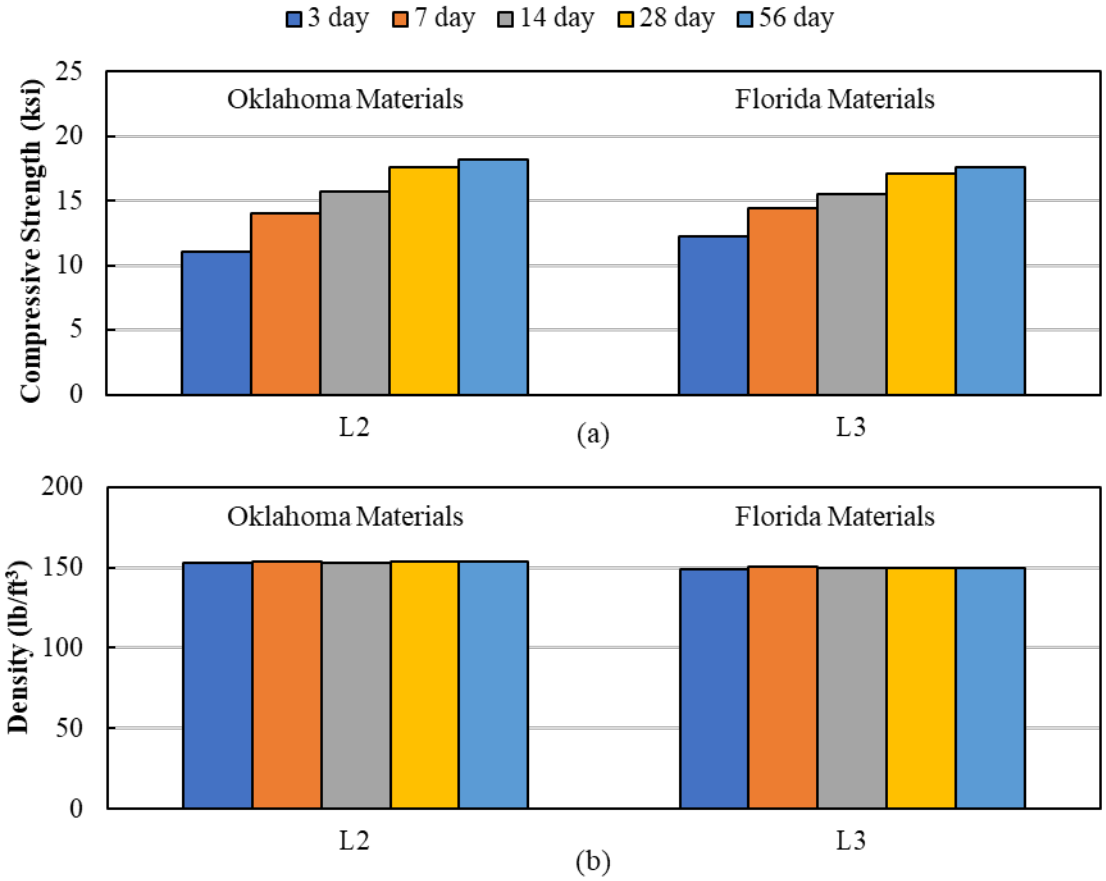

Figure 5.23: Effect of material source on (a) compressive strength and (b) density

The percent difference between the specimens that were moist-cured and those that were not moist cured for compressive strength and density is shown in Figure 5.24. The moist curing of the cylinders did not have a significant effect on the compressive strength or density of the specimens. The average of all the results was 0.8 percent higher compressive strength and 0.3 percent higher density for specimens that were moist cured compared to those that were kept in the capped cylinders until testing. Moist curing likely did not have a significant effect on compressive strength and density because of the low permeability of UHPC.

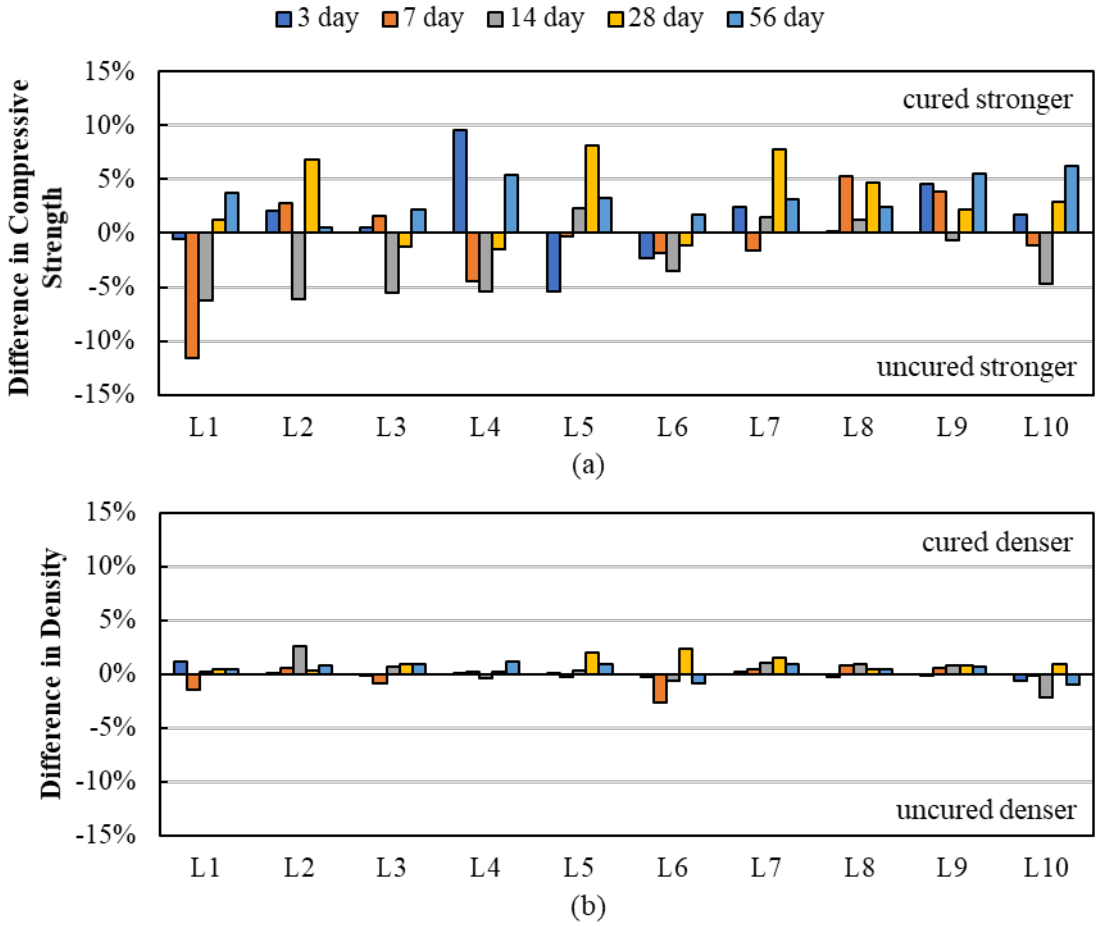

Figure 5.24: Effect of moist curing on (a) compressive strength and (b) density

5.6.4. Modulus of Elasticity Results

Modulus of elasticity was measured using 3 in. by 6 in. cylinders at 28 days for moist-cured and uncured samples. The modulus of elasticity was measured using ASTM C469 [63] as discussed in §5.5.4. A summary of the average measured modulus of elasticity for all large-scale batches is shown in Table 5.7. The measured modulus for the large-scale batches was between 7,100 and 9,500 ksi, which is in the same range for UHPC (4,250 to 8,000 ksi) found by previous researchers [8].

Moist curing did lead to a higher modulus of elasticity on average for all the specimens; the average modulus of all the moist cured samples was 7.5 percent higher than the average of all the uncured samples, as shown in Table 5.7. The effect of moist curing was more pronounced in the samples cast to investigate fiber type and fiber content (L3 and L5 to L10). L1 and L4 were positively influenced by moist curing; this is likely due to lower permeability due to better particle packing for L1 and lower w/b for L4.

Table 5.7: Results of modulus of elasticity

Mix.	w/b	Sand:UFR	Fiber		Modulus of Elasticity (ksi)		
			Type	*Content*	*Uncured*	*Cured*	*Avg.*
L1	0.20	0.7:0.3	OL	2.0%	8,867	8,734	8,767
L2	0.20	1:0	OL	2.0%	8,495	8,937	8,826
L3	0.20	1:0	OL	2.0%	7,247	7,979	7,796
L4	0.18	1:0	OL	2.0%	9,471	9,035	9,144
L5	0.20	1:0	HF	2.0%	7,863	9,202	8,867
L6	0.20	1:0	A	1.5%	8,241	9,415	9,122
L7	0.20	1:0	OL	4.0%	8,038	9,007	8,765
L8	0.20	1:0	HF	4.0%	7,884	8,940	8,676
L9	0.20	1:0	Sy	2.0%	7,158	7,699	7,293
L10	0.20	1:0	Sy	1.0%	7,865	8,241	8,147
				Average =	8,113	8,719	8,540

The average measured modulus of elasticity for the large-scale batches used to evaluate fiber type and fiber content are shown in Figure 5.25. Increasing fiber content from 2 to 4 percent increased the modulus by an average of 12.2 percent for the Dramix OL 13/.20 (OL) fibers; going from 7,796 ksi for L3 to 8,765 ksi for L7). Increasing the fiber content from 2 to 4 percent decreased the average modulus for the Hiper Fiber Type A (HF) by 2.2 percent, going from 8,867 ksi for L5 to 8,676 ksi for L8. There is an inherent uncertainty in modulus testing, which may have been the cause of the slight difference between measured moduli.

The modulus of samples with HF fibers at 2 percent was 13.7 percent higher than the modulus of samples with OL fibers at 2 percent (comparing L5 and L3). The modulus of samples with 4 percent fibers were similar between those with HF and OL fibers (comparing L7 and L8). The modulus of the samples with the Dramix 4D 65/35BG (A) was higher than the samples with HF and OL fibers.

The use of synthetic fibers led to the lowest stiffness among the samples (see L9 and L10). Decreasing the synthetic fiber content from 2 to 1 percent increased the modulus by 11.7 percent.

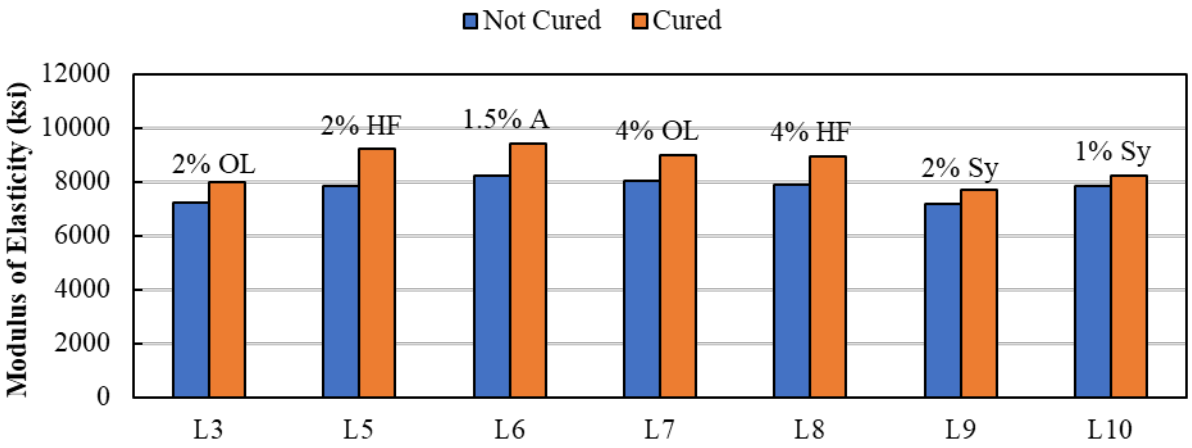

Figure 5.25: Effect of fiber type and content on modulus of elasticity

The average stress versus strain plots for the large-scale batches used to evaluate fiber type and fiber content are shown in Figure 5.26.

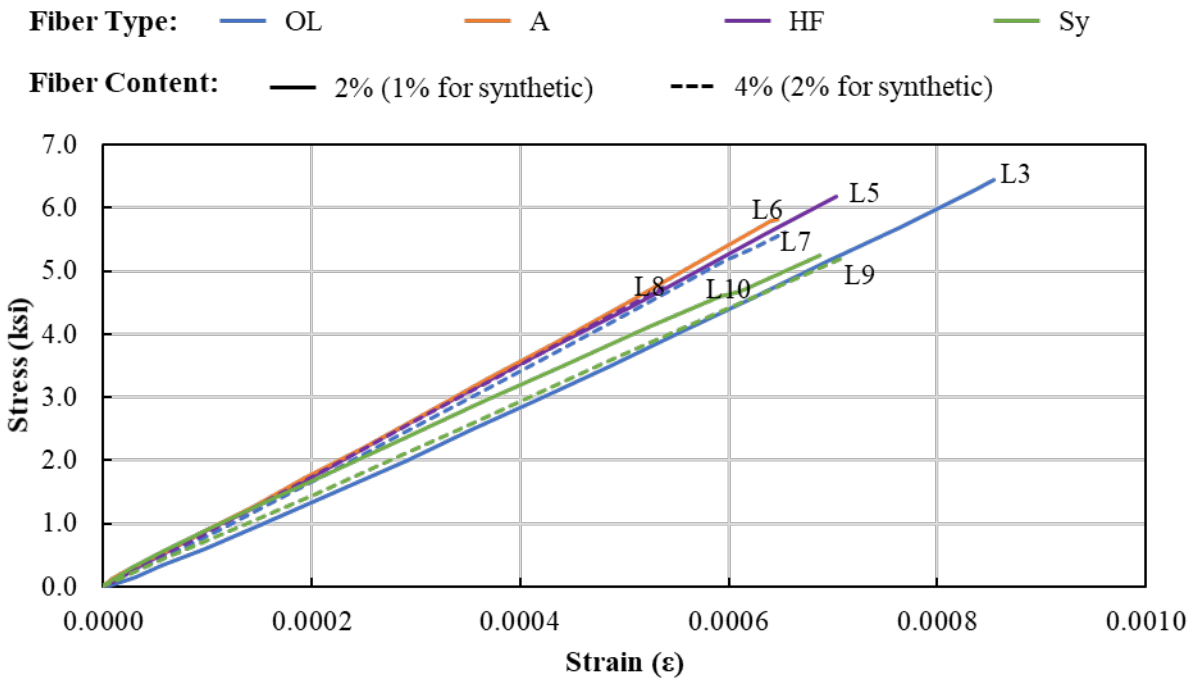

Figure 5.26: Effect of fiber type and content on the modulus of elasticity

The measured average modulus of elasticities for the large-scale batches used to evaluate the effect of w/b and UFR and the source of the constituent materials are shown in Figure 5.27. A lower w/b led to an increase in the modulus of elasticity; samples with w/b of 0.18 (L4) had an average 17.3 percent larger modulus than the similar samples with w/b of 0.20 (L3). The use of UFR also increased the average modulus of elasticity; samples with 30 percent UFR replacement

(L1) had an average 12.5 percent higher modulus than the similar samples with all fine masonry sand (L3).

The samples with material from Oklahoma (OK, L2) had an average 13.2 percent higher modulus than the similar sample with materials from south Florida (FL, L3).

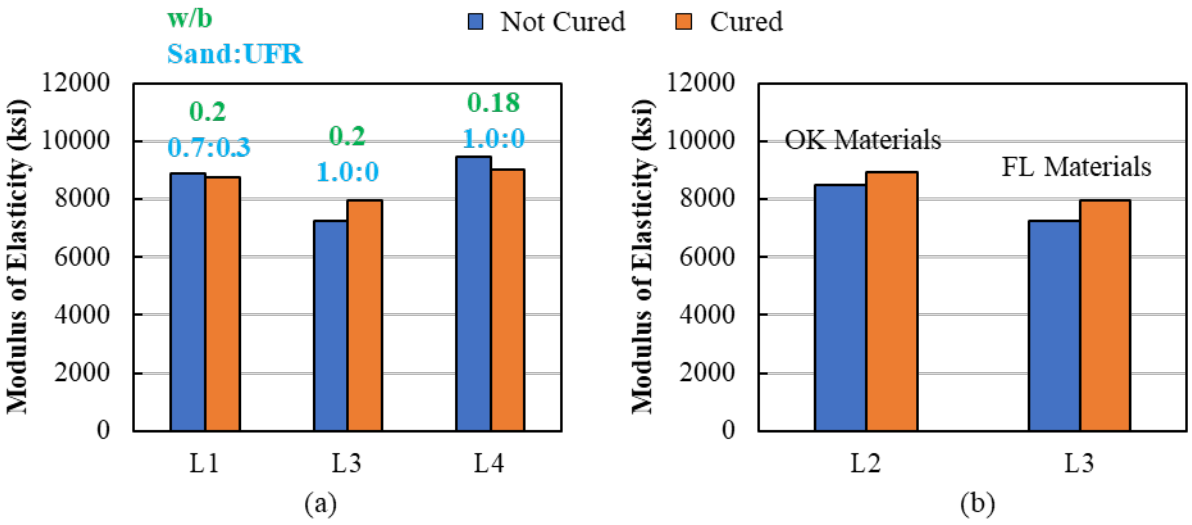

Figure 5.27: Effect of (a) w/b and UFR and (b) material source on modulus of elasticity

5.6.5. Splitting Tensile Strength Results

Splitting tensile strength tests were conducted on both moist cured (3 samples) and uncured samples (3 samples) at 28 days after casting the UHPC. Results of the average splitting tensile strength tests for all large-scale batches are summarized in Table 5.8. Similar to the compressive strength, moist curing did not have an effect on the splitting tensile strength, see similar averages in Table 5.8.

Table 5.8: Splitting tensile strength at 28 days

Mix.	**w/b**	**Sand:UFR**	**Fiber**		**Split Tensile Strength (ksi)**		
			Type	*Content*	*Uncured*	*Cured*	*Avg.*
L1	0.20	0.7:0.3	OL	2.0%	2.68	2.54	2.61
L2	0.20	1:0	OL	2.0%	2.49	2.76	2.62
L3	0.20	1:0	OL	2.0%	2.61	2.73	2.67
L4	0.18	1:0	OL	2.0%	2.81	2.87	2.84
L5	0.20	1:0	HF	2.0%	3.06	2.80	2.93
L6	0.20	1:0	A	1.5%	2.45	2.33	2.39
L7	0.20	1:0	OL	4.0%	2.80	2.90	2.85

Mix.	w/b	Sand:UFR	Fiber		Split Tensile Strength (ksi)		
			Type	*Content*	*Uncured*	*Cured*	*Avg.*
L8	0.20	1:0	HF	4.0%	2.85	2.75	2.80
L9	0.20	1:0	Sy	2.0%	1.45	1.30	1.38
L10	0.20	1:0	Sy	1.0%	1.46	1.53	1.49

The average measured splitting tensile strength for the large-scale batches used to evaluate fiber type and fiber content are shown in Figure 5.28. There was a slight increase in the average tensile strength with an increased fiber content for the Dramix OL 13/.20 (OL) fibers (L3 and L7), increasing from 2.67 ksi to 2.85 ksi (6.7 percent increase). There was actually a slight decrease in the splitting tensile strength with increased fiber content for the Hiper Fiber Type A (HF) fibers (L5 and L8), decreasing from 2.93 ksi to 2.80 ksi (4.4 percent decrease). The OL and HF fibers had similar splitting tensile strengths in general. The Dramix 4D 65/35BG (A) had the lowest splitting tensile strength for the steel fibers, 2.39 ksi average for L6. The synthetic fibers had a 47 percent lower splitting tensile strength than the steel fibers on average (2.71 ksi average for steel fibers compared to 1.44 ksi average for synthetic fibers).

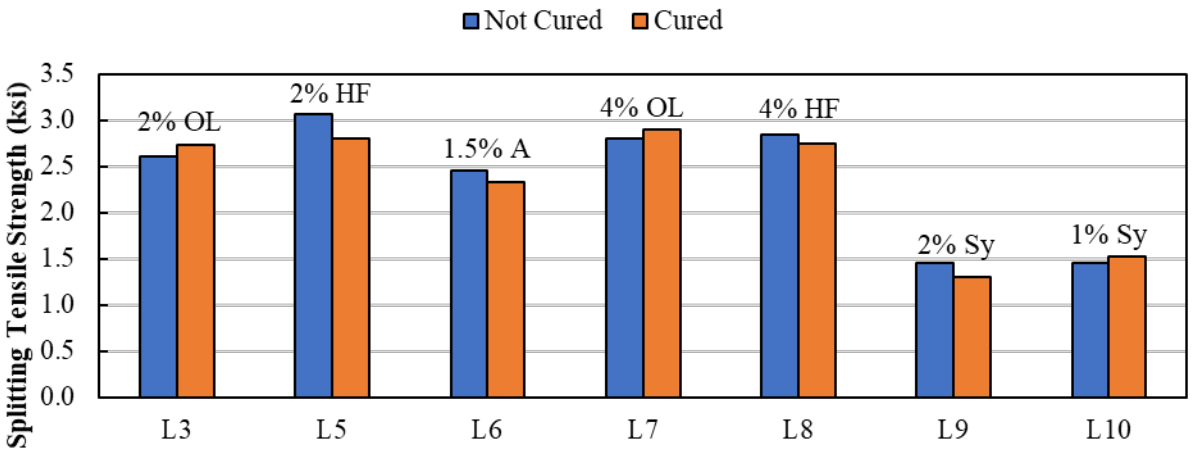

Figure 5.28: Effect of fiber type and content on splitting tensile strength

The splitting tensile strengths for the large-scale batches cast to investigate w/b and UFR content are shown in Figure 5.29. Using a w/b ratio of 0.18 led to an increase in the splitting tensile strength of 6.4 percent (average of 2.67 ksi for L3 and 2.84 ksi for L4). Using UFR led to a slight (2.3 percent) decrease in the splitting tensile strength (average of 2.61 ksi for L1 and 2.67 ksi for L3).

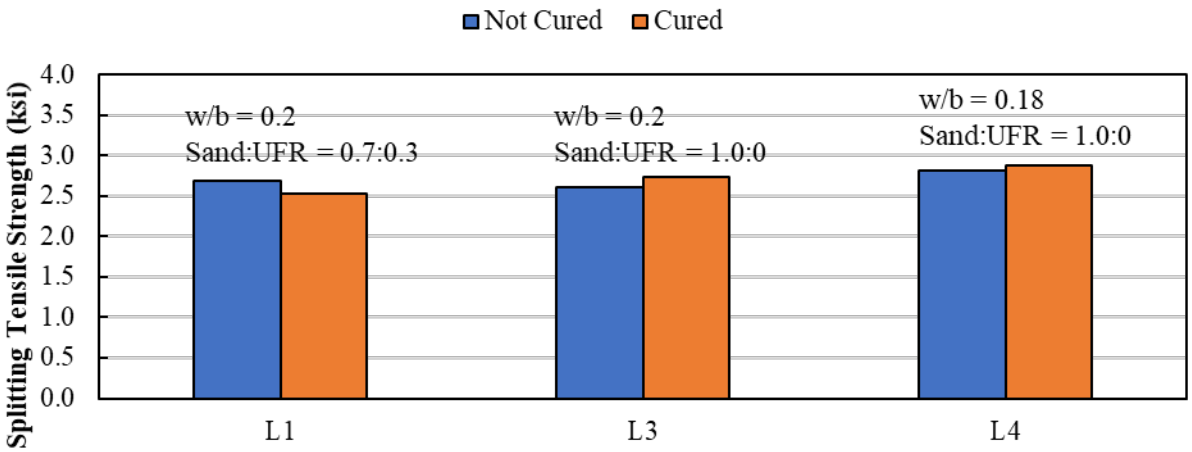

Figure 5.29: Effect of w/b and UFR on splitting tensile strength

The splitting tensile strength for the similar large-scale batches with Oklahoma (OK, L2) and south Florida (FL, L3) materials are shown in Figure 5.30. The mixtures with the FL materials had a slightly higher (1.7 percent) splitting tensile strength compared to the mixtures with OK materials.

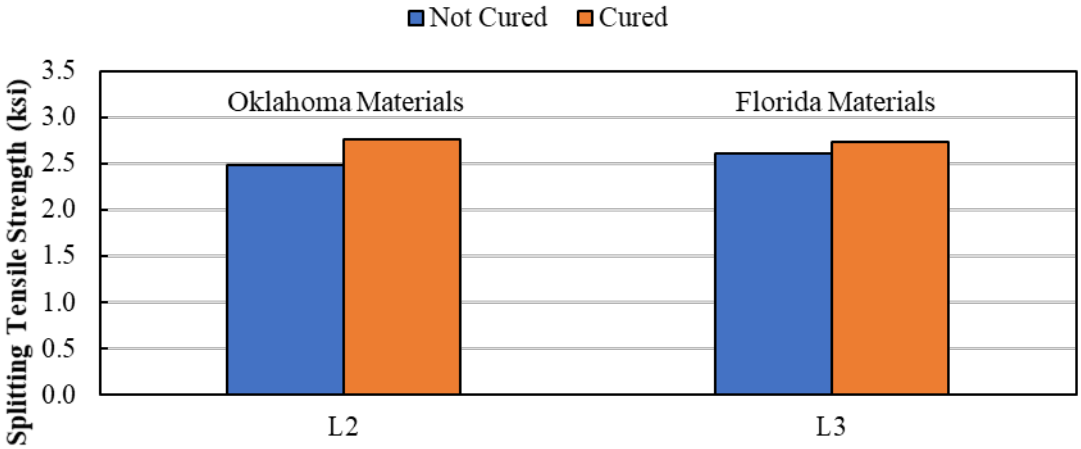

Figure 5.30: Effect of material source on splitting tensile strength

5.6.6. Modulus of Rupture Results

Modulus of rupture (MOR) tests were conducted on 3 in. by 3 in. by 11 in. prism beams to measure the flexural strength of UHPC samples. This test can be considered as an indirect way of evaluating the tensile behavior of UHPC. The MOR test was performed based on ASTM C78 [62] as described in §5.5.6. Equipment capable of testing the direct tensile strength of the UHPC was not available to the research team at the time of this project. A summary of the average MOR results is shown in Table 5.9. The average splitting tensile strength from §5.6.5 are also

included in Table 5.9 for comparison. On average, the MOR test resulted in a 7.6 percent higher estimated tensile strength than the splitting tensile strength test. MOR and splitting tensile strengths were within 10 percent of each other for L1, L3, L4, L7, and L9.

Table 5.9: Average measured modulus of rupture for large-scale batches

Mix.	w/b	Sand:UFR	Fiber		MOR (ksi)	Avg. Split Tensile Strength (ksi)	Percent Difference
			Type	*Content*			
L1	0.20	0.7:0.3	OL	2.0%	2.83	2.61	7.8%
L2	0.20	1:0	OL	2.0%	-*	2.62	-
L3	0.20	1:0	OL	2.0%	2.49	2.67	-7.3%
L4	0.18	1:0	OL	2.0%	2.89	2.84	1.8%
L5	0.20	1:0	HF	2.0%	3.65	2.93	19.8%
L6	0.20	1:0	A	1.5%	3.24	2.39	26.0%
L7	0.20	1:0	OL	4.0%	3.13	2.85	8.9%
L8	0.20	1:0	HF	4.0%	4.05	2.80	30.9%
L9	0.20	1:0	Sy	2.0%	1.34	1.38	-3.3%
L10	0.20	1:0	Sy	1.0%	1.29	1.49	-15.8%
				Average =	2.77	2.46	7.6%

*Modulus of rupture for the L2 mix design was initially found based on a 3-point-load test setup; additional samples could not be cast due to limited amount of material from OU. Modulus or rupture strengths were found using a 4-point-load test setup for all other mixes.

The average measured MOR for the large-scale batches used to evaluate fiber type and fiber content are shown in Figure 5.31. An increased fiber content increased the average MOR for both Dramix OL 13/.20 (OL) and Hiper Fiber Type A (HF) fibers; increasing from 2 to 4 percent fiber content increased the MOR by 25.8 percent for the OL fibers and 10.9 percent for the HF fibers. The HF led to a higher MOR than the OL fibers for similar fiber contents: 46.8 percent higher MOR for 2 percent and 29.4 percent higher for 4 percent fiber contents. The difference in MOR between OL and HF was unexpected since these fibers have the same dimensions and specified properties.

The Dramix 4D 65/35BG (A) had a MOR higher than the OL fibers, but less than the HF fibers. The MOR for the synthetic fibers was about half of the MOR for batches with 2 percent OL fibers.

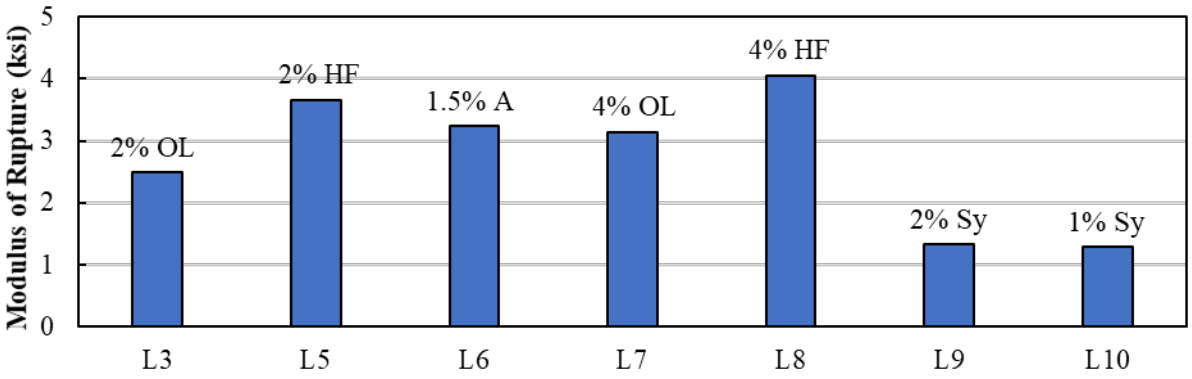

Figure 5.31: Effect of fiber type and fiber content on modulus of rupture

The average flexural stress versus displacement curves for the large-scale batches used to evaluate fiber type and fiber content are shown in Figure 5.32. These curves show the average peak flexural stress and the ductility of the beams in flexure before failure. This behavior is much different than typical concrete MOR beams, which fail immediately after cracking.

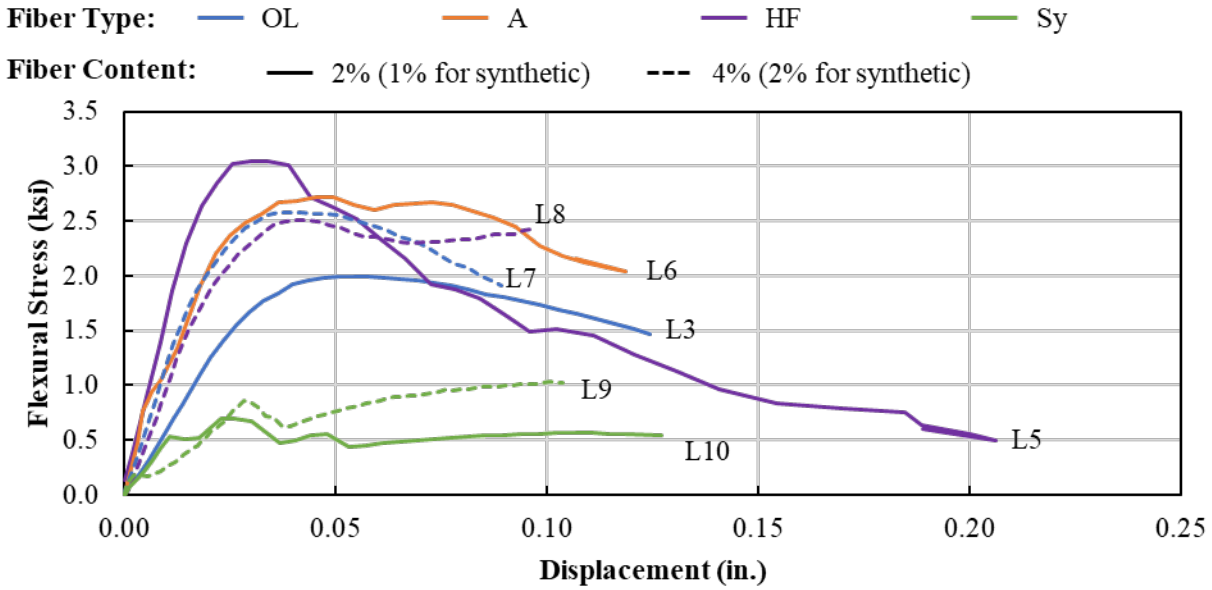

Figure 5.32: Flexural stress versus midspan displacement curves for samples investigating the effect of fiber type and content on the modulus of rupture

The measured MOR used to evaluate the effect of w/b and UFR content are shown in Figure 5.33. The average MOR was 16.3 percent higher when the w/b was decreased from 0.20 to 0.18. The MOR was 13.6 percent higher for the specimens with a 30 percent UFR replacement.

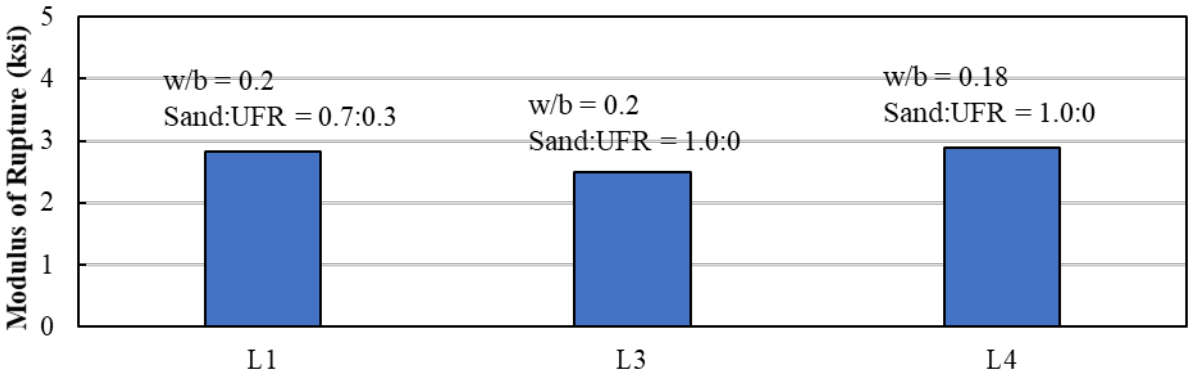

Figure 5.33: Effect of w/b and UFR on modulus of rupture

The average flexural stress versus displacement curves for the large-scale batches used to evaluate w/b and UFR are shown in Figure 5.34.

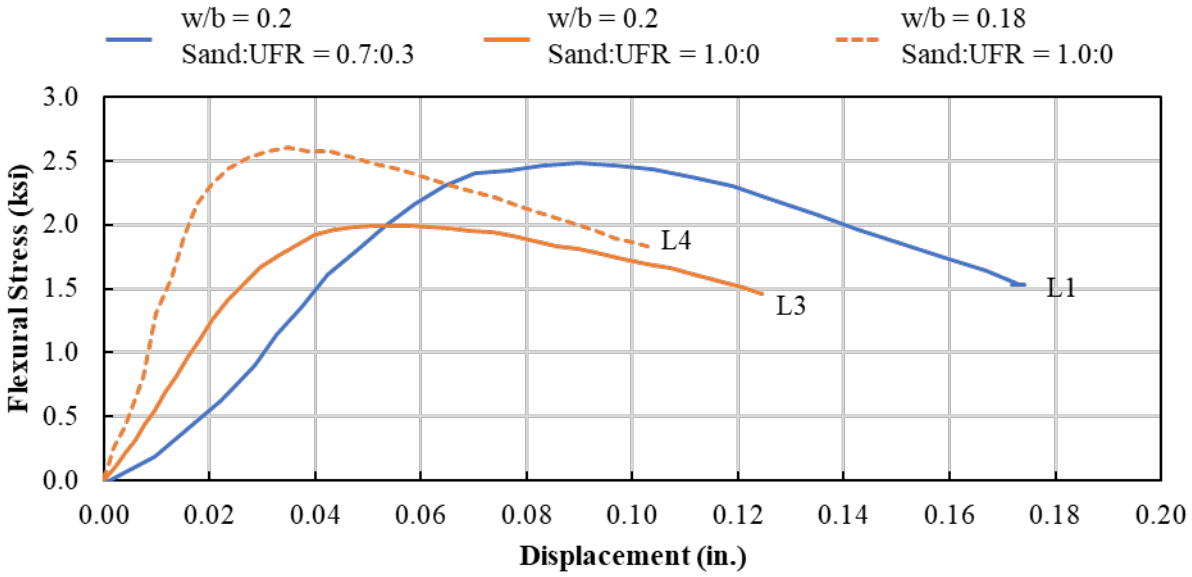

Figure 5.34: Flexural stress versus midspan displacement curves for samples investigating the effect of w/b and using UFR on the modulus of rupture

5.6.7. Bulk Resistivity Test Results

Many current uses for UHPC require good chloride penetration resistance especially where it is used in structural elements subject to marine or deicer exposures or in contact with chloride-containing soils or groundwater, e.g., joints, overlays, splash zone repairs. The bulk resistivity test was performed according to ASTM C1760-12 [60] as described in §5.5.7. The average bulk resistivity readings for all large-scale batches are summarized in Table 5.10. The steel fibers seemed to influence the results. The researchers could not find any bulk resistivity comparison

points for UHPC, so two additional mixtures were tested using Ductal® (one with 0 percent fibers, D1, and one with 2 percent fibers, D2). The measurement shown for D1 was based on the maximum range for the Resipod device.

Table 5.10: Bulk resistivity test results

Mix.	w/b	Sand:UFR	Fiber		Bulk Resistivity (kΩ.cm)					
			Type	*Content*	*3 day*	*7 day*	*14 day*	*28 day*	*56 day*	*90 day*
L1	0.20	0.7:0.3	OL	2.0%	1.4	2.3	4.9	6.6	12.9	21.9
L2	0.20	1:0	OL	2.0%	1.1	3.6	5.0	5.4	11.7	23.1
L3	0.20	1:0	OL	2.0%	4.5	7.0	9.6	15.5	23.8	38.9
L4	0.18	1:0	OL	2.0%	3.1	6.5	9.9	15.5	31.7	56.5
L5	0.20	1:0	HF	2.0%	5.2	8.2	8.3	11.7	23.8	44.9
L6	0.20	1:0	A	1.5%	3.9	5.4	7.5	10.9	16.3	31.9
L7	0.20	1:0	OL	4.0%	2.2	4.2	8.6	11.6	16.2	31.2
L8	0.20	1:0	HF	4.0%	1.4	3.0	7.1	9.4	13.1	25.0
L9	0.20	1:0	Sy	2.0%	9.7	13.7	30.4	59.2	114.8	182.1
L10	0.20	1:0	Sy	1.0%	8.7	11.5	27.2	64.3	137.6	183.4
D1	Ductal®		OL	0.0%	204.5	204.5	204.5	204.5	204.5	204.5
D2	Ductal®		OL	2.0%	9.7	15.1	26.2	47.1	78.3	125.3

The typical classification of permeability measurements for bulk resistivity and surface resistivity are shown in Table 5.11 based on Nugent [86]. The measured bulk resistivity for all large-scale batches would be in the very low classification for concrete permeability.

Table 5.11: Classification of permeability measurements by test method [86]

Classification	RCP (C)	Bulk Resistivity (kΩ-cm)	Surface Resistivity (kΩ-cm)
High	> 4000	< 5	< 12
Moderate	2000 to 4000	5 to 10	12 to 21
Low	1000 to 2000	10 to 20	21 to 37
Very Low	100 to 1000	20 to 200	37 to 254
Negligible	< 100	> 200	> 254

The average measured bulk resistivity over time for the large-scale batches used to evaluate fiber type and fiber content are shown in Figure 5.35. The specimens with steel fibers had significantly smaller bulk resistivity measurements than those without steel fibers or with

synthetic fibers. The measured bulk resistivity of the mixtures with synthetic fibers (L9 and L10) was about 3.5 times larger that of the similar mixtures with steel fibers (L3 and L5 to L8).

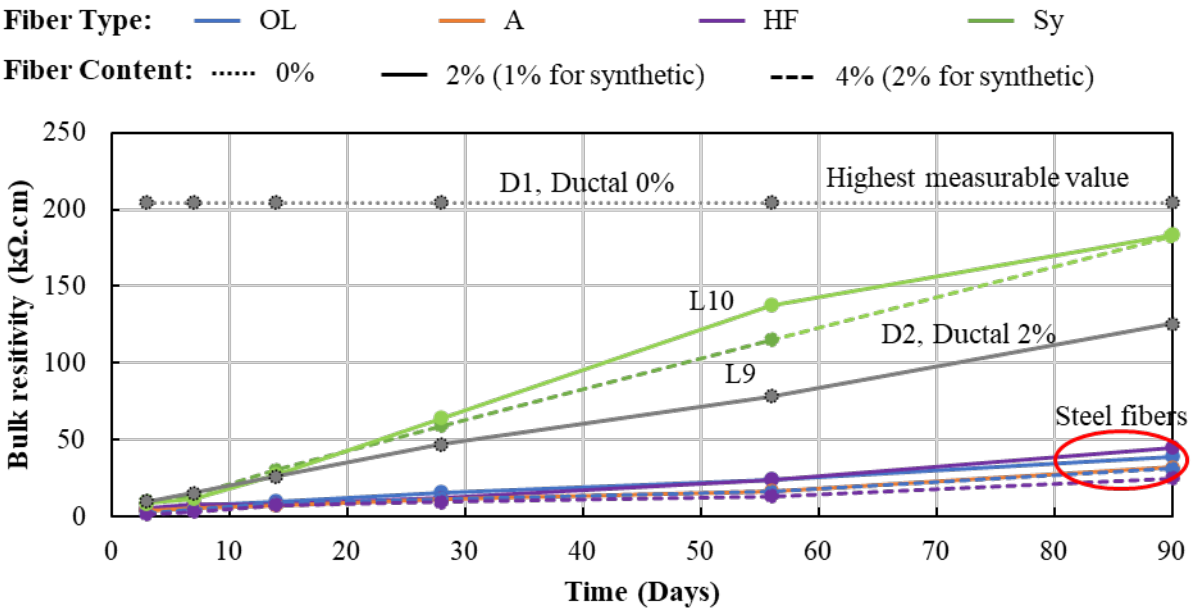

Figure 5.35: Effect of fiber type and content on bulk resistivity

The average measured bulk resistivity over time for the large-scale batches used to evaluate steel fiber type and content are shown in Figure 5.36. A higher fiber content led to a lower bulk resistivity measurement: going from 2 to 4 percent fibers decreased the bulk resistivity by 44 percent for HF fibers and 20 percent for OL fibers.

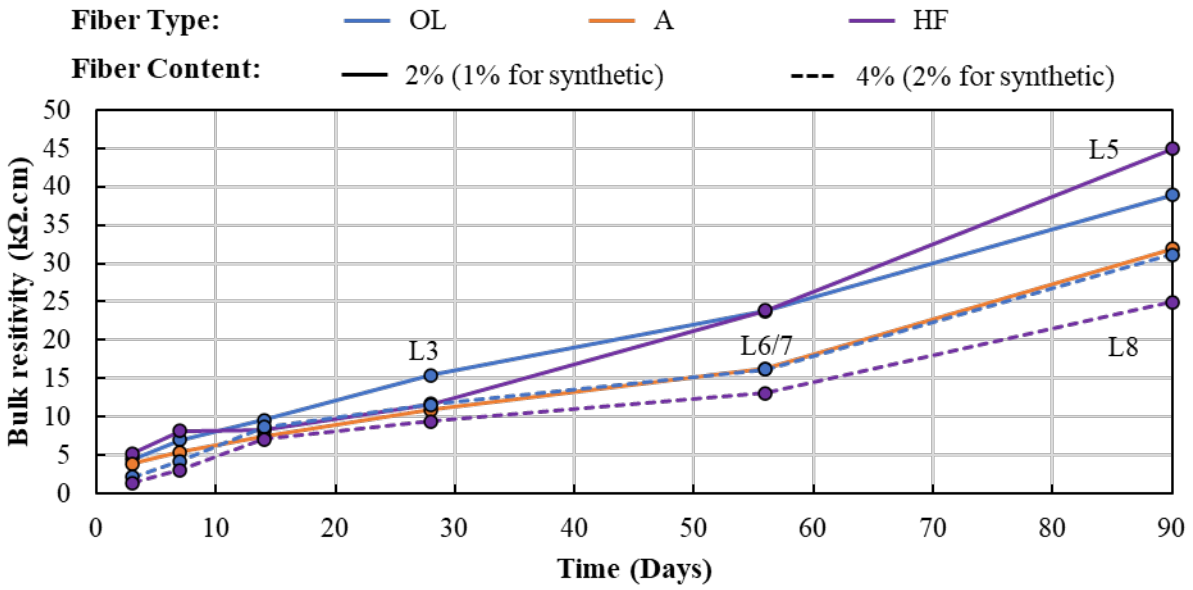

Figure 5.36: Effect of steel fiber type and content on bulk resistivity

The measured bulk resistivity values used to evaluate the effect of w/b and UFR content are shown in Figure 5.37. The bulk resistivity was 45 percent higher at 90 days for w/b of 0.18 compared to 0.20, which is consistent with the specimens with w/b of 0.18 having a lower permeability. The bulk resistivity was lower for the specimens with UFR than those without. It is unclear why the use of UFR led to lower bulk resistivity, but this could have had to do with fiber alignment in the UFR specimens.

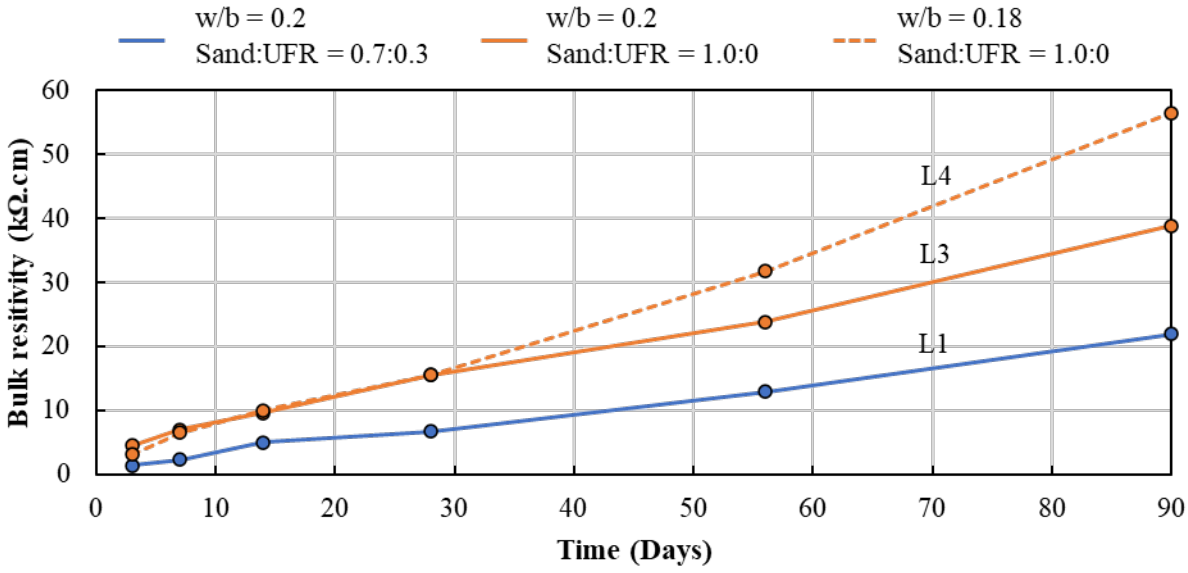

Figure 5.37: Effect of w/b and UFR on bulk resistivity

The bulk resistivity for the similar large-scale batches with Oklahoma (OK, L2) and south Florida (FL, L3) materials are shown in Figure 5.38. The specimens with FL materials had a 68 percent higher bulk resistivity than those with the OK materials.

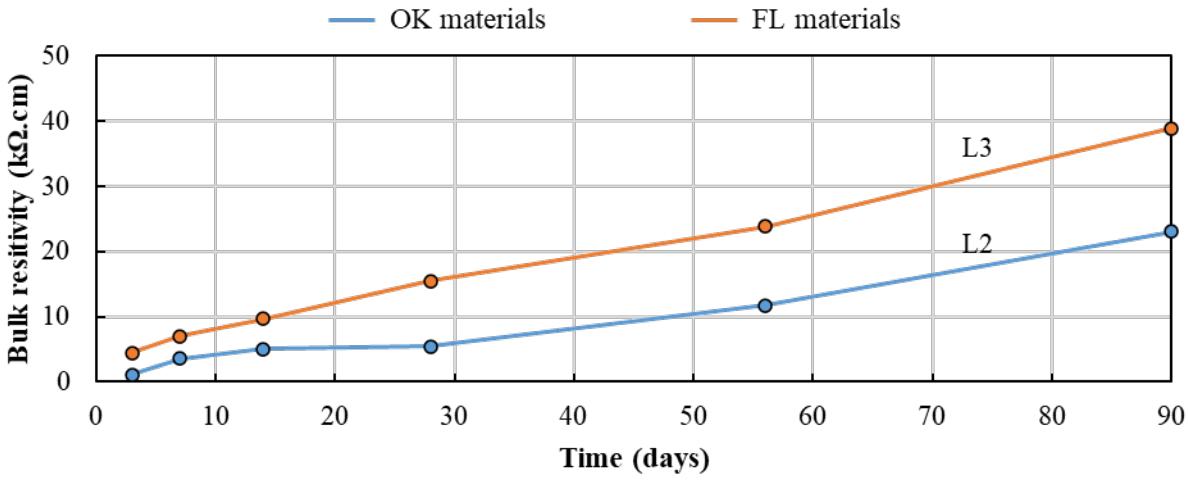

Figure 5.38: Effect of material source on bulk resistivity

In general, the presence of steel fibers in UHPC seems to influence the reading of bulk resistivity. The fibers help to create a path for current flow with less resistance than the concrete matrix itself, as illustrated in Figure 5.39. Specimens with synthetic fibers with similar fiber content would give a better approximation of the bulk resistivity of the concrete matrix with fibers.

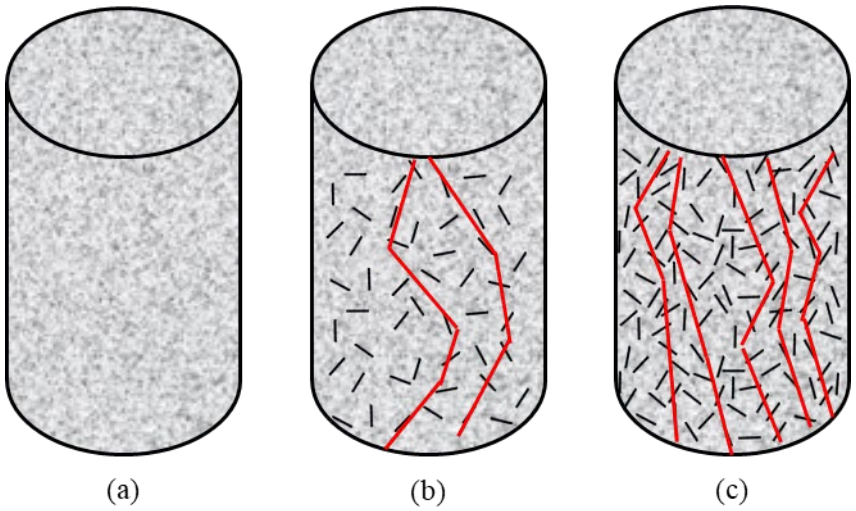

Figure 5.39: Schematic of formation of the conductive path in cylinder samples; (a) 0% fiber content, (b) medium fiber content, and (c) high fiber content

No additional weight or clamping was applied to the bulk resistivity end plates for the general testing. An additional study was performed on the bulk resistivity samples when the samples were between 178 and 200 days old to investigate the effect of different clamping forces on the change in bulk resistivity reading with change in clamping force. Different numbers of half-pound weights were stacked on top of the top electrical plate to investigate if there was any effect on the readings. A summary of the raw data readings for the four samples from L1 are shown in Table 5.12. The additional weight provided on the testing apparatus decreased the resistivity by an average of 0.5 percent for all the test specimens (ranging between 0 and 2.2 percent).

Table 5.12: Example of raw bulk resistivity readings under different weights from L1 samples

L1 Sample	**K (A/L)**	**Bulk Resistivity Readings (kΩ-cm)**							
		0.0 lb	*0.5 lb*	*1.0 lb*	*1.5 lb*	*2.0 lb*	*2.5 lb*	*3.0 lb*	*3.5 lb*
1	1.78	491	487	484	483	482	481	481	480
2	1.73	588	586	585	584	583	583	583	583
3	1.70	363	360	359	359	358	358	357	356
4	1.71	529	528	528	527	527	526	526	526

The results were also compared to four-point Wenner array probe resistivity readings when the samples were between 178 and 200 days also using the Resipod device. The resistivity measured

by the Resipod was modified based on two different correction factors from Morris et al. [87] and the Resipod Operating Instructions [85]. Morris et al. [87] proposed Figure 5.40 for determining the correction factor. The following values can be determined based on the cylinder dimensions and probe spacing for the Resipod device.

$$\frac{L}{a} = \frac{8"}{1.5"} = 11.1 \qquad \frac{d}{a} = \frac{4"}{1.5"} = 2.67$$

Using these values in Figure 5.40 gives a correction factor of k = 2.0.

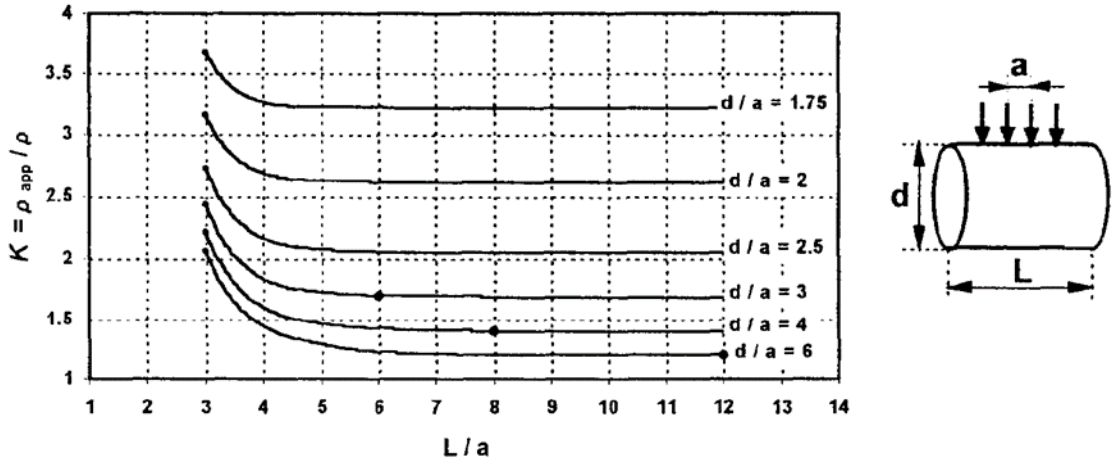

Figure 5.40: Cell constant correction to determine concrete resistivity [87]

The Resipod Operating Instructions [85] recommends the geometric correction factor shown in Equation 5-7.

$$k = \frac{2\pi}{1.09 - \frac{0.527}{d/a} + \frac{7.34}{\left(d/a\right)^2}} \qquad \text{Equation 5-7}$$

$$k = \frac{2\pi}{1.09 - \frac{0.527}{4"/1.5"} + \frac{7.34}{\left(4"/1.5"\right)^2}} = 3.26$$

A comparison between the average bulk resistivity and average four-point Wenner array probe using the two different correction factors are shown in Figure 5.41. Results should be consistent between the bulk resistivity and Wenner array probe measurements. There is a reasonable consistency between bulk resistivity and Wenner array probe measurements using the Morris et al. [87] correction factor for mixes L1 through L8 (average difference of 17 percent). There was a larger difference using the correction from the Resipod Operating Instructions [85] (average difference of 44 percent).

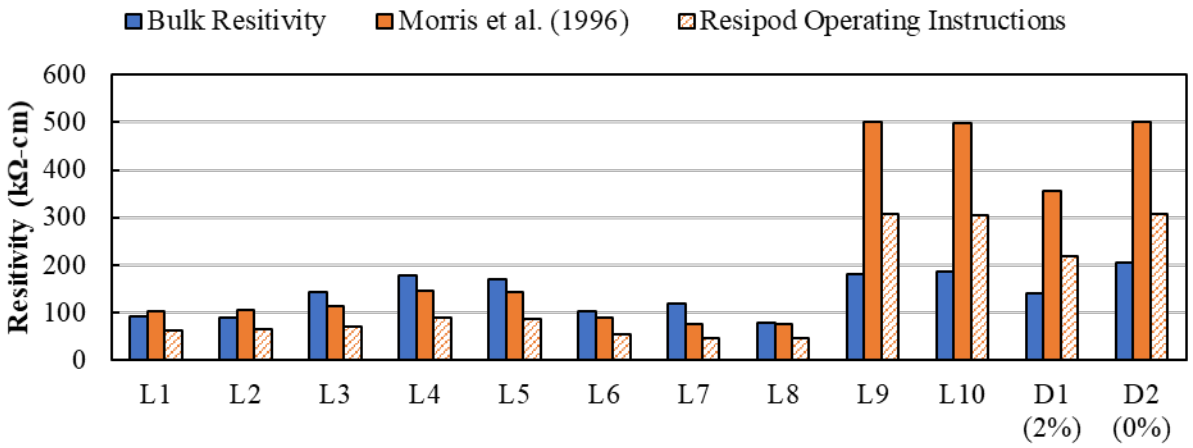

Figure 5.41: Comparison between bulk resistivity and 4-point Wenner array probe measurements using the average of all test results in each mix design

There was noticeably more variation between readings for the Wenner array probe measurements compared to those from the bulk resistivity. The mean, standard deviation, and coefficient of variation for the resistivity measurements taken on samples from the large-scale batches are shown in Table 5.13. For L1 through L8, the average coefficient of variation for the bulk resistivity measurements was 0.153 compared to 0.222 for the measurements using the Wenner array probe. The increased variability for the Wenner array probe may have been due to the steel fiber distribution in the samples having a larger impact on the measurement than in the bulk resistivity test.

Table 5.13: Mean, standard deviation, and coefficient of variation for resistivity measurements taken on large-scale batch samples

Mix		***L1***	***L2***	***L3***	***L4***	***L5***	***L6***	***L7***	***L8***	***L9***	***L10***
Bulk Resistivity	*Mean*	90.8	89.6	142.5	177.5	170.6	102.6	118.9	78.0	179.5	185.9
	St. Dev.	18.0	8.8	32.6	7.6	7.2	16.9	39.4	9.1	1.6	5.9
	CoV	0.198	0.098	0.228	0.043	0.042	0.165	0.331	0.117	0.009	0.032
Wenner Array Probe	*Mean*	103.2	106.0	114.7	146.0	141.9	90.1	76.3	76.5	500.0	499.2
	St. Dev.	24.8	24.3	17.1	22.5	13.9	36.2	19.5	18.9	0.0	2.7
	CoV	0.240	0.229	0.149	0.154	0.098	0.402	0.255	0.247	0.000	0.005

Bulk resistivity appears to be more consistent than four-point resistivity measurements using the Wenner array probe.

5.6.8. Shrinkage Results

Shrinkage was measured on 6 in. by 12 in. cylinders using vibrating wire strain gauges (VWSG) using the procedure described in §5.5.7. Three specimens were prepared per large batch, and all were connected to the data acquisition center. Unfortunately, due to some issues (e.g., power

shut down, software programing issues, and human errors) some early readings were lost. The research team is planning on repeating the shrinkage tests for the mixture designs with incomplete data.

A summary of the available shrinkage data for the large-scale batches is provided in Table 5.14 with shrinkage strains highlighted at 7, 30, and 90 days after casting.

Table 5.14: Summary of shrinkage strains for large-scale batches (will be updated later for other mixtures)

Mix.	**w/b**	**Sand:UFR**	**Fiber**		**Shrinkage Strain (με)**		
			Type	*Content*	*7-day*	*30-day*	*90-day.*
L1	0.20	0.7:0.3	OL	2.0%	-	-	-
L2	0.20	1:0	OL	2.0%	-	-	-
L3	0.20	1:0	OL	2.0%	-	-	-
L4	0.18	1:0	OL	2.0%	451	521	552
L5	0.20	1:0	HF	2.0%	450	530	560
L6	0.20	1:0	A	1.5%	413	496	526
L7	0.20	1:0	OL	4.0%	593	668	718
L8	0.20	1:0	HF	4.0%	470	555	594
L9	0.20	1:0	Sy	2.0%	403	475	552
L10	0.20	1:0	Sy	1.0%	513	600	670
				Average =	470	549	596

The shrinkage development over time during the first few months after casting for four of the large-scale batches is shown in Figure 5.42. A higher volume (2 percent versus 1 percent) of synthetic fibers led to an average 21.4 percent decrease in the total measured shrinkage strain at 90 days after casting.

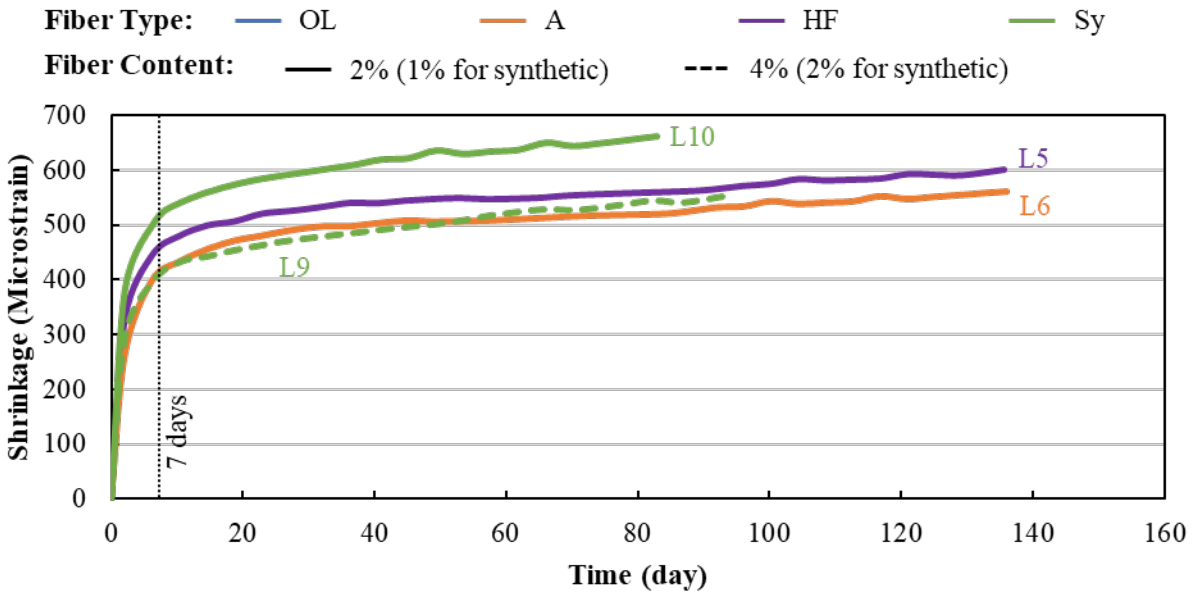

Figure 5.42: Effect of fiber type and content on shrinkage

5.7. Summary and Observations

Ten (10) large-scale batches were cast to investigate the effect of (a) different fiber types and fiber contents, (b) w/b and UFR content, and (c) source of constituent materials on the performance of the developed UHPC mixtures. The following tests were performed to determine the mechanical properties of the UHPC mixtures:

- Flowability
- Setting time
- Compressive strength
- Modulus of elasticity
- Splitting tensile strength
- Modulus of rupture
- Bulk resistivity
- Shrinkage

Some of main observations from the large-scale batches are listed below (organized by test).

1. **Flowability**: Flow should be kept between 8 and 10 inches to help prevent fiber settlement and ensure sufficient workability and working time. This was achieved using a HRWR dosage between 22 and 29.4 oz./cwt. A typical dosage of 27.5 oz./cwt could be used for all mixtures with w/b of 0.20 and with only fine masonry sand (i.e., no UFR).
2. **Set Time**: Initial set times varied between 4.3 and 6.3 hours; final set times varied between 8.0 and 11.5 hours. Mixtures with higher fiber contents had shorter final set times. Lower w/b and UFR substitution had shorter initial and final set times.

3. **Compressive Strength**: Mixtures with steel fibers, w/b of 0.2, and no UFR had average compressive strengths between 17.0 and 17.6 ksi at 28 days. There was no clear trend between steel fiber type and fiber content and compressive strength. The mixtures with synthetic fibers had a 36 percent lower strength than steel fibers for 2 percent synthetic fibers and 12.4 percent lower strength for 1 percent synthetic fibers (at 28 days). Decreasing the w/b from 0.20 to 0.18 slightly increased the compressive strength (between 2 and 6 percent depending on concrete age). The compressive strength for the concrete with materials from Oklahoma had a slightly higher compressive strength (around 3 percent higher). Moist curing did not consistently affect the compressive strength.
4. **Density**: The average measured density of the UHPC varied between 148 and 155 pcf for the mixtures with steel fibers. The average measured density was less for the mixtures with synthetic fibers, between 141 and 145 pcf. Mixtures with 4 percent steel fibers had about a 3 percent higher density than the similar mixtures with 2 percent steel fibers. The higher amount of synthetic fibers (2 percent) decreased the density of the mix by about 2 percent compared to the 1 percent synthetic fiber mixture.
5. **Modulus of Elasticity**: The average modulus of elasticity varied between 7,796 and 9,144 ksi for the mixtures with steel fibers and 7,293 and 8,147 ksi for mixtures with synthetic fibers. Increasing the steel fiber content from 2 to 4 percent increased the modulus by an average of 12.2 percent for OL fibers and decreased modulus by 2.2 percent for HF fibers. The use of 2 percent HF fibers produced samples with a 13.7 percent higher modulus than similar samples with OL fibers. Samples with 4 percent of OL and HF fibers had comparable moduluses. The use of synthetic fibers led to the lowest moduluses among the large-scale batches. A lower w/b and use of UFR increased the modulus. Samples made with the Oklahoma materials had an average 13.2 percent higher modulus than those made with materials from south Florida. Moist curing of samples led to an average 7.5 higher modulus than those not moist cured.
6. **Splitting Tensile Strength**: The average splitting tensile strength varied between 2.39 and 2.93 ksi for the mixtures with steel fibers and 1.38 and 1.49 ksi for mixtures with synthetic fibers. There was a slight increase in splitting tensile strength when increasing from 2 to 4 percent OL fibers and a slight decrease for HF fibers. Decreasing the w/b to 0.18 increased the average splitting tensile strength by 6.4 percent compared to w/b of 0.20. Using UFR decreased the splitting tensile strength slightly (2.3 percent). Moist curing did not consistently affect the splitting tensile strength of the samples.
7. **Modulus of Rupture**: The average modulus of rupture varied between 2.49 ksi and 4.05 for the mixtures with steel fibers and 1.29 and 1.34 for synthetic fibers. An increased steel fiber content (2 to 4 percent) increased the average MOR for samples with OL and HF fibers. The use of HF fibers led to the highest MOR. The Dramix 4D 65/35BG (A) had a higher MOR than the OL fibers but less than HF fibers. The MOR increased with a w/b of 0.18 (compared to w/b of 0.20) and with the use of UFR.
8. **Bulk Resistivity**: All mixtures had average bulk resistivities in the very low classification of permeability measurements. The presence of steel fibers dramatically decreased the bulk resistivity. Higher steel fiber contents led to lower bulk resistivity.

9. **Shrinkage**: The average shrinkage strains were 470, 549, and 596 microstrain for 7, 30, and 90 days after casting. Shrinkage was only measured in some of the large-scale batches at the time of this report. Additional samples were being constructed to measure shrinkage in the other mixtures.

The best mix design based on the large-scale batches is summarized in Table 5.15.

Table 5.15: Proposed non-proprietary UHPC mix designs

Mix.	Cement Type	W/B	Mix Proportions						Fiber		Admixtures	
			ag/cm	*C*	*S*	*SF*	*FA*	*UFR*	*Type*	*Content (%)*	*HRWR (oz./cwt)*	*VMA (oz./cwt)*
L3	Titan Type I/II	0.20	1.0	0.6	0.3	0.1	1.00	0.00	HF or OL	2.0	27.5	0
L1	Titan Type I/II	0.20	1.0	0.6	0.3	0.1	0.70	0.30	HF or OL	2.0	29.5	0

The approximate cost of these mixtures was determined based costs obtained from the suppliers of the different materials. The approximate costs do not include any freight costs to ship the materials.

- Type I/II Cement: $100/ton
- Silica Fume: $1,000/ton
- Slag: $100/ton
- Fine Masonry Sand: $15/ton
- UFR: currently not a commercial product
- HRWR: $0.15 per oz.
- VMA: $0.14 per oz.
- Fibers: $2.00/lb.
- Water: $0.004/gallon ($0.00048/lb)

Using these costs, the cost for the proposed mix is around $800 per cubic yard (with around $530 per cubic yard of this amount being for the steel fibers).

CHAPTER 6. NON-PROPRIETARY UHPC WORKSHOP

6.1. Introduction

A technology transfer workshop was held as part of the 2019 International ABC Conference in Miami to share the performance, observations, and recommendations for the "ABC-UTC Non-Proprietary UHPC Mix" project from all the partner universities. This workshop was coordinated by the University of Oklahoma (OU) and involved presentations by each partner university. The workshop also involved a lab demonstration of mixing of the UHPC mixture. Details for the lab demonstration were coordinated by OU and FIU.

6.2. Workshop Descriptions

The workshop descriptions from the 2019 International ABC Conference Program are shown below. Both workshops were coordinated by Royce Floyd (OU).

- ***W-03: Non-Proprietary UHPC for ABC, Part 1: Mix Development and Material Properties***: Ultra-high performance concrete (UHPC) has the potential to provide significant benefits in many applications for ABC due to its superior mechanical and durability properties. This workshop will cover the basics of non-proprietary UHPC mix development, material properties, and applications of non-proprietary UHPC mix designs for ABC. It will include presentations on the need for non-proprietary UHPC, mix design development and material selection, non-proprietary UHPC material properties, effect of regionally available materials on mix performance, results of ongoing research sponsored by the ABC-UTC on structural behavior and durability of non-proprietary UHPC, and a summary of research conducted by other states and entities.
- ***W-07: Non-Proprietary UHPC for ABC, Part 2: Demonstration and Implementation***: Non-proprietary UHPC has the potential to be a viable option for ABC applications requiring performance exceeding that of conventional concrete. The differences in mixing, placement, finishing, curing, and testing methods required for UHPC compared to conventional concrete are best understood by practical exposure. This workshop will include demonstration of mixing, placement, and testing of non-proprietary UHPC with hands-on participation by the workshop attendees. It will also include a presentation on the upcoming ABC-UTC "Guide for ABC-UTC Non-Proprietary UHPC" and panel discussion that will identify important elements to consider when specifying non-proprietary UHPC.

6.3. Lab Demonstration

Two small mixtures (0.15 ft^3) and one large mixture (2.2 ft^3) were cast during the demonstration. Different steps in the UHPC mixing process were highlighted during the demonstration, including weighing and preparing the materials, the importance of moisture content of aggregates, mixing, pouring, and cylinder sample demolding and grinding process were explained in detail. A spread flow test was conducted on the different mixtures. Different custom formwork were created for the demonstration to show the self-compacting quality of the UHPC: one with congested rebar and the other in the shape of the FIU logo. Some photographs from the lab demonstration portion of the workshop are shown in Figure 6.1 and Figure 6.2.

(a) (b) (c)

Figure 6.1: Flowability Test; (a) overdosed HRWR mix, (b) and (c) regular HRWR dosage mix

(a) (b)

Figure 6.2: Pouring UHPC; (a) congested rebar formwork and (b) FIU logo formwork

CHAPTER 7. SUMMARY AND CONCLUSIONS

Ultra-high performance concrete (UHPC) is generally known as a cementitious composite material with compressive strength (greater than 18 ksi) and high tensile strength (greater than 1 ksi) [1], [3]. UHPC is continually becoming more popular among academia, engineers, and owners due to its unique properties. Commercially available UHPC products offer consistent quality and material properties, but their use has been limited due to their high cost, which can be 25 to 30 times more expensive than conventional concrete.

The research effort conducted under this project aimed to study the effect of different variables, including fiber type, fiber content, cement type, cement content, HRWR dosage, VMA dosage, w/b, and UFR content, on the final mechanical properties of UHPC mixtures. Knowledge gained from this investigation was then used to develop a non-proprietary UHPC mix design, labeled "ABC-UTC Non-Proprietary UHPC Mix," made with local materials achieving the necessary mechanical properties and durability for use in bridge components, repair, and connections. A total of 115 small-scale batches (0.15 ft^3) and 10 large-scale batches (2.2 ft^3) were cast to investigate the different variables and develop the final mixture design.

Some of the major conclusions from this research are summarized below:

1. Particle packing theory can be used with simple spreadsheets as a first step in the UHPC mixture development phase.
2. The fine aggregate moisture content affected the repeatability of the UHPC mixtures. Fine aggregates should be oven dried to ensure consistent material properties can be achieved.
3. Type I/II or Lehigh White cement resulted in similar compressive strengths and workability. Type III cement led to higher compressive strength but shortened the working time for the UHPC.
4. A water-to-binder ratio between 0.18 and 0.20 produced the highest compressive strength while maintaining a good flow and working time. The water content in the chemical admixtures can affect the compressive strength and should be considered when determining how much water should be added to a mixture.
5. Flow should be kept between 8 and 10 inches to help prevent fiber settlement and ensure sufficient workability and working time. This was achieved using a HRWR dosage between 22 and 29.4 oz./cwt. A typical dosage of 27.5 oz./cwt could be used for all mixtures with w/b of 0.20 and with only fine masonry sand (i.e., no UFR).
6. VMA content did not influence the compressive strength. VMA can be used at dosages less than 10 oz./cwt to stabilize heavier steel fibers in the mixtures.
7. The use of fibers with 0.5-inch length, 0.008-inch diameter, and tensile strength of 400 ksi led to the best overall performance of the UHPC. This size fiber reasonably distributed in the mixture without the addition of any VMA.
8. Uncoated fibers with high zinc contents can lead to an expansive reaction in the UHPC that greatly decreases its strength. This reaction can be observed in small-scale (0.15 ft^3) trial batches.

9. The use of synthetic fibers led to lower compressive strength, density, modulus of elasticity, and tensile strength compared to similar mixtures with steel fibers. The use of synthetic fibers did lead to higher bulk resistivity than similar mixtures with steel fibers.
10. Higher steel fiber contents (2 versus 4 percent) generally led to higher tensile strength but similar compressive strength and modulus of elasticity. Higher steel fiber contents also decreased the bulk resistivity.
11. The use of ultra-fines recovery (UFR) materials at a 30 percent replacement generally led to improved performance. In the small-scale batches, its use was found to increase compressive strengths by 10 to 15 percent. The large-scale batches resulted in similar compressive strength and modulus of elasticity, and higher tensile strength. More HRWR is needed for mixtures with UFR to achieve flows between 8 and 10 inches.
12. All mixtures had average bulk resistivities in the very low classification of permeability measurements. The presence of steel fibers dramatically decreased the bulk resistivity. Higher steel fiber contents led to lower bulk resistivity.
13. The average shrinkage strains were 470, 549, and 596 microstrain for 7, 30, and 90 days after casting.

Two mix designs were developed based on the availability of UFR and summarized in Table 7.1. These mixtures gave compressive strengths close to the 18-ksi minimum and had modulus of rupture strengths above the 1.5-ksi first crack and 2.0-ksi peak minimum values typically used for UHPC [3].

Table 7.1: Proposed non-proprietary UHPC mix designs

Mix.	**Cement Type**	**W/B**	**Mix Proportions**						**Fiber**		**Admixtures**	
			ag/cm	*C*	*S*	*SF*	*FA*	*UFR*	*Type*	*Content (%)*	*HRWR (oz./cwt)*	*VMA (oz./cwt)*
1	Titan Type I/II	0.20	1.0	0.6	0.3	0.1	1.00	0.00	HF or OL	2.0	27.5	0
2	Titan Type I/II	0.20	1.0	0.6	0.3	0.1	0.70	0.30	HF or OL	2.0	29.5	0

These mix designs can be used with the procedure outlined in §4.2 to determine the specific amounts of material to use based on the desired quantity of UHPC.

REFERENCES

[1] B. Graybeal, "Ultra-High-Performance Concrete--| Federal Highway Administration," *Accedido marzo*, vol. 23, 2015.

[2] R. Karim, M. Najimi, and B. Shafei, "Assessment of transport properties, volume stability, and frost resistance of non-proprietary ultra-high performance concrete," *Construction and Building Materials*, vol. 227, p. 117031, 2019.

[3] M. K. Tadros et al., "Implementation of Ultra-High-Performance Concrete in Long-Span Precast Pretensioned Elements for Concrete Buildings and Bridges," *Precast/Prestressed Concrete Institute (PCI)*, Jan. 2020.

[4] K. Wille, A. E. Naaman, and G. J. Parra-Montesinos, "Ultra-High Performance Concrete with Compressive Strength Exceeding 150 MPa (22 ksi): A Simpler Way.," *ACI materials journal*, vol. 108, no. 1, 2011.

[5] M. Berry, R. Snidarich, and C. Wood, "Development of Non-Proprietary Ultra-High Performance Concrete," Montana Dept. of Transportation Research Programs, 2017.

[6] B. Graybeal, "UHPC in the US Highway Infrastructure," *Designing and Building with UHPFRC, Marseille, France*, 2009.

[7] H. Russel and B. Graybeal, "Ultra-High-Performance Concrete: A State-of-the-Art Report for the Bridge Community. Federal Highway Administration; McLean, VA," 2013.

[8] B. Graybeal, "Design and construction of field-cast UHPC connections.," United States. Federal Highway Administration, 2019.

[9] D. Garber and E. Shahrokhinasab, "Performance Comparison of In-Service, Full-Depth Precast Concrete Deck Panels to Cast-in-Place Decks," Accelerated Bridge Construction University Transportation Center (ABC-UTC), 2019.

[10] ACI Committee 239, "Ultra-High Performance Concrete: An Emerging Technology Report (ACI 239R-18)," *Farmington Hills, MI: American Concrete Institute*, 2018.

[11] Association Francaise de Normalisation (AFNOR), "Concrete - Ultra-high performance fibre-reinforced concrete - Specifications, performance, production and conformity.," *AFNOR France*, pp. 18–470, France 2016.

[12] American Society for Testing and Materials (ASTM), "C1856/C1856M - 17 - Standard Practice for Fabricating and Testing Specimens of Ultra-High Performance Concrete," 2017.

[13] Canadian Standards Association, "CSA A23.1 Concrete materials and methods of concrete construction, Annex U - Ultra-high Performance Concrete (UHPC).," *Mississauga, Ontario: Canadian Standards Associatoin.*, 2019.

[14] B. Graybeal, "Design and construction of field-cast UHPC connections.," United States. Federal Highway Administration, 2014.

[15] Swiss Society of Engineers and Architects (SIA). (2016)., “SIA 2052 Béton fibré ultra-performant (BFUP) - Matériaux, dimensionnement et exécution (Ultra-High Performance Fibre Reinforced Cement-based Composites [UHPFRC]- Construction material, dimensioning and application).,” *Zurich: SIA.*, 2016.

[16] Z. Haber, I. D. la Varga, B. A. Graybeal, B. Nakashoji, and R. El-Helou, “Properties and Behavior of UHPC-Class Materials,” Federal Highway Administration (FHWA), FHWA-HRT-18-036, Mar. 2018.

[17] J. Resplendino, “State of the art of design and construction of UHPFRC structures in France,” 2012, pp. 27–41.

[18] C. Sosa Cardenas, I. M. Mantawy, and A. Azizinamini, “Repair of Timber Piles Using Ultra-High-Performance Concrete,” 2021.

[19] A. Azizinamini, S. Rehmat, and A. Sadeghnejad, “Enhancing resiliency and delivery of bridge elements using ultra-high performance concrete as formwork,” *Transportation Research Record*, vol. 2673, no. 5, pp. 443–453, 2019.

[20] A. Khodayari, I. M. Mantawy, and A. Azizinamini, “Introducing a New Connection Detail for Connecting Prefabricated Barrier to Concrete Deck Using UHPC,” 2021.

[21] J. Juhart, N. Randl, W. Schneider, and A. Pichler, “Study on the Application of UHPC for Precast Tunnel Segments,” in *International Symposium on Ultra High Performance Concrete*, 2012, pp. 981–988.

[22] H. Aoude, S. De Carufel, and C. Melançon, “Blast Behavior of One-Way Panel Components Constructed with UHPC,” 2016, vol. 1, no. 1.

[23] S. Sritharan and G. M. Schmitz, “Design of tall wind turbine towers utilizing UHPC,” presented at the 2nd International Symposium on Ultra-High Performance Fibre-Reinforced Concrete (UHPFRC). Marseille, France, 2013.

[24] S. Aaleti, B. Petersen, and S. Sritharan, “Design guide for precast UHPC waffle deck panel system, including connections,” 2013.

[25] J. Heimann, “The implementation of full depth UHPC waffle bridge deck panels,” United States. Federal Highway Administration, 2013.

[26] “hhbc-consulting - UHPC Onshore windmill tower and foundation.” / (accessed Feb. 25, 2021).

[27] P. Acker and M. Behloul, “Ductal® technology: A large spectrum of properties, a wide range of applications,” 2004, pp. 11–23.

[28] P. Fontana *et al.*, “Composite UHPC façade elements with functional surfaces,” *HiPerMat 2016*, pp. 9–11, 2016.

[29] “Ductal® | Innovative UHPC Solution,” *Ductal*®, Jul. 27, 2015. https://www.ductal.com/en (accessed Feb. 25, 2021).

[30] Utah Department of Transportation (UDOT), "Performance of Accelerated Bridge Construction Projects in Utah: As of August 2016 (Lessons Learned Report)," 2016.

[31] B. A. Graybeal, "Material property characterization of ultra-high-performance concrete," United States. Federal Highway Administration. Office of Infrastructure …, 2006.

[32] P. Li, Q. Yu, and H. Brouwers, "Effect of coarse basalt aggregates on the properties of Ultra-high Performance Concrete (UHPC)," *Construction and Building Materials*, vol. 170, pp. 649–659, 2018.

[33] A. Arora, Y. Yao, B. Mobasher, and N. Neithalath, "Fundamental insights into the compressive and flexural response of binder-and aggregate-optimized ultra-high performance concrete (UHPC)," *Cement and Concrete Composites*, vol. 98, pp. 1–13, 2019.

[34] S. El-Tawil, M. Alkaysi, A. E. Naaman, W. Hansen, and Z. Liu, "Development, Characterization and Applications of a Non Proprietary Ultra High Performance Concrete for Highway Bridges," Michigan Dept. of Transportation, 2016.

[35] M. S. Meddah, S. Zitouni, and S. Belâabes, "Effect of content and particle size distribution of coarse aggregate on the compressive strength of concrete," *Construction and Building Materials*, vol. 24, no. 4, pp. 505–512, 2010.

[36] M. Alkaysi and S. El-Tawil, "Effects of variations in the mix constituents of ultra high performance concrete (UHPC) on cost and performance," *Materials and Structures*, vol. 49, no. 10, pp. 4185–4200, 2016.

[37] Z. B. Haber and B. A. Graybeal, "Experimental Evaluation of Prefabricated Deck Panel Connections," 2015.

[38] B. A. Graybeal, "Development of Non-Proprietary Ultra-High-Performance Concrete for Use in the Highway Bridge Sector: TechBrief," United States. Federal Highway Administration, 2013.

[39] R. Yu, P. Spiesz, and H. Brouwers, "Effect of nano-silica on the hydration and microstructure development of Ultra-High Performance Concrete (UHPC) with a low binder amount," *Construction and Building Materials*, vol. 65, pp. 140–150, 2014.

[40] A. Tafraoui, G. Escadeillas, S. Lebaili, and T. Vidal, "Metakaolin in the formulation of UHPC," *Construction and Building Materials*, vol. 23, no. 2, pp. 669–674, 2009.

[41] A. M. Matos, S. Nunes, C. Costa, and J. L. Barroso-Aguiar, "Characterization of non-proprietary UHPC for use in rehabilitation/strengthening applications," in *Rheology and Processing of Construction Materials*, Springer, 2019, pp. 552–559.

[42] M. Berry, "Feasibility of Non-Proprietary Ultra-High Performance Concrete (UHPC) for Use in Highway Bridges in Montana: Phase II Field Application," 2018.

[43] S. El-Tawil, Y.-S. Tai, J. A. Belcher II, and D. Rogers, "Open-Recipe Ultra-High-Performance Concrete," *Formwork*, p. 33, 2020.

[44] A. J. Giesler, S. B. Applegate, and B. D. Weldon, “Implementing nonproprietary, ultra-high-performance concrete in a precasting plant,” *PCI Journal*, vol. 61, no. 6, pp. 68–80, 2016.

[45] T. Looney, A. McDaniel, J. Volz, and R. Floyd, “Development and characterization of ultra-high performance concrete with slag cement for use as bridge joint material,” *Development*, vol. 1, no. 02, 2019.

[46] A. Neville and an O. M. C. Safari, *Properties of Concrete, Fifth Edition*. 2012. Accessed: Feb. 22, 2021. [Online]. Available: https://www.safaribooksonline.com/complete/auth0oauth2/&state=/library/view//9780273786337/?ar

[47] American Society for Testing and Materials (ASTM), “C109/C109M - Standard Test Method for Compressive Strength of Hydraulic Cement Mortars (Using 2-in. or [50-mm] Cube Specimens),” 2016.

[48] A. Tafraoui, G. Escadeillas, and T. Vidal, “Durability of the ultra high performances concrete containing metakaolin,” *Construction and Building Materials*, vol. 112, pp. 980–987, 2016.

[49] R. Yu, P. Spiesz, and H. Brouwers, “Development of an eco-friendly Ultra-High Performance Concrete (UHPC) with efficient cement and mineral admixtures uses,” *Cement and Concrete Composites*, vol. 55, pp. 383–394, 2015.

[50] E. Shahrokhinasab, F. D. Chitty, M. Vahedi, and S. Zolfagharysaravi, “Improvement of Concrete Characterization Using Nanosilica,” *Computational Engineering and Physical Modeling*, vol. 4, no. 2, pp. 39–52, 2021.

[51] A. Nasution, I. Imran, and M. Abdullah, “Improvement of concrete durability by nanomaterials,” *Procedia Engineering*, vol. 125, pp. 608–612, 2015.

[52] A. Ehsani, M. Nili, and K. Shaabani, “Effect of nanosilica on the compressive strength development and water absorption properties of cement paste and concrete containing Fly Ash,” *KSCE Journal of Civil Engineering*, vol. 21, no. 5, pp. 1854–1865, 2017.

[53] A. Çevik, R. Alzeebaree, G. Humur, A. Niş, and M. E. Gülşan, “Effect of nano-silica on the chemical durability and mechanical performance of fly ash based geopolymer concrete,” *Ceramics International*, vol. 44, no. 11, pp. 12253–12264, 2018.

[54] A. M. Fadzil, M. M. Norhasri, M. Hamidah, M. Zaidi, and J. M. Faizal, “Alteration of nano metakaolin for ultra high performance concrete,” in *InCIEC 2013*, Springer, 2014, pp. 887–894.

[55] M. M. Norhasri, M. Hamidah, A. M. Fadzil, and O. Megawati, “Inclusion of nano metakaolin as additive in ultra high performance concrete (UHPC),” *Construction and Building Materials*, vol. 127, pp. 167–175, 2016.

[56] A. E. Naaman, “Fiber reinforced concrete: Five decades of progress,” 2018, pp. 22–25.

[57] A. E. Naaman, *Fiber reinforced cement and concrete composites*. Techno Press 3000, 2018.

[58] M. Lachemi, K. Hossain, V. Lambros, P.-C. Nkinamubanzi, and N. Bouzoubaa, "Performance of new viscosity modifying admixtures in enhancing the rheological properties of cement paste," *Cement and concrete research*, vol. 34, no. 2, pp. 185–193, 2004.

[59] J. S. Lawler, M. K. Tadros, M. Lampton, and E. N. Wagner, "Development of Non-Proprietary UHPC for Florida Precast Applications," 2019, vol. 2, no. 1.

[60] American Society for Testing and Materials (ASTM), "ASTM C1760-12-Standard Test Method for Bulk Electrical Conductivity of Hardened Concrete," 2012.

[61] American Society for Testing and Materials (ASTM), "C39/C39M-21 - Standard Test Method forCompressive Strength of Cylindrical Concrete Specimens," 2021.

[62] American Society for Testing and Materials (ASTM), "C78/C78M-18 - Standard Test Method for Flexure Strength of Concrete (Using Simple Beam with Third-Point Loading)," 2018.

[63] American Society for Testing and Materials (ASTM), "C469/C469M-14 - Standard Test Method for Static Modulus of Elasticity and Poisson's Ratio of Concrete in Compression," 2014.

[64] American Society for Testing and Materials (ASTM), "C496/C496M-17 - Standard Test Method for Splitting Tensile Strength of Cylindrical Concrete Specimens," 2017.

[65] American Society for Testing and Materials (ASTM), "C1437-20 - Standard Test Method for Flow of Hydraulic Cement Mortar," 2020.

[66] American Society for Testing and Materials (ASTM), "C403/C403M - 16 - Standard Test Method for Time of Setting of Concrete Mixtures by Penetration Resistance," 2016.

[67] American Society for Testing and Materials (ASTM), "C230/C230M - 21 - Standard Specification for Flow Table for Use in Tests of Hydraulic Cement," 2021.

[68] A. Andreasen, "Über die Beziehung zwischen Kornabstufung und Zwischenraum in Produkten aus losen Körnern (mit einigen Experimenten)," *Kolloid-Zeitschrift*, vol. 50, no. 3, pp. 217–228, 1930.

[69] D. Dinger and J. Funk, "Predictive process control of crowded particulate suspensions," 1994.

[70] Z. Rong, W. Sun, H. Xiao, and W. Wang, "Effect of silica fume and fly ash on hydration and microstructure evolution of cement based composites at low water–binder ratios," *Construction and Building Materials*, vol. 51, pp. 446–450, 2014.

[71] S. A. Fennis and J. C. Walraven, "Using particle packing technology for sustainable concrete mixture design," *Heron, 57 (2012) 2*, 2012.

[72] H. Brouwers and H. Radix, "Self-compacting concrete: the role of the particle size distribution," 2005, pp. 109–118.

[73] S. Pradhan, S. Kumar, and S. V. Barai, “Recycled aggregate concrete: Particle Packing Method (PPM) of mix design approach,” *Construction and Building Materials*, vol. 152, pp. 269–284, 2017.

[74] A. Rahul, M. Santhanam, H. Meena, and Z. Ghani, “3D printable concrete: Mixture design and test methods,” *Cement and Concrete Composites*, vol. 97, pp. 13–23, 2019.

[75] D. P. Bentz, “Influence of water-to-cement ratio on hydration kinetics: simple models based on spatial considerations,” *Cement and concrete research*, vol. 36, no. 2, pp. 238–244, 2006.

[76] X. Pang, “The effect of water-to-cement ratio on the hydration kinetics of Portland cement at different temperatures,” 2015, vol. 13, p. 16.

[77] D. M. Kirby and J. J. Biernacki, “The effect of water-to-cement ratio on the hydration kinetics of tricalcium silicate cements: Testing the two-step hydration hypothesis,” *Cement and Concrete Research*, vol. 42, no. 8, pp. 1147–1156, 2012.

[78] A. J. Giesler, S. B. Applegate, and B. D. Weldon, “Implementing nonproprietary, ultra-high-performance concrete in a precasting plant,” *PCI Journal*, vol. 61, no. 6, pp. 68–80, 2016.

[79] T. Looney, A. McDaniel, J. Volz, and R. Floyd, “Development and characterization of ultra-high performance concrete with slag cement for use as bridge joint material,” *Development*, vol. 1, no. 02, 2019.

[80] “Viscosity Modifying Admixtures (VMAs) in Concrete,” *The Constructor*, Dec. 02, 2018. https://theconstructor.org/concrete/viscosity-modifying-admixture-vma-concrete/5903/ (accessed Apr. 09, 2021).

[81] “Mortar Penetration Resistance Apparatus.” https://www.humboldtmfg.com/mortar-penetration-resistance-apparatus.html (accessed Apr. 23, 2021).

[82] “Compressometer, Extensometer with LSCT.” https://www.humboldtmfg.com/compressometerextensometer-with-lsct.html (accessed Apr. 23, 2021).

[83] B. A. Graybeal, “Development of Non-Proprietary Ultra-High-Performance Concrete for Use in the Highway Bridge Sector: TechBrief,” United States. Federal Highway Administration, 2013.

[84] “Bulk Resistivity Accessory,” *GlobalGilson.com*. https://www.globalgilson.com/bulk-resistivity-accessory (accessed Mar. 15, 2021).

[85] Proceq SA, “Resipod Family Operating Instructions,” p. 28, 2017.

[86] J. T. Nugent, “Chloride Penetration Resistance of Concrete: An Examination and Comparison of Short-Term Testing Methods,” Thesis, Jan. 2020.

[87] W. Morris, E. I. Moreno, and A. A. Sagues, “Practical Evaluation of Resistivity of Concrete in Test Cylinders using a Wenner Array Probe,” *Cement and Concrete Research*, vol. 26, no. 12, pp. 1779–1787, 1996.

APPENDIX A. SPREADSHEET DEVELOPMENT FOR NON-PROPRIETARY UHPC MIXTURE DESIGN

A spreadsheet was developed to aid in the mix design procedure based on the particle packing analysis. The particle size distribution (PSD) analysis results are input in the spreadsheet and curves for each material developed, as shown in Figure A.1.

		Cement	Slag	Silica Fume	Sand	UFR
mm(μm/1000)	μm	Average	Average	Average	Average	Average
0.001	1	4.93	5.60	1.17	3.72	0.15
0.002	2	9.68	11.49	2.27	3.72	0.28
0.003	3	14.35	17.49	3.38	3.73	0.41
0.004	4	18.78	23.31	4.48	3.73	0.53
0.005	5	22.83	28.78	5.58	3.74	0.66
0.006	6	26.52	33.88	6.82	3.74	0.79
0.007	7	29.95	38.66	8.06	3.74	0.92
0.008	8	33.17	43.14	9.30	3.75	1.04
0.010	10	39.23	51.30	11.77	3.76	1.30
0.012	12	44.94	58.46	13.44	3.77	1.55
0.014	14	50.36	64.68	14.35	3.78	1.81
0.016	16	55.49	70.04	15.27	3.78	2.06
0.018	18	60.32	74.65	16.18	3.79	2.32
0.020	20	64.82	78.58	17.10	3.80	2.57
0.022	22	68.97	81.95	17.59	3.81	2.83
0.024	24	71.76	84.02	18.09	3.82	3.08
0.025	25	74.54	86.09	18.26	3.83	3.21
0.028	28	79.34	89.35	18.80	3.84	3.59
0.030	30	82.13	91.12	19.15	3.85	3.85
0.032	32	84.62	92.64	19.51	3.86	4.10
0.034	34	86.83	93.92	19.79	3.87	4.36
0.036	36	88.77	95.01	20.07	3.87	4.61
0.037	37	89.63	95.48	20.21	3.88	4.74
0.038	38	90.48	95.94	20.33	3.88	4.87
0.040	40	91.98	96.73	20.57	3.89	6.02
0.043	43	93.87	97.68	20.93	3.91	7.75
0.044	44	94.40	97.93	21.05	3.91	8.33
0.045	45	94.93	98.19	21.15	3.92	8.91
0.050	50	96.99	99.13	21.64	3.94	11.79
0.053	53	97.90	99.49	21.94	3.95	13.52
0.055	55	98.40	99.67	22.10	3.96	14.67
0.056	56	98.62	99.74	22.18	3.96	15.25
0.060	60	99.31	99.94	22.50	3.98	17.55
0.063	63	99.57	99.97	22.74	4.00	19.28
0.066	66	99.84	99.99	22.93	4.01	21.01
0.071	71	99.99	100.00	23.24	4.03	23.89
0.074	74	100.00	100.00	23.43	4.05	25.62
0.075	75	100.00	100.00	23.48	4.05	26.20
0.080	80	100.00	100.00	23.71	4.27	30.14
0.085	85	100.00	100.00	23.94	4.49	34.08
0.088	88	100.00	100.00	24.08	4.63	36.44
0.090	90	100.00	100.00	24.13	4.71	38.02
0.095	95	100.00	100.00	24.26	5.51	41.96
0.112	112	100.00	100.00	24.71	8.22	55.36
0.125	125	100.00	100.00	25.06	10.29	65.60
0.150	150	100.00	100.00	25.72	14.27	85.30
0.210	210	100.00	100.00	27.88	41.53	99.90
0.500	500	100.00	100.00	100.00	100.00	100.00

(a)

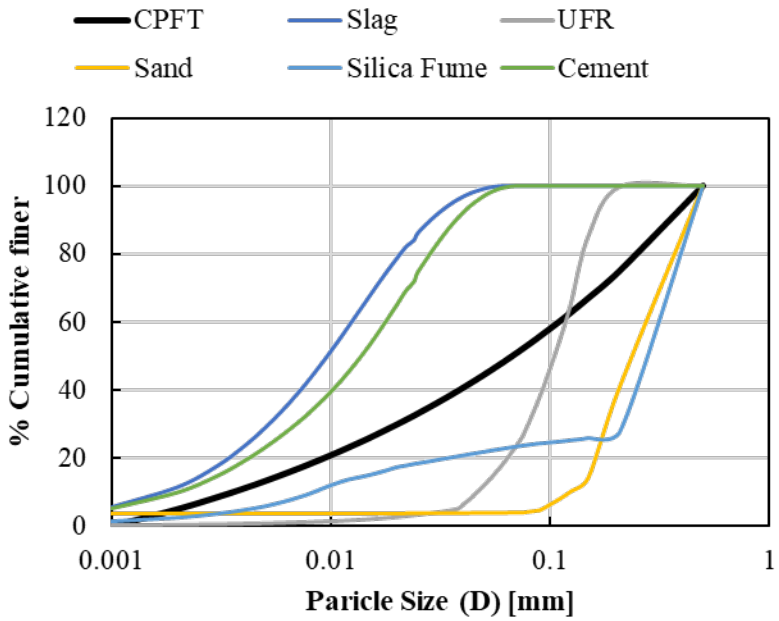

(b)

Figure A.1: Particle size distribution (PSD) analysis inputs, (a) data and (b) plot

The proportions of the different constituent materials can be input for up to nine different mix designs, as shown in Figure A.2. The total proportion of the materials should equal 2.0. A cementitious material to fine aggregate ratio (cm:agg) of 1:1 was used for most of the mix designs in this research, so the sum of the proportion of cementitious materials should equal 1.0 and sum of the sand and UFR should equal 1.0. The minimum particle size (D_{min}), maximum particle size (D_{max}), and distribution modulus (q) are also inputs in the spreadsheet. These values are used to determine the idealized particle size distribution curve using Equation A-1.

$$D(P) = \frac{D^q - D_{min}^q}{D_{max}^q - D_{min}^q} \qquad \text{Equation A-1}$$

This is discussed in more detail in Chapter 3.

Proportions						
Mixes	Cement	Slag	Silica Fume	Sand	UFR	
OPT#1	0.60	0.30	0.10	1.00	0.00	2.00
OPT#2	0.65	0.25	0.10	1.00	0.00	2.00
OPT#3	0.70	0.20	0.10	1.00	0.00	2.00
OPT#4	0.67	0.23	0.10	1.00	0.00	2.00
OPT#5	0.67	0.30	0.13	0.90	0.00	2.00
OPT#6	0.60	0.30	0.10	0.90	0.10	2.00
OPT#7	0.60	0.30	0.10	0.80	0.20	2.00
OPT#8	0.60	0.30	0.10	0.70	0.30	2.00
OPT#9	0.60	0.30	0.10	0.60	0.40	2.00

	Cells required to be filled by user

Other Inputs	
D_{min} [mm] =	0.001
D_{max} [mm] =	0.5
q =	0.25

Figure A.2: Input fields for proportions of different mix designs

The particle size distribution curves are developed for all the proposed mix designs based on the distribution curves of the constituent materials, shown in Figure A.1, and the input proportions, shown in Figure A.2. A sample of some of these curves alongside the idealized particle size distribution curve are shown in Figure A.3. The proportions were varied to decrease the distance between the actual and idealized curves.

Distribution Curves for Optimized Mixture Options								
OPT#1	OPT#2	OPT#3	OPT#4	OPT#5	OPT#6	OPT#7	OPT#8	OPT#9
4.2	4.2	4.2	4.2	4.2	4.1	3.9	3.7	3.5
6.6	6.6	6.5	6.5	6.8	6.4	6.3	6.1	5.9
9.0	8.9	8.8	8.9	9.3	8.8	8.6	8.5	8.3
11.2	11.1	11.0	11.1	11.8	11.1	10.9	10.7	10.6
13.3	13.2	13.0	13.1	14.0	13.2	13.0	12.8	12.7
15.2	15.1	14.9	15.0	16.1	15.1	15.0	14.8	14.7
17.1	16.8	16.6	16.8	18.0	16.9	16.8	16.6	16.5
18.8	18.5	18.3	18.4	19.9	18.6	18.5	18.4	18.2
21.9	21.6	21.3	21.5	23.3	21.8	21.7	21.6	21.4
24.8	24.5	24.1	24.3	26.4	24.7	24.6	24.5	24.4
27.4	27.1	26.7	26.9	29.2	27.3	27.2	27.1	27.0
29.8	29.4	29.1	29.3	31.8	29.7	29.6	29.6	29.5
32.0	31.6	31.3	31.5	34.2	31.9	31.9	31.8	31.7
34.0	33.6	33.3	33.5	36.3	33.9	33.9	33.8	33.7
35.8	35.4	35.1	35.3	38.3	35.7	35.7	35.6	35.6
36.9	36.6	36.3	36.5	39.5	36.9	36.9	36.8	36.8
38.1	37.8	37.5	37.7	40.8	38.1	38.0	38.0	38.0
40.1	39.8	39.6	39.7	42.9	40.1	40.0	40.0	40.0
41.2	41.0	40.7	40.9	44.2	41.2	41.2	41.2	41.2
42.2	42.0	41.8	41.9	45.2	42.2	42.2	42.2	42.2
43.1	42.9	42.7	42.8	46.2	43.1	43.1	43.1	43.2
43.8	43.7	43.5	43.6	47.0	43.9	43.9	43.9	44.0
44.2	44.0	43.9	44.0	47.4	44.2	44.2	44.3	44.3
44.5	44.4	44.2	44.3	47.8	44.5	44.6	44.6	44.7
45.1	45.0	44.8	44.9	48.4	45.2	45.3	45.4	45.5
45.8	45.7	45.6	45.7	49.2	46.0	46.2	46.4	46.6
46.0	45.9	45.8	45.9	49.4	46.2	46.5	46.7	46.9
46.2	46.1	46.1	46.1	49.7	46.5	46.7	47.0	47.2
47.0	47.0	46.9	46.9	50.5	47.4	47.8	48.2	48.6
47.4	47.3	47.3	47.3	50.9	47.8	48.3	48.8	49.3
47.6	47.5	47.5	47.5	51.1	48.1	48.6	49.2	49.7
47.6	47.6	47.6	47.6	51.2	48.2	48.8	49.3	49.9
47.9	47.9	47.9	47.9	51.5	48.6	49.3	49.9	50.6
48.0	48.0	48.0	48.0	51.6	48.8	49.5	50.3	51.1
48.1	48.1	48.1	48.1	51.7	49.0	49.8	50.7	51.5
48.2	48.2	48.2	48.2	51.8	49.2	50.2	51.2	52.1
48.2	48.2	48.2	48.2	51.8	49.3	50.4	51.4	52.5
48.2	48.2	48.2	48.2	51.8	49.3	50.4	51.5	52.6
48.3	48.3	48.3	48.3	52.0	49.6	50.9	52.2	53.5
48.4	48.4	48.4	48.4	52.1	49.9	51.4	52.9	54.4
48.5	48.5	48.5	48.5	52.1	50.1	51.7	53.3	54.9
48.6	48.6	48.6	48.6	52.2	50.2	51.9	53.6	55.2
49.0	49.0	49.0	49.0	52.6	50.8	52.6	54.4	56.3
50.3	50.3	50.3	50.3	53.8	52.7	55.1	57.4	59.8
51.4	51.4	51.4	51.4	54.8	54.2	56.9	59.7	62.5
53.4	53.4	53.4	53.4	56.6	57.0	60.5	64.1	67.6
67.2	67.2	67.2	67.2	69.0	70.1	73.0	75.9	78.8
100.0	100.0	100.0	100.0	100.0	100.0	100.0	100.0	100.0

(a)

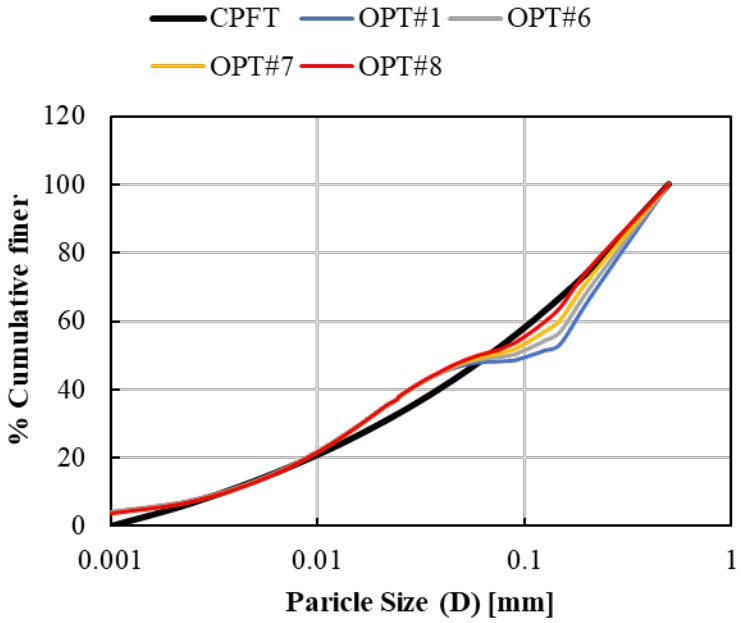

(b)

Figure A.3: Resulting PSD curves for the mix designs, (a) data and (b) plot

A comparison of different distribution moduli (q) was also conducted using the developed spreadsheet, as shown in Figure A.4. A value of q = 0.25 was selected based on previous literature.

A table was also developed in the spreadsheet to determine the required amount of material for all the test specimens, as shown in Figure A.5. A total of 2.2 ft^3 was determined for all the specimens in the test program.

q =	0.25
mm(μm/1000)	CPFT
0.001	0.0
0.002	5.1
0.003	8.5
0.004	11.1
0.005	13.3
0.006	15.2
0.007	16.8
0.008	18.3
0.01	20.9
0.012	23.1
0.014	25.1
0.016	26.8
0.018	28.4
0.02	29.9
0.022	31.3
0.024	32.5
0.025	33.2
0.028	34.9
0.03	35.9
0.032	37.0
0.034	37.9
0.036	38.9
0.037	39.3
0.038	39.8
0.04	40.6
0.043	41.9
0.044	42.3
0.045	42.6
0.05	44.5
0.053	45.5
0.055	46.2
0.056	46.5
0.06	47.8
0.063	48.7
0.066	49.6
0.071	51.0
0.074	51.8
0.075	52.1
0.08	53.4
0.085	54.6
0.088	55.3
0.09	55.8
0.095	56.9
0.112	60.4
0.125	62.9
0.15	67.0
0.21	75.3
0.5	100.0

Comparison of Different *n*

q =	0.1	0.19	0.25	0.37	1
	0.0	0.0	0.0	0.0	0.0
	8.3	6.2	5.1	3.3	0.2
	13.5	10.3	8.5	5.6	0.4
	17.3	13.4	11.1	7.5	0.6
	20.3	15.8	13.3	9.1	0.8
	22.8	18.0	15.2	10.5	1.0
	24.9	19.8	16.8	11.8	1.2
	26.8	21.5	18.3	12.9	1.4
	30.1	24.3	20.9	15.0	1.8
	32.7	26.7	23.1	16.8	2.2
	35.0	28.8	25.1	18.5	2.6
	37.1	30.7	26.8	20.0	3.0
	38.9	32.4	28.4	21.3	3.4
	40.5	34.0	29.9	22.6	3.8
	42.0	35.4	31.3	23.8	4.2
	43.4	36.7	32.5	25.0	4.6
	44.1	37.4	33.2	25.5	4.8
	45.9	39.1	34.9	27.1	5.4
	47.0	40.2	35.9	28.1	5.8
	48.1	41.3	37.0	29.0	6.2
	49.1	42.3	37.9	30.0	6.6
	50.0	43.2	38.9	30.8	7.0
	50.5	43.7	39.3	31.3	7.2
	50.9	44.1	39.8	31.7	7.4
	51.8	45.0	40.6	32.5	7.8
	53.0	46.2	41.9	33.7	8.4
	53.4	46.6	42.3	34.1	8.6
	53.8	47.0	42.6	34.5	8.8
	55.6	48.9	44.5	36.3	9.8
	56.6	49.9	45.5	37.3	10.4
	57.2	50.6	46.2	38.0	10.8
	57.5	50.9	46.5	38.3	11.0
	58.7	52.1	47.8	39.6	11.8
	59.6	53.0	48.7	40.5	12.4
	60.4	53.9	49.6	41.4	13.0
	61.7	55.3	51.0	42.8	14.0
	62.4	56.1	51.8	43.7	14.6
	62.7	56.3	52.1	43.9	14.8
	63.8	57.6	53.4	45.3	15.8
	64.9	58.7	54.6	46.5	16.8
	65.5	59.4	55.3	47.3	17.4
	66.0	59.9	55.8	47.8	17.8
	66.9	60.9	56.9	49.0	18.8
	70.0	64.3	60.4	52.7	22.2
	72.0	66.6	62.9	55.4	24.8
	75.5	70.5	67.0	60.0	29.9
	82.0	78.1	75.3	69.5	41.9
	100.0	100.0	100.0	100.0	100.0

(a)

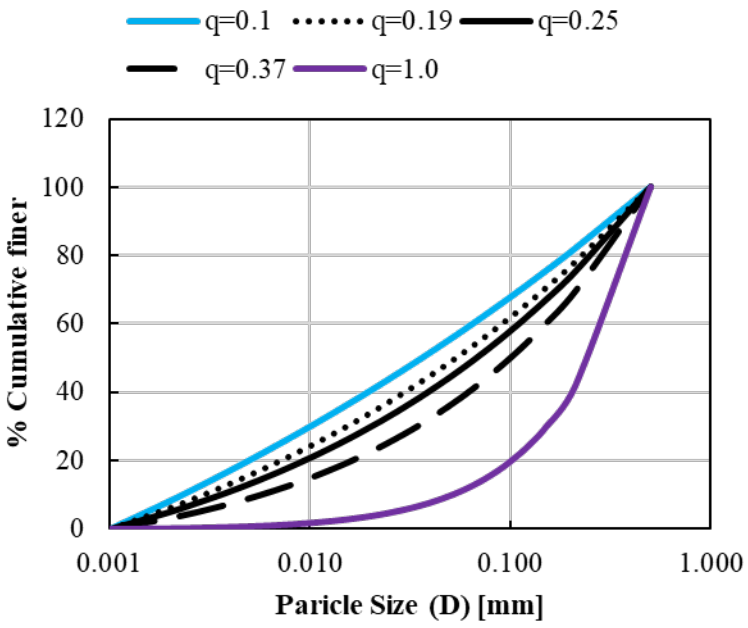

(b)

Figure A.4: Effect of different q values on the idealized PSD curve, (a) data and (b) plot

Tests per mix

	Properties	Test Method	Specimen Shape	d (in)	L (in)	V (in^3)	Total Quantity	V_{tot} (in^3)	V_{tot} (ft^3)
1	Flowability	ASTM C1437	n/a	-	-	17.9	3	53.7	0.03
2	Compression Strength	ASTM C39 ASTM C109	cylinder	3	6	42.4	6	254.5	0.15
3	Modulus of Elasticity and Poisson's Ratio	ASTM C469	cylinder	4	8	100.5	3	301.6	0.17
4	Splitting Tensile Strength	ASTM C496	cylinder	3	6	42.4	3	127.2	0.07
5	Flexural Strength	ASTM C78	prism	3	11	99.0	3	297.0	0.17
6	Direct Tension	FHWA	prism	2	17	68.0	3	204.0	0.12
7	Total Shrinkage	Embedded VWGs	cylinder	6	12	339.3	3	1017.9	0.59
8	Compressive Creep	Embedded VWGs	cylinder	4	8	100.5	0	0.0	0.00
9	Setting Time	ASTM C403	cylinder	6	6	169.6	3	508.9	0.29
10	Freeze-Thaw Resistance	ASTM C666	prism	3	11	99.0	0	0.0	0.00
11	Rapid Chloride Ion Permeability	ASTM C1202	cylinder	4	8	100.5	0	0.0	0.00
								Total volume per mix =	1.60
								20% extra =	0.32
								Total with extra =	1.92
								Taotal Based on desiner decision =	2.2

Figure A.5: Spreadsheet used to determine the UHPC quantity required per mix

A spreadsheet was also developed to convert the proportions for a mix design into the actual amount of material required for a cubic yard, cubic foot, and desired amount of material. This spreadsheet is shown in Figure A.6.

Specified Proportions for Mix	
Fiber Content %	2
Fiber Density (g/cm^3)	7.85
Fiber Density (lb/ft^3)	490
w/b	0.20
HRWR (oz./cwt)	27.5
VMA (oz./cwt)	0
Type I Cement (proportion)	0.60
Slag	0.30
Silica Fume	0.10
Fine sand	1.00
UFR	0.00
Total unit	2.00
No fiber UHPC mix density (lb/ft^3)	148.6

Material per 1 yd^3	
% Fibers (by volume) =	*2*
Type I Cement [lb/yd^3] =	1180
Slag [lb/yd^3] =	590
Silica Fume [lb/yd^3] =	197
w/cm =	0.2
Water [lb/yd^3] =	393
Fine Masonry Sand [lb/yd^3] =	1966
UFR [lb/yd^3] =	0
Steel Fibers [lb/yd^3] =	265
Steel Fibers [%] =	2.0
Glenium 7920 [oz./cwt] =	27.5
cwt of cementitious material / yd^3 =	19.7
Glenium 7920 [oz/yd^3] =	541
MasterMatrix VMA 358 [oz./cwt] =	0.0
MasterMatrix VMA 358 [oz/yd^3] =	0.0

Material per 1 ft^3	
% Fibers (by volume) =	*2*
Type I Cement [lb/ft^3] =	43.7
Slag [lb/ft^3] =	21.8
Silica Fume [lb/ft^3] =	7.3
Water [lb/ft^3] =	14.6
Fine Masonry Sand [lb/ft^3] =	72.8
UFR [lb/ft3] =	0.0
Steel Fibers [lb/ft^3] =	9.8
Glenium 7920 [oz/ft^3] =	20.0
MasterMatrix VMA 358 [oz/ft^3] =	0.0

Materials for [ft^3] =	2.2
% Fibers (by volume) =	2.0
Type I Cement [lb/mix] =	96.1
Slag [lb/mix] =	48.1
Silica Fume [lb/mix] =	16.0
Water [lb/mix] =	32.0
Fine Masonry Sand [lb/mix] =	160.2
UFR [lb/mix] =	0.0
Steel Fibers [lb/mix] =	21.6
Glenium 7920 [oz/mix] =	44.1
MasterMatrix VMA 358 [oz/mix] =	0.0

Figure A.6: Spreadsheets used to determine the amount of material to use for specific mixes

APPENDIX B. RESULTS FROM SMALL-SCALE BATCHES

Detailed results from all small-scale batches are summarized in this section. All the results from the small-scale batches are summarized in the following tables:

- **Table B.1**: Initial mixtures cast with masonry cement and fine aggregate with natural moisture condition (Series OU).
- **Table B.2**: Second series of tests (Series A) with Type I/II cement and fine aggregate with natural moisture condition.
- **Table B.3**: Third series of tests (Series B) with Type I/II cement and fine aggregate with natural moisture condition. This series was used to continue refinement of the mix design and investigate proportions of cementitious materials and w/b ratios.
- **Table B.4**: Fourth series of tests (Series C) all with oven-dried fine aggregate. This series was used to further investigate all the experimental variables and develop the final mix designs to be used for the large-scale batches.

The mixture proportions, flow table results, measured density, and compressive strengths are shown in the tables. The compressive strength and density were generally measured at 3, 7, and 28 days. Generally, the average results from two cylinder tests are shown in the tables.

Table B.1: Initial mixtures with masonry cement and natural moisture aggregate (OU series)

Mix.	Fiber Type	Vol. %	w*/b	w/b	Agg./b	C	Slag	SF	Sand	UFR	Cement Type	HRWR (oz/cwt)	VMA (oz/cwt)	Flow Table (in)	f'c (ksi)			Density (lb/ft^3)		
															3	*7*	*28*	*3*	*7*	*28*
OU1	-	0	0.21	0.20	1	0.60	0.30	0.10	1	0	C-M	15.77	0.00	-	4.1	3.8	7.1	121.6	122.7	119.4
OU2	A	2	0.21	0.20	1	0.60	0.30	0.10	1	0	C-M	15.77	0.00	7.00	5.1	6.6	9.5	-	136.5	134.8
OU3	-	0	0.21	0.20	1	0.60	0.30	0.10	1	0	C-M	31.54	0.00	-	4.2	5.8	7.5	120.8	121.2	121.0
OU4	-	0	0.21	0.20	1	0.60	0.30	0.10	1	0	C-M	23.66	0.00	-	4.0	5.1	6.7	114.8	116.2	116.4
OU5	-	0	0.17	0.16	1	0.60	0.30	0.10	1	0	C-M	23.66	0.00	-	5.5	5.7	8.2	126.5	119.5	122.7
OU6	-	0	0.19	0.18	1	0.60	0.30	0.10	1	0	C-M	25.23	0.00	-	3.3	4.3	4.5	110.3	109.3	109.9
OU7	A	2	0.18	0.17	1	0.60	0.30	0.10	1	0	C-M	23.66	0.00	-	3.4	4.2	5.2	110.1	109.6	109.9

Table B.2: Series A; mixtures with Type I/II cement and natural moisture content in aggregates

Mix.	Fiber Type	Vol. %	w*/b	w/b	Agg./b	C	Slag	SF	Sand	UFR	Cement Type	HRWR (oz/cwt)	VMA (oz/cwt)	Flow Table (in)	f'c (ksi)			Density (lb/ft^3)		
															3	*7*	*28*	*3*	*7*	*28*
A1	-	0	0.21	0.20	1	0.60	0.30	0.10	1	0	C-T-I/II	31.54	0.00	-	9.9	10.6	-	140.2	140.5	-
A2	-	0	0.19	0.18	1	0.60	0.30	0.10	1	0	C-T-I/II	24.19	0.00	-	10.9	13.0	-	145.2	145.5	-
A3	-	0	0.18	0.17	1	0.60	0.30	0.10	1	0	C-T-I/II	20.31	0.00	-	10.3	11.0	-	139.1	139.3	-
A4	A	1	0.19	0.18	1	0.60	0.30	0.10	1	0	C-T-I/II	18.99	0.00	-	8.8	10.9	-	138.2	141.2	-
A5	A	2	0.19	0.18	1	0.60	0.30	0.10	1	0	C-T-I/II	19.52	0.00	-	9.8	11.0	-	146.3	145.4	-
A6	-	0	0.19	0.18	1	0.60	0.30	0.10	1	0	C-T-I/II	15.75	0.00	-	8.1	10.1	-	130.2	137.7	-
A7	-	0	0.19	0.18	1	0.60	0.30	0.10	1	0	C-T-I/II	16.76	0.00	-	9.0	11.2	-	137.4	137.8	-
A8	-	0	0.19	0.18	1	0.60	0.30	0.10	1	0	C-T-I/II	16.48	0.00	-	8.5	-	9.7	142.7	142.5	-
A9	-	0	0.19	0.18	1	0.60	0.30	0.10	1	0	C-T-I/II	15.56	0.00	-	-	8.4	10.9	-	137.6	138.7
A10	A	1	0.19	0.18	1	0.60	0.30	0.10	1	0	C-T-I/II	15.56	0.00	-	-	10.3	11.0	-	141.1	139.8
A11	A	2	0.19	0.18	1	0.60	0.30	0.10	1	0	C-T-I/II	15.56	0.00	-	-	8.4	12.3	-	143.8	146.5
A12	OL	1	0.19	0.18	1	0.60	0.30	0.10	1	0	C-T-I/II	15.56	0.00	-	8.7	10.8	11.9	142.2	143.6	142.2
A13	OL	2	0.19	0.18	1	0.60	0.30	0.10	1	0	C-T-I/II	15.56	0.00	-	9.8	10.1	11.7	145.0	144.5	142.6
A14	H	1	0.19	0.18	1	0.60	0.30	0.10	1	0	C-T-I/II	15.56	0.00	-	5.6	7.6	10.1	139.1	138.7	138.4
A15	H	2	0.19	0.18	1	0.60	0.30	0.10	1	0	C-T-I/II	15.56	0.00	-	4.7	6.5	8.7	141.6	140.4	142.1
A16	OL	1	0.19	0.18	1	0.60	0.30	0.10	1	0	C-T-I/II	15.56	0.00	-	-	9.9	11.7	-	139.4	139.3
A17	OL	2	0.19	0.18	1	0.60	0.30	0.10	1	0	C-T-I/II	15.56	0.00	-	-	10.5	12.7	-	144.4	142.9
A18	-	0	0.19	0.18	1	0.60	0.25	0.15	1	0	C-T-I/II	15.56	0.00	-	6.5	8.2	10.5	134.8	133.2	132.4

Mix.	Fiber Type	Vol. %	w*/b	w/b	Agg./b	C	Slag	SF	Sand	UFR	Cement Type	HRWR (oz/cwt)	VMA (oz/cwt)	Flow Table (in)	f'c (ksi)			Density (lb/ft^3)		
															3	*7*	*28*	*3*	*7*	*28*
A19	H	1	0.19	0.18	1	0.60	0.25	0.15	1	0	C-T-I/II	15.56	0.00	-	6.3	9.5	11.1	137.8	136.0	136.1
A20	H	2	0.18	0.17	1	0.60	0.25	0.15	1	0	C-T-I/II	15.56	0.00	-	5.9	8.7	10.6	138.1	136.9	136.1

Table B.3: Series B; optimization process with natural moisture aggregates

Mix.	Fiber Type	Vol. %	w*/b	w/b	Agg./b	C	Slag	SF	Sand	UFR	Cement Type	HRWR (oz/cwt)	VMA (oz/cwt)	Flow Table (in)	f'c (ksi)			Density (lb/ft^3)		
															3	*7*	*28*	*3*	*7*	*28*
B1	-	0	0.21	0.20	1	0.60	0.30	0.10	1	0	C-T-I/II	15.75	0.00	-	7.2	9.0	12.6	134.9	135.8	138.6
B2	-	0	0.21	0.20	1	0.60	0.25	0.15	1	0	C-T-I/II	15.75	0.00	-	6.9	7.8	10.3	133.8	131.2	130.8
B3	-	0	0.21	0.20	1	0.65	0.25	0.10	1	0	C-T-I/II	15.75	0.00	-	9.0	9.6	13.6	140.8	140.1	140.5
B4	-	0	0.21	0.20	1	0.65	0.20	0.15	1	0	C-T-I/II	15.75	0.00	-	7.6	8.4	11.4	137.3	137.3	135.9
B5	-	0	0.21	0.20	1	0.70	0.20	0.10	1	0	C-T-I/II	15.75	0.00	-	7.9	8.6	12.8	137.5	139.4	139.2
B6	-	0	0.21	0.20	1	0.70	0.15	0.15	1	0	C-T-I/II	15.75	0.00	-	7.5	8.0	11.6	136.4	135.1	136.2
B7	-	0	0.21	0.20	1	0.65	0.23	0.13	1	0	C-T-I/II	15.75	0.00	-	7.4	7.9	11.3	134.7	134.0	135.8
B8	-	0	0.21	0.20	1	0.70	0.18	0.13	1	0	C-T-I/II	15.75	0.00	-	7.1	8.3	11.7	135.2	136.4	135.6
B9	-	0	0.21	0.20	1	0.65	0.25	0.10	1	0	C-T-I/II	18.31	0.00	-	7.5	4.8	13.4	140.3	139.3	144.6
B10	H	2	0.21	0.20	1	0.65	0.25	0.10	1	0	C-T-I/II	18.31	0.00	-	8.8	8.8	15.0	144.2	143.3	144.2
B11	-	0	0.19	0.18	1	0.60	0.30	0.10	1	0	C-T-I/II	23.81	0.00	-	10.5	13.3	15.5	146.8	146.2	146.1
B12	-	0	0.19	0.18	1	0.65	0.23	0.13	1	0	C-T-I/II	18.31	0.00	-	8.6	9.8	11.7	135.2	136.0	137.5
B13	-	0	0.21	0.20	1	0.65	0.23	0.13	1	0	C-T-I/II	18.31	0.00	-	7.9	10.0	14.0	140.4	141.0	142.5
B14	-	0	0.21	0.20	1	0.70	0.18	0.13	1	0	C-T-I/II	18.31	0.00	-	7.7	9.3	12.7	138.7	137.8	140.4
B15	H	1	0.21	0.20	1	0.65	0.25	0.10	1	0	C-T-I/II	15.75	0.00	-	6.9	10.3	12.6	141.6	141.7	141.9
B16	H	2	0.21	0.20	1	0.65	0.25	0.10	1	0	C-T-I/II	15.75	0.00	-	6.3	10.8	13.6	139.3	140.4	140.8
B17	-	0	0.19	0.18	1	0.60	0.30	0.10	1	0	C-T-I/II	23.81	0.00	-	9.6	13.6	18.0	144.4	145.4	146.4
B18	-	0	0.19	0.18	1	0.65	0.25	0.10	1	0	C-T-I/II	23.81	0.00	-	9.2	11.5	16.8	145.2	145.1	146.0
B19	-	0	0.19	0.18	1	0.70	0.20	0.10	1	0	C-T-I/II	23.81	0.00	-	10.9	13.1	15.1	146.7	146.4	146.8
B20	H	2	0.19	0.18	1	0.60	0.30	0.10	1	0	C-T-I/II	23.81	0.00	-	9.8	13.0	15.2	145.2	144.7	144.8
B21	OL	1.5	0.18	0.18	1	0.60	0.30	0.10	1	0	C-T-I/II	11.17	0.00	-	6.6	8.4	10.9	134.6	136.1	137.1
B22	OL	2	0.19	0.18	1	0.60	0.30	0.10	1	0	C-T-I/II	23.81	0.00	-	7.4	10.0	15.2	144.1	146.0	149.0
B23	-	0	0.21	0.20	1	0.60	0.30	0.10	1	0	C-T-I/II	23.81	0.00	-	8.9	12.0	16.6	143.3	145.0	146.0
B24	-	0	0.21	0.20	1	0.60	0.30	0.10	1	0	C-T-I/II	21.97	0.00	-	10.0	11.2	15.8	145.0	134.6	145.8

Mix.	Fiber Type	Vol. %	w*/b	w/b	Agg./b	C	Slag	SF	Sand	UFR	Cement Type	HRWR (oz/cwt)	VMA (oz/cwt)	Flow Table (in)	f'_c (ksi)			Density (lb/ft^3)		
															3	*7*	*28*	*3*	*7*	*28*
B25	OL	2	0.21	0.20	1	0.60	0.30	0.10	1	0	C-T-I/II	21.97	0.00	11.00	9.0	12.5	16.7	149.3	150.2	149.6
B26	OL	2	0.21	0.20	1	0.60	0.30	0.10	1	0	C-T-I/II	20.14	0.00	11.00	8.1	12.9	16.0	146.2	146.1	145.2
B27	OL	2	0.21	0.20	1	0.60	0.30	0.10	1	0	C-T-I/II	18.31	0.00	11.00	9.7	11.1	15.5	144.6	148.0	142.4
B28	OL	2	0.21	0.20	1	0.60	0.30	0.10	1	0	C-T-I/II	16.48	0.00	11.00	4.5	5.4	11.0	136.6	138.6	139.1
B29	OL	2	0.14	0.14	1	0.60	0.30	0.10	1	0	C-T-I/II	11.47	0.00	-	7.0	10.4	10.7	137.5	138.1	138.0
B30	OL	2	0.16	0.16	1	0.60	0.30	0.10	1	0	C-T-I/II	12.60	0.00	-	6.6	9.2	9.0	135.8	135.5	136.4
B31	-	0	0.19	0.18	1	0.60	0.30	0.10	1	0	C-T-I/II	23.81	0.00	-	9.3	12.5	13.0	145.2	145.2	144.9
B32	-	0	0.20	0.18	1	0.60	0.30	0.10	1	0	C-T-I/II	41.93	0.00	-	10.8	13.9	15.8	148.4	148.9	149.2
B33	-	0	0.19	0.18	1	0.60	0.30	0.10	1	0	C-T-I/II	24.17	0.00	-	-	13.6	14.6	-	153.3	148.2

Table B.4: Series C; optimization process with oven-dried aggregates

Mix.	Fiber Type	Vol. %	w*/b	w/b	Agg./b	C	Slag	SF	Sand	UFR	Cement Type	HRWR (oz/cwt)	VMA (oz/cwt)	Flow Table (in)	f'_c (ksi)			Density (lb/ft^3)		
															3	*7*	*28*	*3*	*7*	*28*
C1	OL	2	0.21	0.20	1	0.60	0.30	0.10	1	0	C-A-I/II	20.60	0.00	10.00	9.4	11.6	12.8	148.4	148.6	148.3
C2	OL	2	0.21	0.20	1	0.60	0.30	0.10	1	0	C-T-I/II	22.25	0.00	9.00	9.5	11.6	14.5	144.9	144.5	144.2
C3	OL	2	0.21	0.20	1	0.60	0.30	0.10	1	0	C-A-I/II	22.25	0.00	8.00	9.7	11.3	13.4	148.9	148.2	150.0
C4	OL	2	0.21	0.20	1	0.60	0.30	0.10	1	0	C-W-I	23.35	0.00	7.50	12.7	13.8	14.8	146.3	146.9	146.2
C5	H	2	0.21	0.20	1	0.60	0.30	0.10	1	0	C-T-I/II	24.72	6.41	11.00	6.7	7.6	9.6	146.1	147.0	145.6
C6	A	2	0.22	0.20	1	0.60	0.30	0.10	1	0	C-T-I/II	24.72	8.24	9.50	9.5	10.9	13.0	146.3	147.3	145.5
C7	OL	2	0.22	0.20	1	0.60	0.30	0.10	1	0	C-A-I/II	24.72	8.24	10.00	9.6	12.2	14.6	150.3	149.3	149.6
C8	OL	2	0.22	0.20	1	0.60	0.30	0.10	1	0	C-T-I/II	24.72	8.24	9.50	9.6	11.1	13.4	146.1	146.0	146.3
C9	OL	2	0.21	0.20	1	0.60	0.30	0.10	1	0	C-A-I/II	18.00	0.00	5.00	9.5	12.3	13.9	147.3	148.4	148.5
C10	OL	2	0.24	0.22	1	0.60	0.30	0.10	1	0	C-A-I/II	24.72	8.24	11.50	9.3	12.1	12.1	151.1	151.6	151.0
C11	OL	2	0.23	0.22	1	0.60	0.30	0.10	1	0	C-T-I/II	19.87	6.50	10.50	9.4	11.9	12.9	145.4	144.4	143.9
C12	H	2	0.23	0.22	1	0.60	0.30	0.10	1	0	C-W-I	22.89	6.50	5.00	8.8	9.3	10.8	143.9	143.9	144.7
C13	H	2	0.23	0.22	1	0.60	0.30	0.10	1	0	C-T-I/II	18.49	6.50	9.00	5.5	6.8	7.2	142.5	141.5	142.0
C14	H	2	0.21	0.20	1	0.60	0.30	0.10	1	0	C-T-I/II	22.89	6.50	9.00	5.1	5.9	7.0	143.0	143.3	144.4
C15	OL	2	0.23	0.22	1	0.60	0.30	0.10	1	0	C-T-I/II	18.31	5.86	7.00	9.9	11.4	14.6	142.4	142.1	144.8
C16	OL	2	0.21	0.20	1	0.60	0.30	0.10	1	0	C-T-I/II	26.55	3.02	10.00	10.2	11.9	15.2	-	148.3	149.0

Mix.	Fiber Type	Vol. %	w*/b	w/b	Agg./b	C	Slag	SF	Sand	UFR	Cement Type	HRWR (oz/cwt)	VMA (oz/cwt)	Flow Table (in)	f'c (ksi)			Density (lb/ft^3)		
															3	*7*	*28*	*3*	*7*	*28*
C17	OL	2	0.25	0.24	1	0.60	0.30	0.10	1	0	C-T-I/II	16.39	2.47	10.50	8.8	10.0	12.5	143.0	142.6	142.8
C18	OL	2	0.23	0.22	1	0.65	0.25	0.10	1	0	C-T-I/II	24.72	1.56	11.00	9.3	12.2	13.9	147.1	147.6	147.5
C19	OL	2	0.23	0.22	1	0.70	0.20	0.10	1	0	C-T-I/II	22.43	2.11	11.00	10.5	10.9	13.7	146.5	146.3	146.4
C20	H	2	-	-	-	-	-	-	-	-	Ductal	-	-	-	-	-	5.6	-	-	149.6
C21	OL	2	0.23	0.22	1	0.65	0.23	0.13	1	0	C-T-I/II	22.16	5.22	9.50	9.3	12.1	13.9	142.0	145.9	145.6
C22	OL	2	0.19	0.17	1	0.60	0.30	0.10	1	0	C-T-I/II	41.97	3.27	8.00	11.0	12.9	-	149.9	148.2	-
C23	H	2	-	-	-	-	-	-	-	-	Ductal	-	-	7.00	-	5.6	5.9	-	135.5	140.9
C24	OL	2	0.20	0.18	1	0.60	0.30	0.10	1	0	C-W-I	34.06	0.00	7.00	11.9	14.5	15.1	147.7	148.4	147.8
C25	OL	2	0.23	0.22	1	0.60	0.30	0.10	1	0	C-W-I	24.72	0.00	9.00	11.2	12.7	13.7	144.4	144.5	144.0
C26	OL	2	0.18	0.17	1	0.60	0.30	0.10	1	0	C-T-I/II	35.52	0.00	7.00	12.7	14.0	15.0	150.2	149.6	150.2
C27	OL	2	0.23	0.22	1	0.60	0.30	0.10	1	0	C-T-I/II	22.89	4.30	11.50	10.0	11.7	12.9	145.2	145.1	145.5
C28	OL	2	0.21	0.20	1	0.60	0.30	0.10	1	0	C-T-I/II	21.70	0.00	6.00	11.4	13.0	15.7	146.8	146.9	147.7
C29	OL	2	0.21	0.20	1	0.60	0.30	0.10	1	0	C-T-I/II	21.70	6.50	7.00	11.3	12.9	15.7	145.7	146.3	147.4
C30	OL	2	0.21	0.20	1	0.60	0.30	0.10	1	0	C-A-I/II	19.81	0.00	6.00	9.8	13.2	14.8	148.9	149.7	149.3
C31	OL	2	0.21	0.20	1	0.60	0.30	0.10	1	0	C-T-I/II	27.47	0.00	10.50	10.0	13.7	13.3	146.7	147.4	148.1
C32	OL	2	0.22	0.20	1	0.60	0.30	0.10	1	0	C-T-I/II	27.47	6.50	9.50	11.1	13.4	15.2	146.1	147.7	147.0
C33	OL	2	0.19	0.18	1	0.60	0.30	0.10	1	0	C-T-I/II	27.47	0.00	9.00	12.4	13.5	15.5	150.5	148.6	149.1
C34	OL	2	0.20	0.18	1	0.60	0.30	0.10	1	0	C-T-I/II	27.47	6.50	8.00	12.0	13.6	16.7	151.1	149.4	148.9
C35	OL	2	0.21	0.20	1	0.60	0.30	0.10	1	0	C-T-I/II	27.47	0.00	10.50	-	13.6	-	-	150.5	-
C36	OL	2	0.22	0.20	1	0.60	0.30	0.10	1	0	C-T-I/II	27.47	6.50	10.50	-	13.9	-	-	150.2	-
C37	OL	2	0.21	0.20	1	0.60	0.30	0.10	1	0	C-T-III	27.47	0.00	9.50	12.8	14.2	17.9	148.4	149.6	149.0
C38	OL	2	0.22	0.20	1	0.60	0.30	0.10	1	0	C-T-III	27.47	6.50	9.50	12.3	14.0	17.3	148.3	147.6	149.3
C39	OL	2	0.19	0.18	1	0.60	0.30	0.10	1	0	C-T-III	27.47	0.00	7.50	13.6	14.9	17.1	149.8	150.1	149.7
C40	OL	2	0.18	0.17	1	0.60	0.30	0.10	1	0	C-T-I/II	29.39	0.00	7.50	-	-	19.2	-	-	156.5
C41	OL	2	0.19	0.17	1	0.60	0.30	0.10	1	0	C-T-I/II	29.39	9.16	7.25	-	-	19.5	-	-	151.6
C42	HF	2	0.21	0.20	1	0.60	0.30	0.10	1	0	C-T-I/II	27.47	0.00	10.00	11.2	13.3	17.9	151.4	146.7	147.8
C43	HF	2	0.22	0.20	1	0.60	0.30	0.10	1	0	C-T-I/II	27.47	6.50	10.00	10.5	13.8	16.7	148.5	148.1	148.5
C44	HF	2	0.19	0.18	1	0.60	0.30	0.10	1	0	C-T-I/II	27.47	0.00	8.50	12.3	14.9	18.8	149.7	149.0	152.0
C45	OL	2	0.21	0.20	1	0.60	0.30	0.10	0.9	0.1	C-T-I/II	27.47	0.00	10.00	10.8	13.4	16.8	145.9	146.6	147.0
C46	OL	2	0.21	0.20	1	0.60	0.30	0.10	0.8	0.2	C-T-I/II	27.47	0.00	8.00	11.5	15.5	17.2	147.9	148.8	148.6
C47	OL	2	0.21	0.20	1	0.60	0.30	0.10	0.7	0.3	C-T-I/II	29.39	0.00	9.00	11.8	15.5	17.1	147.6	147.4	147.9
C48	OL	2	0.21	0.20	1	0.60	0.30	0.10	0.65	0.35	C-T-I/II	29.39	0.00	8.00	11.1	14.6	17.8	146.9	146.3	148.6

Mix.	Fiber Type	Vol. %	w*/b	w/b	Agg./b	C	Slag	SF	Sand	UFR	Cement Type	HRWR (oz/cwt)	VMA (oz/cwt)	Flow Table (in)	f'_c (ksi)			Density (lb/ft^3)		
															3	*7*	*28*	*3*	*7*	*28*
C49	-	0	0.20	0.16	1	0.60	0.30	0.10	0.65	0.35	C-T-I/II	85.15	0.00	6.00	-	11.5	14.3	-	140.0	-
C50	-	0	0.20	0.16	1	0.60	0.30	0.10	0.65	0.35	C-T-I/II	85.15	0.00	6.50	-	12.0	13.5	-	140.4	-
C51	-	0	0.19	0.15	1	0.60	0.30	0.10	0.65	0.35	C-T-I/II	92.84	0.00	7.50	-	10.9	15.0	-	138.8	-
C52	OL	2	0.20	0.18	1	0.60	0.30	0.10	0.8	0.2	C-T-I/II	38.08	0.00	9.50	12.0	14.6	18.5	150.7	150.4	151.1
C53	OL	2	0.20	0.18	1	0.60	0.30	0.10	0.7	0.3	C-T-I/II	38.08	0.00	9.25	11.7	14.3	18.3	150.1	150.1	152.3

APPENDIX C. RESULTS FROM LARGE-SCALE BATCHES

Detailed results from the large-scale experimental section are summarized in this section. A summary of the mixture proportions, compressive strengths, density, modulus of elasticity, modulus of rupture, and splitting tensile strength are summarized in Table C.1 and Table C.2.

Table C.1: Large-scale UHPC batches -mix proportions, compressive strength, and density

Mix.	Fiber Type	Vol. %	w*/b	w/b	Agg./b	C	Slag	SF	Sand	UFR	Cement Type	HRWR (oz/cwt)	VMA (oz/cwt)	Flow Table (in)	f'c (ksi)					Density (lb/ft^3)				
															3	*7*	*14*	*28*	*56*	*3*	*7*	*14*	*28*	*56*
L1	OL	2	0.21	0.20	1	0.60	0.30	0.10	0.7	0.3	C-T-I/II	29.4	0.00	9.50	11.8	14.6	15.5	16.7	18.1	149.5	151.0	149.4	149.4	149.6
L2	OL	2	0.21	0.20	1	0.60	0.30	0.10	1	0	C-A-I/II	22.0	0.00	10.00	11.0	14.0	15.7	17.6	18.2	153.1	153.4	152.9	153.5	153.2
L3	OL	2	0.21	0.20	1	0.60	0.30	0.10	1	0	C-T-I/II	27.5	0.00	10.50	12.2	14.4	15.5	17.1	17.6	148.8	150.8	149.8	149.6	149.5
L4	OL	2	0.19	0.18	1	0.60	0.30	0.10	1	0	C-T-I/II	27.5	0.00	8.00	12.0	14.9	16.4	17.8	18.1	150.4	151.6	151.0	151.1	151.5
L5	HF	2	0.21	0.20	1	0.60	0.30	0.10	1	0	C-T-I/II	27.5	0.00	9.50	12.1	14.3	15.4	17.5	18.0	148.4	147.6	149.0	148.5	149.9
L6	A	1.5	0.21	0.20	1	0.60	0.30	0.10	1	0	C-T-I/II	27.5	4.49	9.50	11.7	14.9	16.2	17.3	17.6	150.6	151.3	151.7	151.4	150.2
L7	OL	4	0.21	0.20	1	0.60	0.30	0.10	1	0	C-T-I/II	27.5	0.00	8.50	12.0	14.3	15.0	17.0	17.1	154.2	155.6	155.8	155.2	155.0
L8	HF	4	0.21	0.20	1	0.60	0.30	0.10	1	0	C-T-I/II	27.5	0.00	9.00	12.8	14.3	15.6	17.3	17.4	154.9	154.9	154.4	155.1	154.4
L9	S	2	0.21	0.20	1	0.60	0.30	0.10	1	0	C-T-I/II	27.5	0.00	9.00	9.7	10.8	11.2	11.1	13.4	141.1	141.6	142.2	142.0	141.4
L10	S	1	0.21	0.20	1	0.60	0.30	0.10	1	0	C-T-I/II	27.5	0.00	9.50	10.9	12.4	13.4	15.4	16.0	143.5	144.3	144.9	144.1	144.5

Table C.2: Large-scale UHPC batches - splitting tensile strength, modulus of elasticity, and modulus of rupture

Mix.	Split T (ksi) - 28days			MOE (ksi) - 28days			MOR(ksi) - 28days
	N.Cured	Cured	Avg.	N.Cured	Cured	Avg.	Avg.
L1	2.68	2.54	2.61	8866.77	8733.62	8766.91	2.827
L2	2.49	2.76	2.62	8494.85	8936.67	8826.22	-
L3	2.61	2.73	2.67	7246.64	7978.68	7795.67	2.489
L4	2.81	2.87	2.84	9471.15	9034.57	9143.72	2.894
L5	3.06	2.80	2.93	7862.58	9201.79	8866.99	3.652
L6	2.45	2.33	2.39	8241.42	9415.38	9121.89	3.235
L7	2.80	2.90	2.85	8038.32	9006.73	8764.63	3.130
L8	2.85	2.75	2.80	7883.74	8940.07	8675.99	4.051
L9	1.45	1.30	1.38	7157.54	7698.71	7292.83	1.336
L10	1.46	1.53	1.49	7865.41	8240.88	8147.01	1.290

The stress versus strain plots used to determine the modulus of elasticity for all the specimens tested for the large-scale batches are shown in Figure C.1 and Figure C.2. The average response of all the specimens is also shown.

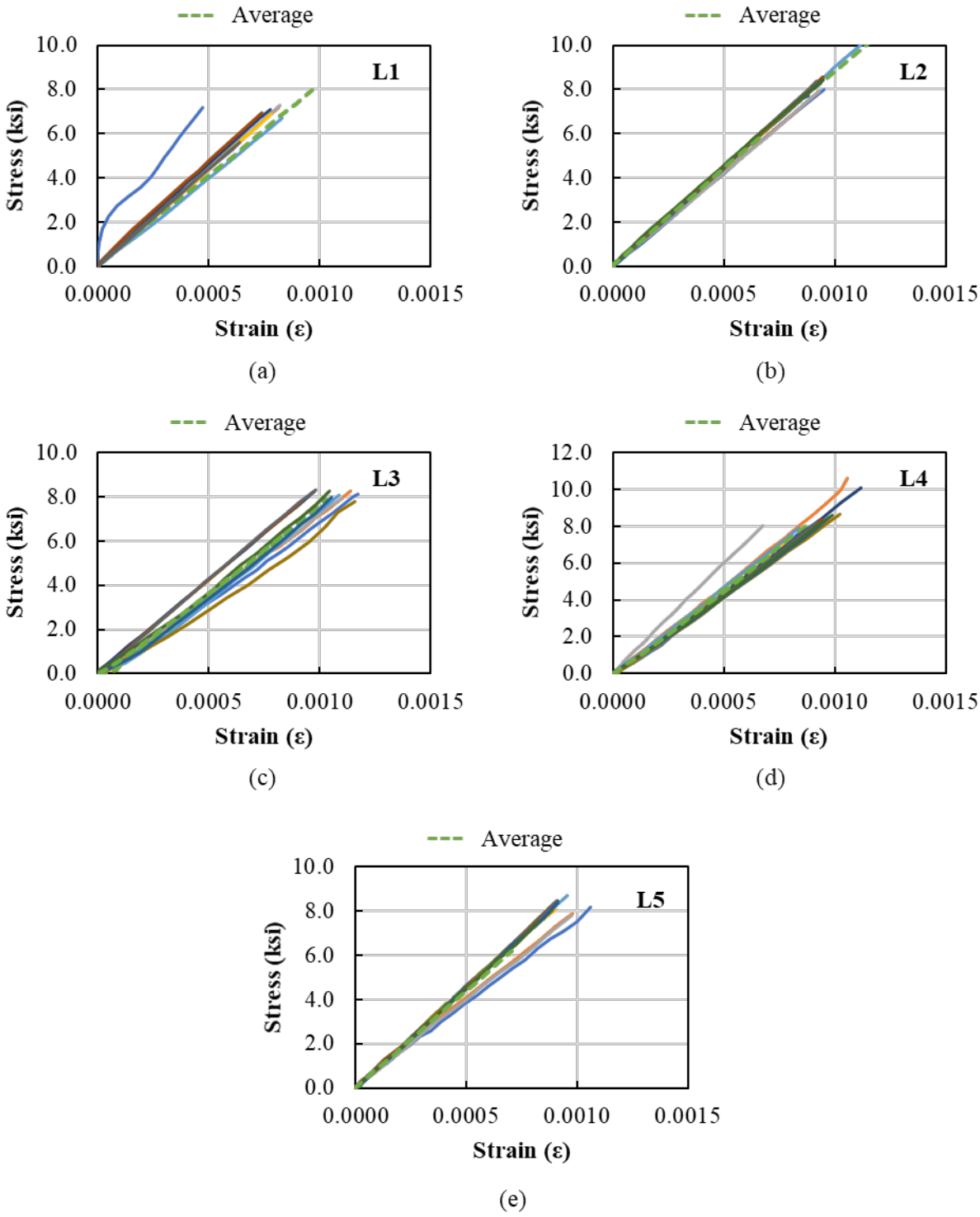

Figure C.1: Stress versus strain plots used to determine modulus of elasticity (L1 to L5)

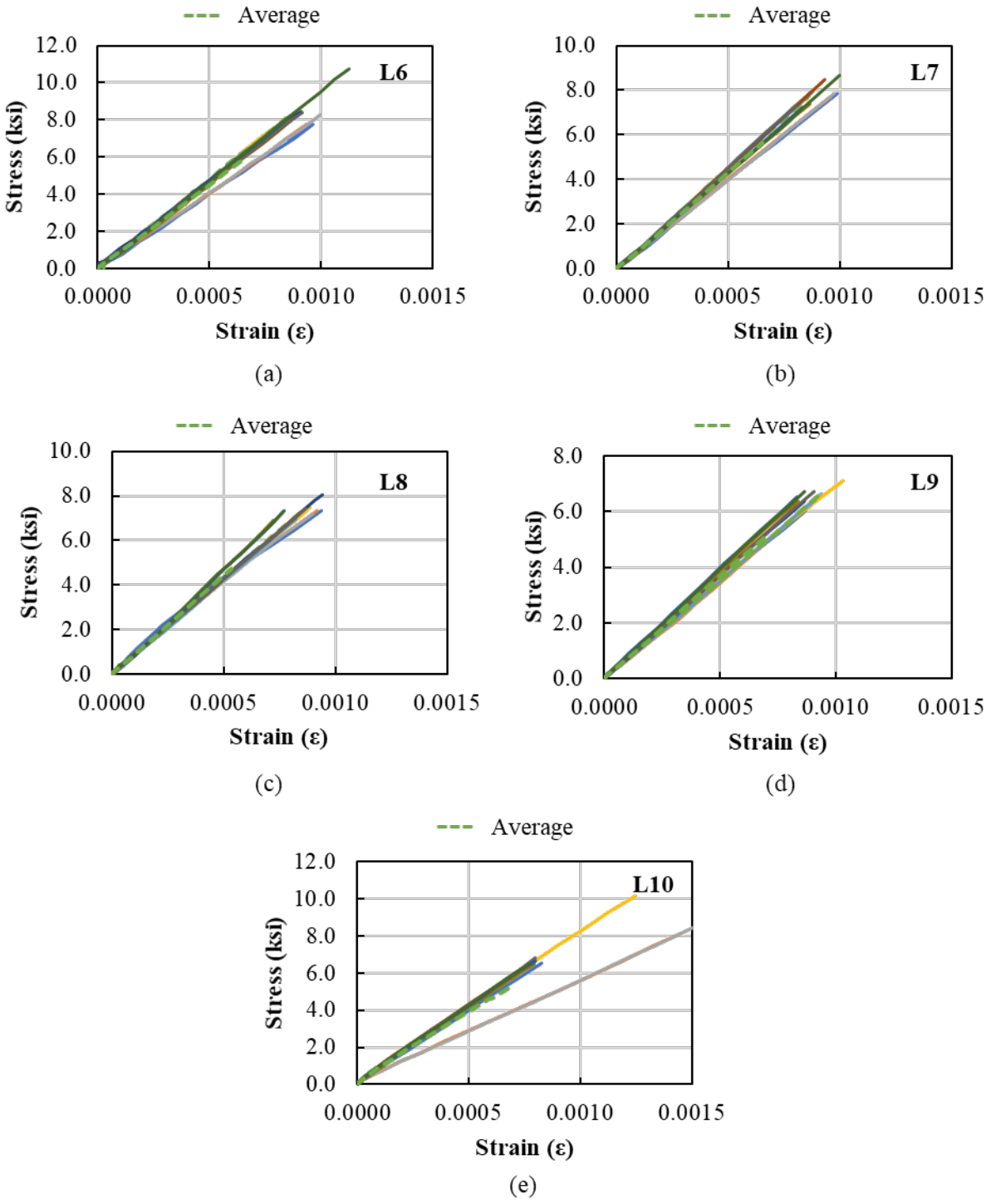

Figure C.2: Stress versus strain plots used to determine modulus of elasticity (L6 to L10)

The flexural stress versus displacement curves obtained during the four-point modulus of rupture testing for all specimens tested for the large-scale batches are shown in Figure C.3 and Figure C.4. These curves were all filtered to eliminate noise using the procedure described in Chapter 5.

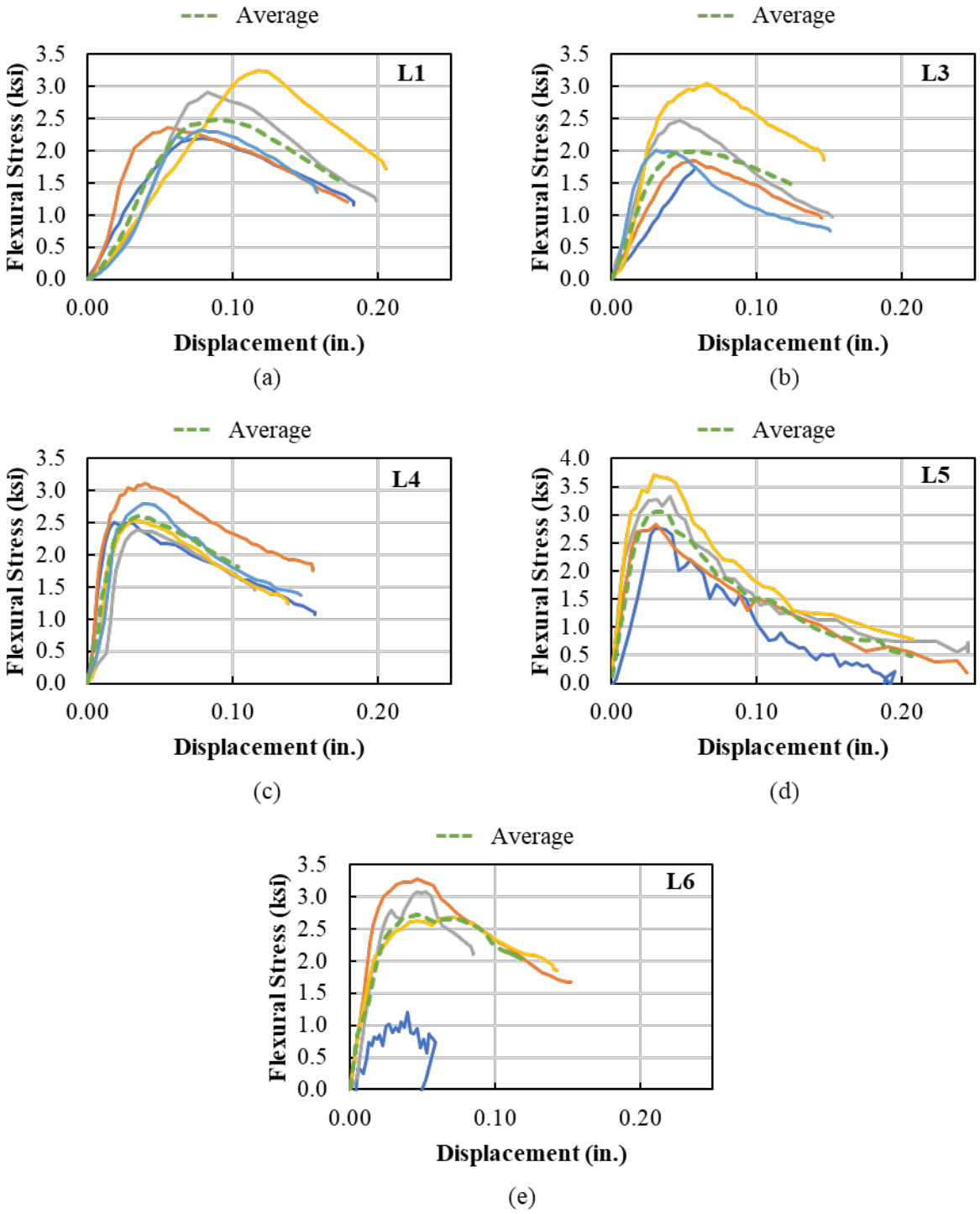

Figure C.3: Flexural stress versus midspan displacement from modulus of rupture testing for L1 and L3 to L6

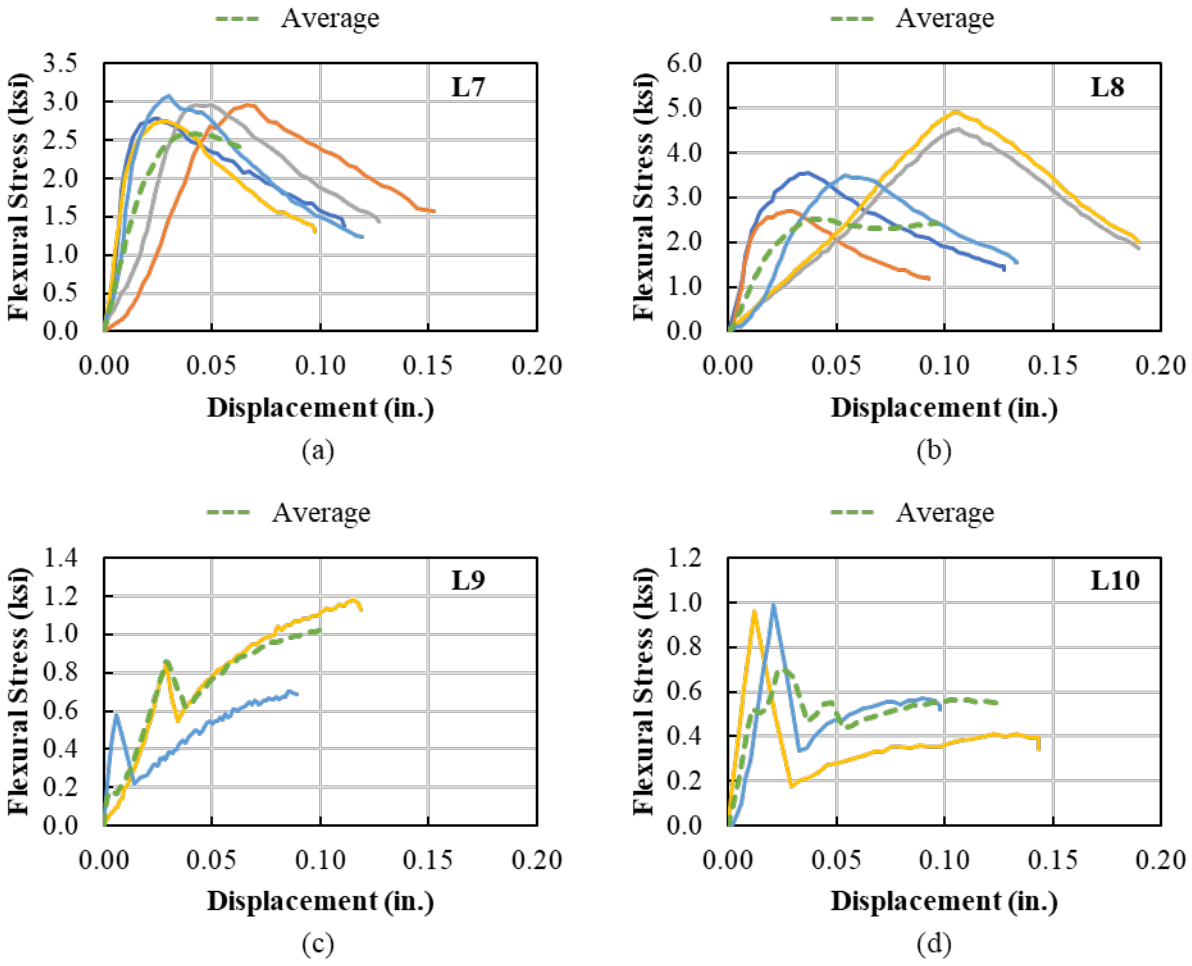

Figure C.4: Flexural stress versus midspan displacement from modulus of rupture testing for L7 to L10

The bulk resistivity readings (raw data) for the specimens with different clamping forces are shown in Table C.3.

Table C.3: Bulk resistivity readings (raw data) with different applied clamping forces

Mix	Cast Date	Age at Test	Sample	K (A/L), in.	Bulk Resistivity Readings under Different Clamping Forces, kΩ-cm								
					0 lb	*0.5 lb*	*1 lb*	*1.5 lb*	*2 lb*	*2.5 lb*	*3 lb*	*3.5 lb*	*4 lb*
L1	7/20/20	280	1	1.78	491	487	484	483	482	481	481	480	480
			2	1.73	588	586	585	584	583	583	583	583	582
			3	1.70	363	360	359	359	358	358	357	356	356
			4	1.71	529	528	528	527	527	526	526	526	525
L2	7/27/20	273	1	1.67	451	449	448	447	446	445	445	444	443
			2	1.68	510	509	509	508	507	506	506	506	505
			3	1.69	480	479	478	477	477	477	477	477	476
			4	1.83	519	518	518	517	517	517	517	517	517
L3	8/7/20	262	1	1.67	563	862	859	858	857	856	855	854	854
			2	1.68	1002	1002	1001	1001	1001	1001	1001	1000	1000
			3	1.73	817	816	815	814	814	814	813	812	811
			4	1.70	780	779	779	778	778	778	777	777	776
L4	8/18/20	251	1	1.72	911	911	911	910	910	909	908	907	906
			2	1.70	1000	1000	1000	1000	1000	1000	1000	1000	1000
			3	1.73	1109	1108	1108	1107	1107	1107	1107	1107	1107
			4	1.68	1000	1000	1000	1000	1000	1000	1000	1000	1000
L5	8/26/20	243	1	1.72	918	917	916	916	916	916	916	915	915
			2	1.80	864	863	862	862	862	862	862	862	862
			3	1.79	952	951	951	951	951	951	951	951	951
			4	1.77	891	890	890	890	890	889	889	889	889
L6	9/1/20	237	1	1.67	584	583	582	582	582	582	582	582	582
			2	1.67	663	662	661	661	661	661	660	660	660
			3	1.75	423	422	421	420	420	420	420	420	420
			4	2.21	468	467	466	466	466	466	466	466	466
L7	9/11/20	227	1	2.56	648	647	647	646	646	645	645	645	645
			2	1.82	508	507	506	505	505	504	504	503	503
			3	1.70	494	493	492	491	491	490	490	490	490
			4	1.77	593	592	592	591	590	590	590	589	589
L8	9/17/20	221	1	1.72	389	388	386	385	384	384	384	383	383
			2	1.70	494	493	492	491	491	491	490	490	490
			3	1.71	385	384	383	383	382	382	382	382	382

Mix	Cast Date	Age at Test	Sample	K (A/L), in.	Bulk Resistivity Readings under Different Clamping Forces, kΩ-cm								
					0 lb	*0.5 lb*	*1 lb*	*1.5 lb*	*2 lb*	*2.5 lb*	*3 lb*	*3.5 lb*	*4 lb*
			4	1.71	448	446	445	444	444	444	444	444	444
L9	10/6/20	202	1	1.71	1000	1000	1000	1000	1000	1000	1000	1000	1000
			2	1.68	1000	1000	1000	1000	1000	1000	1000	1000	1000
			3	1.68	1000	1000	1000	1000	1000	1000	1000	1000	1000
			4	1.68	1000	1000	1000	1000	1000	1000	1000	1000	1000
L10	10/21/20	187	1	1.72	1000	1000	1000	1000	1000	1000	1000	1000	1000
			2	1.71	1000	1000	1000	1000	1000	1000	1000	1000	1000
			3	1.83	1000	1000	1000	1000	1000	1000	1000	1000	1000
			4	1.73	1000	1000	1000	1000	1000	1000	1000	1000	1000
D1 (2%)	10/30/20	178	1	1.92	689	688	686	685	684	683	683	683	683
D2 (0%)	10/30/20	178	1	1.95	1000	1000	1000	1000	1000	1000	1000	1000	1000
			2	1.90	1000	1000	1000	1000	1000	1000	1000	1000	1000

APPENDIX D. TESTING DATA COLLECTION SHEETS

Data from all tests were recorded in data collection sheets and stored on a cloud server. A sample of some of the data collections sheets are shown in Figure D.1 (compression strength testing), Figure D.2 (split cylinder testing), and Figure D.3 (modulus of rupture).

Compressive Strength Testing

ABC-UTC - Non-Proprietary UHPC Mix Design

g to lb 0.002204623

Date 7/23/2020

Time 11:00 AM

Initials *ES*

Mixture *L1-3 day*

Test #:	1	2	3	4	5	6
Cylinder ID:	L1-1 (n/cured)	L1-2 (n/cured)	L1-3 (n/cured)	L1-4 (cured)	L1-5 (cured)	L1-6 (cured)
Mass of Cylinder before Capping [lb]:	3.4180	3.3060	3.3130	3.3415	3.3925	3.4285
Length of Cylinders [in]:	5.5830	5.4375	5.4360	5.4405	5.4990	5.5465
	5.5840	5.4385	5.4465	5.4420	5.4985	5.5475
	5.5770	5.4410	5.4485	5.4435	5.4955	5.5470
Diameter of Cylinders [in]:	3.0040	3.0010	3.0030	3.0030	3.0020	3.0020
	3.0050	3.0040	3.0040	3.0045	3.0030	3.0035
Ultimate Load [kips]:	80.95	87.1	84.15	83.3	79.45	88.3
Failure Mode:	Type 4	Type 4	Type 4	Type 4	Type 1	Type 4

Figure D.1: Example data collection sheet for compression strength testing

Split Cylinder Testing

ABC-UTC - Non-Proprietary UHPC Mix Design

Date 8/17/2020

Time 11:00 AM

Initials *ES*

Mixture *FIU1-2% OL fibers- 28days*

Test #:	1 - NC	2 - NC	3 - NC	4 - C	5 - C	6 - C
Cylinder ID:	FIU1-SP1	FIU1-SP2	FIU1-SP3	FIU1-SP4	FIU1-SP5	3.5045
Mass of Cylinder before Capping [g]:	3.256	3.4615	3.4195	3.4015	3.5025	5.7325
Length of Cylinders [in]:	5.255	5.6435	5.537	5.429	5.709	5.731
	5.256	5.649	5.538	5.428	5.7105	5.7305
	5.2555	5.65	5.539	5.4305	5.711	3.003
Diameter of Cylinders [in]:	3.003	3.001	3.001	3.0005	3.0015	3.003
	3.0035	3.005	3.0015	3.0015	3.002	3.0015
Ultimate Load [kips]:	71.74	69.55	66.24	63.1	58.8	67.25

Figure D.2: Example of data collection sheet for split cylinder testing

Modulus of Rupture Test

ABC-UTC - Non-Proprietary UHPC Mix Design

Date 8/17/2020

Time 9:00 AM

Initials *E.S*

Mixture *L1-FIU1-2% OL fibers*

Test #:		1 - NC	2 -NC	3 - C	4 - C
Beam ID:		FIU1-MOR1	FIU2-MOR2	FIU2-MOR3	FIU2-MOR4
Mass of Beam before Capping [lb]:		8.5868	8.1271	8.2865	8.4433
Span Length [in]:		6	6	6	6
Ultimate Load [kips]:		8.9	9.5	7.9	9.1
Location of Failure (middle third, outside by < 5%, or outside by > 5%):		MT	MT	MT	MT
Width at Fracture Plane	Top Width [in]:	3.145	3.008	2.9855	2.889
	Middle Width [in]:	3.1145	3.007	3.001	2.885
	Bottom Width [in]:	3.139	3.014	3.003	2.8845
Height at Fracture Plane	Left Height [in]:	2.924	2.885	3.0185	3.1645
	Center Height [in]:	2.935	2.8915	2.9985	3.163
	Right Height [in]:	2.957	2.881	2.993	3.1655

Figure D.3: Example of data collection sheet for modulus of rupture testing